

AD-A153 678

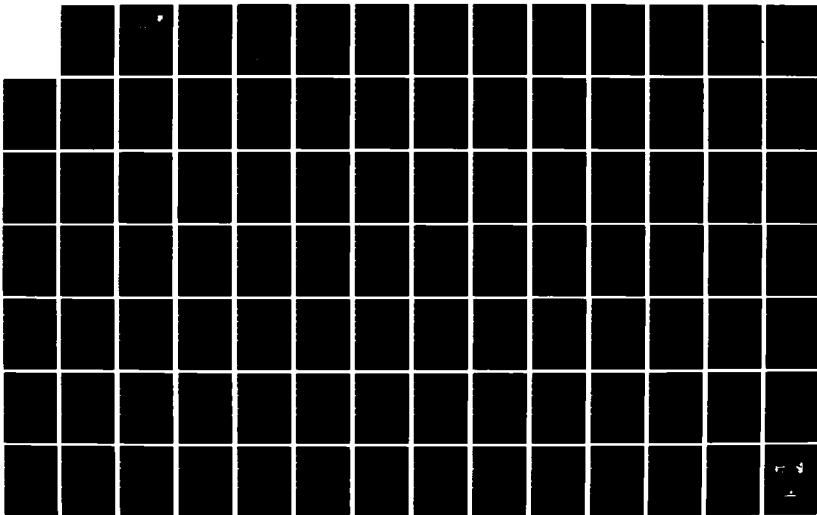
BASIC EMC (ELECTROMAGNETIC COMPATIBILITY) TECHNOLOGY
ADVANCEMENT FOR C3 S. (U) SOUTHEASTERN CENTER FOR
ELECTRICAL ENGINEERING EDUCATION INC S.
D A KOOPMAN ET AL. AUG 84

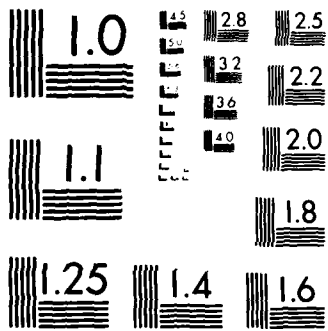
1/2

UNCLASSIFIED

F/G 20/14

NL





MICROCOPY RESOLUTION TEST CHART
NATIONAL BUREAU OF STANDARDS 1963-A

1009

①

AD-A153 678

RADC-TR-82-286, Vol IVd (of six)
Final Technical Report
August 1984



**BASIC EMC TECHNOLOGY ADVANCEMENT
FOR C³ SYSTEMS - Modeling Crosstalk
In Balanced Twisted Pairs**

Southeastern Center for Electrical Engineering Education

Dawn A. Koopman and Clayton R. Paul

APPROVED FOR PUBLIC RELEASE; DISTRIBUTION UNLIMITED

F30602-81-C-0062

**ROME AIR DEVELOPMENT CENTER
Air Force Systems Command
Griffiss Air Force Base, NY 13441**

**DTIC
ELECTE
MAY 15 1985
S D
B**

DTIC FILE COPY

85 5 13 024

BASIC EMC TECHNOLOGY ADVANCEMENT FOR C³ SYSTEMS

This report has been reviewed by the RADC Public Affairs Office (PA) and is releasable to the National Technical Information Service (NTIS). At NTIS it will be releasable to the general public, including foreign nations.

RADC-TR-82-286, Volume IVd (of six) has been reviewed and is approved for publication.

APPROVED: *Roy F. Stratton*
ROY F. STRATTON
Project Engineer

APPROVED:

W. S. Tuthill
W. S. TUTHILL, Colonel, USAF
Chief, Reliability & Compatibility Division

FOR THE COMMANDER:

John A. Ritz
JOHN A. RITZ
Acting Chief, Plans Office

If your address has changed or if you wish to be removed from the RADC mailing list, or if the addressee is no longer employed by your organization, please notify RADC (RBCT) Griffiss AFB NY 13441. This will assist us in maintaining a current mailing list.

Do not return copies of this report unless contractual obligations or notices on a specific document requires that it be returned.

TABLE OF CONTENTS

	<u>PAGE</u>
List of Figures	iv
List of Plots	vii
Chapter I - Introduction	1
Chapter II - Low-Frequency Model for Three Conductor Lines	15
Chapter III - Crosstalk in the Unbalanced Twisted-Pair Configuration	28
Chapter IV - The Unbalanced Twisted-Pair Generator and Receptor Circuits	53
Chapter V - Crosstalk in the Balanced Twisted-Pair	86
Chapter VI - Summary and Conclusions	119
Appendix A	124
Appendix B	144
References	156

S DTIC
ELECTE **D**
MAY 15 1985
B

Approved For	
<input checked="" type="checkbox"/>	
Special	
Priority Codes	
Special	
A-1	



LIST OF FIGURES

<u>FIGURE</u>		<u>PAGE</u>
1-1	The single wire receptor configuration	3
1-2	The SWP receptor configuration	4
1-3	The TWP receptor configuration	6
1-4	TWP terminated in differential line drivers and line receivers.	7
1-5	TWP balanced by means of a center- tapped transformer.	9
1-6	(a) The TWP (b) The "Abrupt-Loop" Model	12
1-7	The "Click" Model.	13
2-1	Typical cross-sectional geometries to which the results apply	16
2-2	The three-conductor transmission line. . . .	17
2-3	The per-unit-length model.	19
2-4	The low-frequency model.	24
2-5	An explanation of inductive coupling and capacitive-coupling in the low-frequency model. (a) Low-impedance loads (b) High-impedance loads.	27
3-1	The single wire to unbalanced TWP experiment.	29
3-2	The single wire to unbalanced SWP configuration	37
3-3	The unbalanced SWP low-frequency approximation	39
3-4	A low-frequency model of the twisted pair. .	46
3-5	An explanation of the sensitivity to twist. SWP denotes straight wire (untwisted) pair and TWP denotes the twisted pair.	51

<u>FIGURE</u>	<u>PAGE</u>
4-1	The TWP to TWP experiment 54
4-2	The SWP to SWP experiment 57
4-3	The low-frequency unbalanced SWP to unbalanced SWP configuration 64
4-4	The low-frequency approximation. (a) Inductive-coupling. (b) Capacitive coupling. 65
5-1	The balanced TWP experiment 88
5-2	View of the experiment. 89
5-3	The LF-428 transformers 90
5-4	View of the experiment at $X = 0$ 91
5-5	Cross-sectional view at $X = 0$ 92
5-6	Cross-sectional view at $X = L$ 93
5-7	The balanced SWP low-frequency approximation. 99
A-1	A general $(n + 1)$ conductor line. 125
A-2	The single generator wire to straight wire pair (SWP) receptor configuration. (a) Longitudinal view. (b) Cross-sectional view 132
A-3	The unbalanced SWP generator circuit to unbalanced SWP receptor circuit. (a) Longitudinal view. (b) Cross-sectional view 136
A-4	The single wire generator circuit to balanced SWP receptor circuit. (a) Longitudinal view. (b) Cross-sectional view 141

<u>FIGURE</u>		<u>PAGE</u>
B-1	The center-tapped transformer	145
B-2	The transformer windings	146
B-3	The equivalent circuit.	150
B-4	The equivalent circuit with its primary winding terminated in impedance R. . . .	151
B-5	A T network.	153
B-6	Equivalent circuit used in Chapter V. . . .	154

LIST OF PLOTS

All plots show voltage transfer ratio versus frequency.

<u>PLOT</u>		<u>PAGE</u>
3-1	(a) - (d) Single wire to unbalanced TWP sensitivity experiment	33 - 36
3-2	(a) - (d) Single wire to unbalanced SWP experiment	41 - 44
4-1	(a) - (d) Unbalanced SWP to unbalanced SWP experiment	58 - 61
4-2	(a) - (d) Unbalanced TWP to unbalanced TWP sensitivity experiment	68 - 71
4-3	(a) - (d) Comparison of single wire to unbalanced TWP and unbalanced TWP to unbalanced TWP, high readings.	75 - 78
4-4	(a) - (d) Comparison of single wire to unbalanced TWP and unbalanced TWP to unbalanced TWP, low readings.	79 - 82
5-1	(a) - (d) Single wire to balanced SWP experiment	95 - 98
5-2	(a) - (d) Single wire to balanced TWP sensitivity experiment	104 - 107
5-3	(a) - (d) Comparison of single wire to unbalanced TWP and single wire to balanced TWP, high readings	109 - 112
5-4	(a) - (d) Comparison of single wire to unbalanced TWP and single wire to balanced TWP, low readings.	113 - 116

CHAPTER I

INTRODUCTION

Electrical devices (computers, radar systems, communication radios, etc.) are interconnected by wires on most present systems. Electromagnetic fields produced by the excitation of these wires will cause unintentional coupling of signals onto nearby wires. This undesired electromagnetic coupling is termed crosstalk. It is important to be able to determine whether these crosstalk signals will cause the devices at the ends of the wires to malfunction. Wires are often grouped together in cable bundles or harnesses. The close proximity of wires in these bundles enhances the possibility that the crosstalk levels will be sufficiently large to cause malfunctions.

The ability to predict crosstalk levels and the means to control crosstalk when it causes a problem are important to optimum system design. If interference of this type is allowed to surface during final system tests, a costly and time consuming retrofit of the wiring or the addition of filters and other interference control measures may be required. Not only is it desirable to be able to predict this crosstalk with mathematical models, but an understanding of the mechanism of crosstalk is essential in designing other wiring configurations which will reduce the level of pick-up.

Several methods of reducing crosstalk have been developed. One method of decreasing the electric field coupling onto a wire is to surround the wire(s) with a cylindrical metal shield. In order to maintain the wire's flexibility, the shield is usually a braided metal covering. Disadvantages of shielding wires are the added weight to a system and the increased complexity of manufacture. Also, depending on how the shield is grounded or terminated, it may or may not provide a significant reduction in crosstalk [1].

The use of pairs of wires placed in close proximity rather than a single wire at a large height above a ground plane return reduces crosstalk caused by magnetic coupling. To explain this effect, consider the case of two wires above a ground plane (Figure 1-1). The excitation of the generator wire (and ground plane return) produces electromagnetic fields about the wire. The amount of magnetic coupling into the receptor circuit is proportional to the area (shaded in Figure 1-1) between the receptor wire and the ground plane. This is because the time rate-of-change of the magnetic flux which penetrates the area between the receptor wire and its return induces, by Faraday's law, an EMF or equivalent voltage source in that circuit. This EMF induces voltages across the loads, Z_{OR} and Z_{LR} , at the ends of the circuit. Extend this concept to the configuration using a straight wire pair (SWP) as the receptor circuit (Figure 1-2). Now the magnetic coupling is proportional to the smaller area between the two wires of the SWP [1].

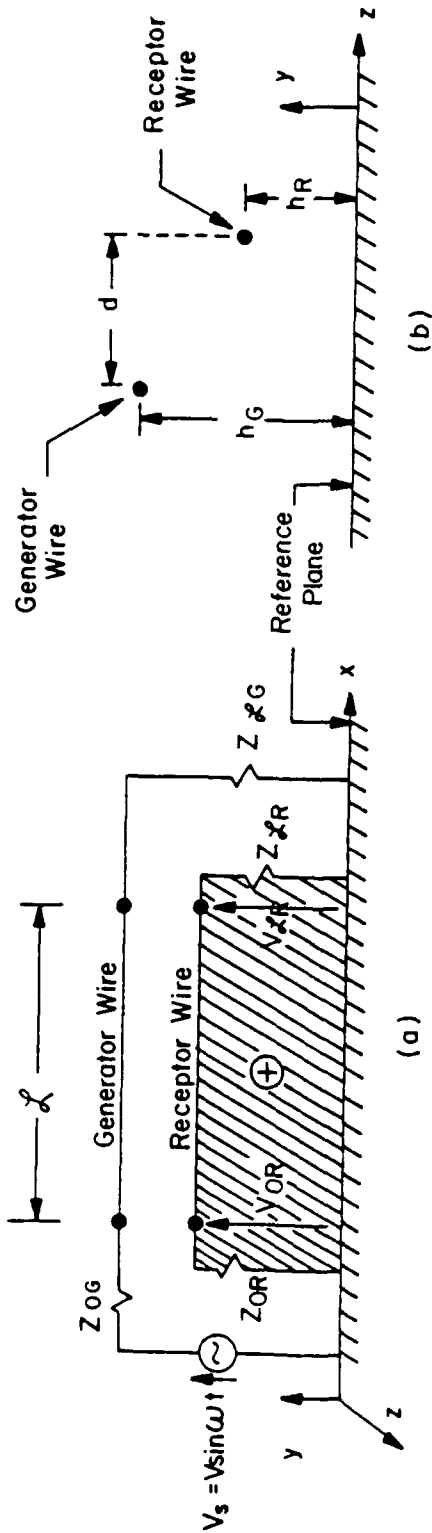


FIGURE 1-1. THE SINGLE WIRE RECEPTOR CONFIGURATION.

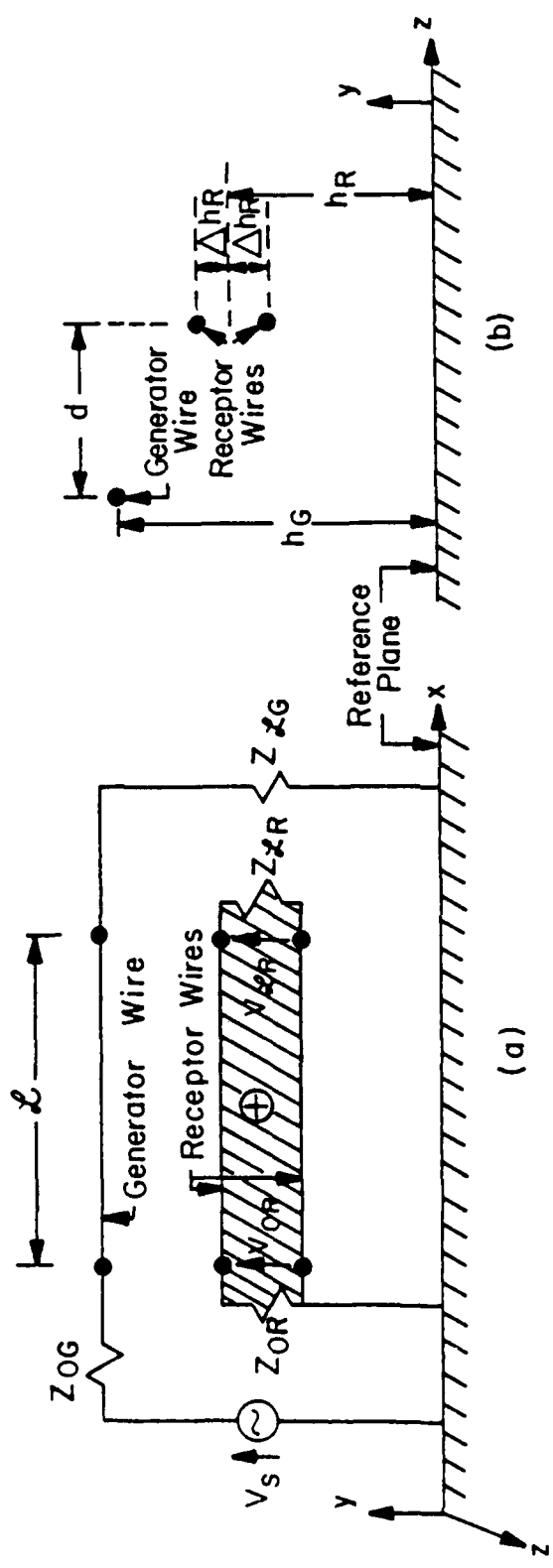


FIGURE 1-2. THE SWP RECEPTOR CONFIGURATION.

A further reduction of the magnetic coupling to the receptor circuit can be gained by twisting the wires of the SWP, resulting in a twisted wire pair (TWP), (Figure 1-3). Assume that the loops of the TWP are of equal dimension. The magnetic field produced by the generator circuit will cause a magnetic flux to penetrate each loop of the TWP. This magnetic flux will cause EMF's of equal magnitude to be developed in the loops. However, since wire positions are interchanged with each half twist of the TWP, the currents induced by the EMF of one loop will cancel the currents induced by the EMF of an adjacent loop. Therefore, if there are an even number of loops, it would seem that the magnetic field crosstalk would be eliminated. For an odd number of loops, the crosstalk due to magnetic field coupling would be diminished to the extent that it would be proportional to the area of one loop of the TWP only [1].

The TWP configuration of Figure 1-3 is referred to as unbalanced with respect to its terminal impedances. By unbalanced, it is meant that at a particular end of the line, the impedance which each wire sees to ground is not the same [1]. Hence, a balanced configuration is one in which each wire sees the same impedance to ground. It is generally accepted that balancing the terminations of a TWP provides a further reduction in crosstalk. For this reason, it is becoming increasingly common to transmit digital data via twisted pairs which are balanced in that they are terminated in differential line drivers and line receivers (Figure 1-4), [3].

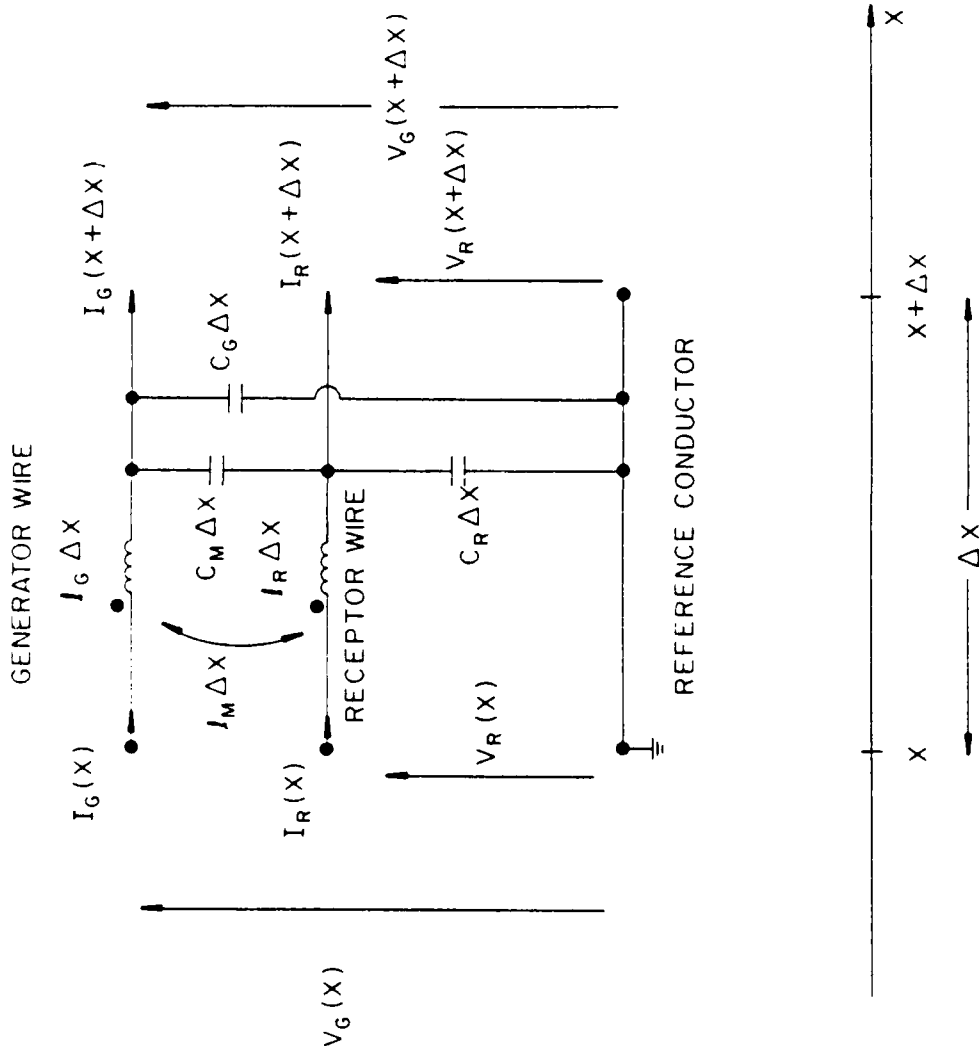


FIGURE 2-3. THE PER-UNIT-LENGTH MODEL.

The transmission line equations can be derived from a ΔX section of the line (Figure 2-3). This ΔX section is characterized by the per-unit-length parameters of the line: the self inductances of the generator and receptor wires, L_G and L_R , the mutual inductance between the two wires, L_m , the self capacitances of the wires, c_G and c_R , and their mutual capacitance, c_m . The transmission line equations, as $\Delta X \rightarrow 0$, are

$$\frac{dV_G(X)}{dX} = -j\omega L_G I_G(X) - j\omega L_m I_R(X) \quad (2-1a)$$

$$\frac{dV_R(X)}{dX} = -j\omega L_m I_G(X) - j\omega L_R I_R(X) \quad (2-1b)$$

$$\frac{dI_G(X)}{dx} = -j\omega (c_G + c_m) V_G(X) + j\omega c_m V_R(X) \quad (2-1c)$$

$$\frac{dI_R(X)}{dx} = j\omega c_m V_G(X) - j\omega (c_R + c_m) V_R(X) \quad (2-1d)$$

In order to simplify the representation and manipulation of these transmission line equations, the per-unit-length parameters will be represented in matrix form. The per-unit-length inductance matrix is defined by

$$\tilde{L} = \begin{bmatrix} L_G & L_m \\ L_m & L_R \end{bmatrix} \quad (2-2a)$$

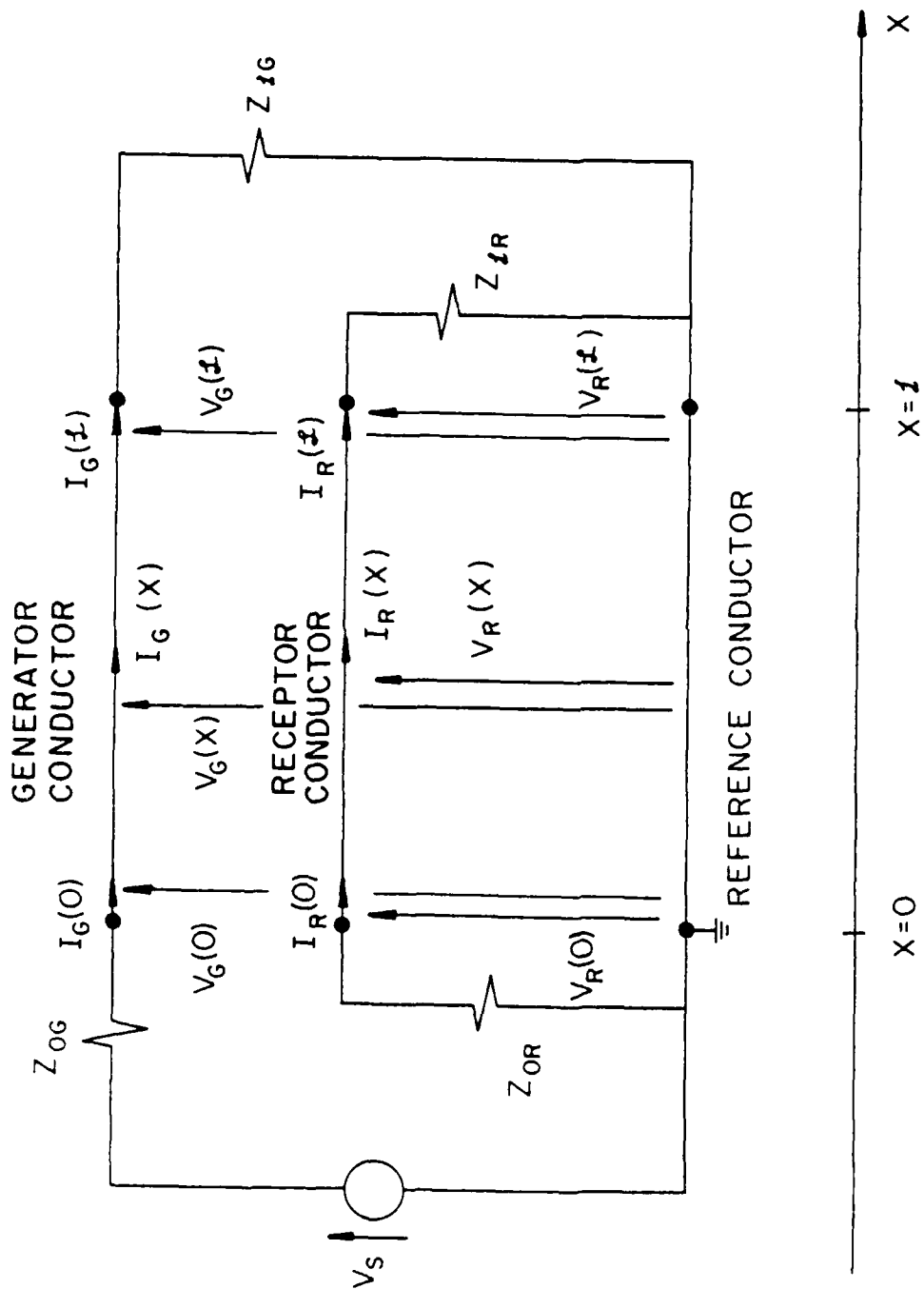


FIGURE 2-2. THE THREE-CONDUCTOR TRANSMISSION LINE.

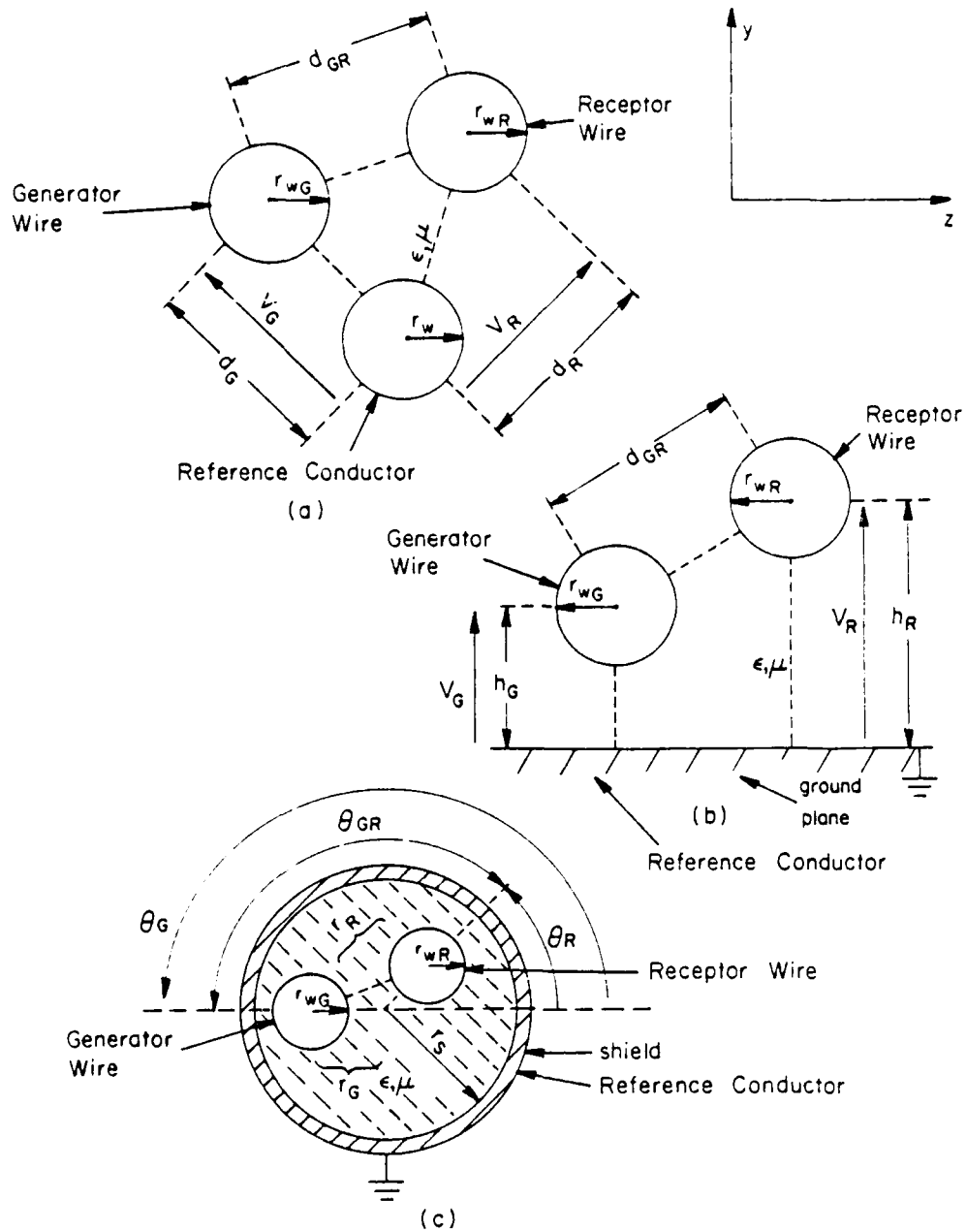


FIGURE 2-1. TYPICAL CROSS-SECTIONAL GEOMETRIES TO WHICH THE RESULTS APPLY.

CHAPTER II

LOW-FREQUENCY MODEL FOR
THREE-CONDUCTOR LINES

As a preliminary to any further examination of the TWP, a simple low-frequency model of the crosstalk for the case of the three-conductor line (Figure 2-1) will be presented [13]. The concepts involved in this analysis are important in explaining the crosstalk of TWP's. This low-frequency model was developed during the process of solving the transmission line equations for the three-conductor line. The configuration consists of a generator wire, a receptor wire and a third conductor which will be referred to as the reference conductor (Figure 2-2). The total line is of length L . A voltage source V_g is applied between one end of the generator wire and the reference conductor. One is then usually interested in determining the voltages $V_R(0)$ and $V_R(L)$ induced at the ends of the receptor wire.

The solution of the transmission line equations (and hence the low-frequency model) is obtained under certain assumptions. The medium surrounding the conductors is homogeneous, linear, isotropic and lossless, and is characterized by permeability μ and permittivity ϵ . Also the line is uniform and the conductors are perfect.

crosstalk from a single wire to an unbalanced TWP [12].

For certain low-impedance loads, it was observed that the cross-talk was very sensitive to slight variations in line twists.

Their explanation for this sensitivity will be used in Chapter IV, when the crosstalk from an unbalanced TWP to an unbalanced TWP is examined. Finally, Chapter V will investigate the crosstalk to a TWP in which the terminal configurations are balanced by means of a center-tapped transformer as in Figure 1-5.

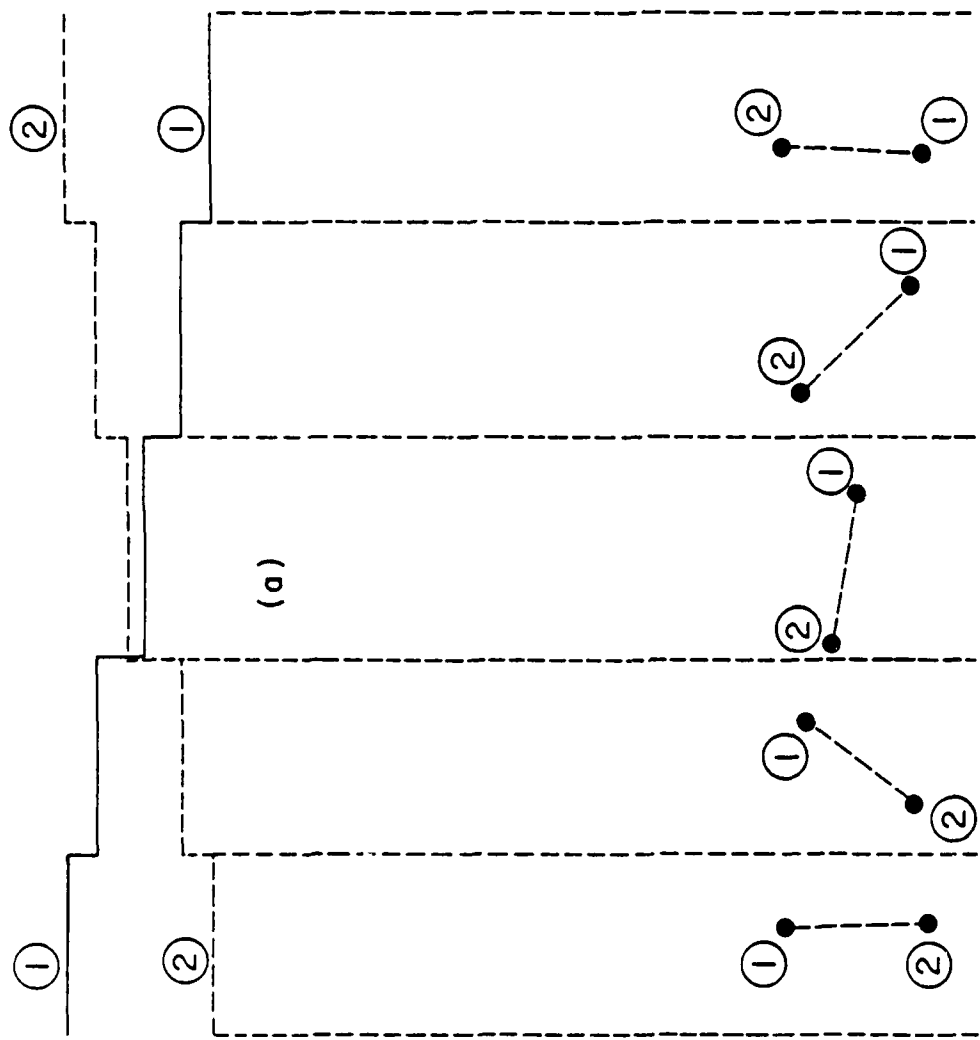
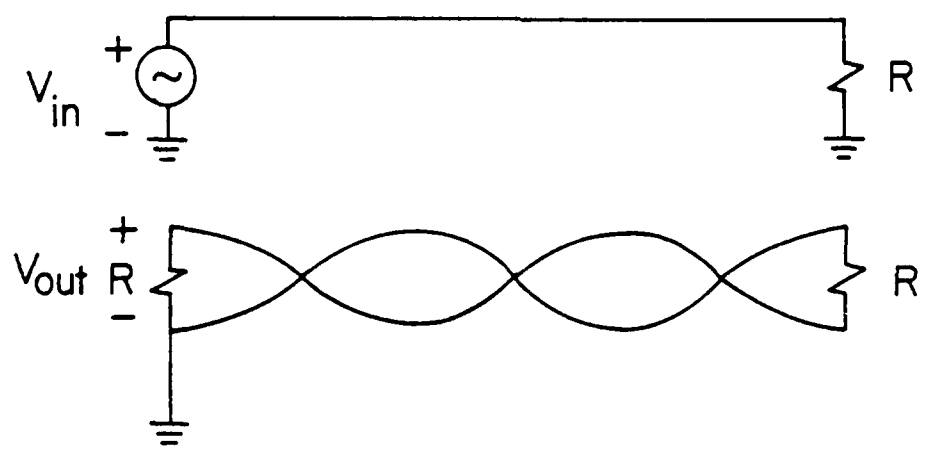
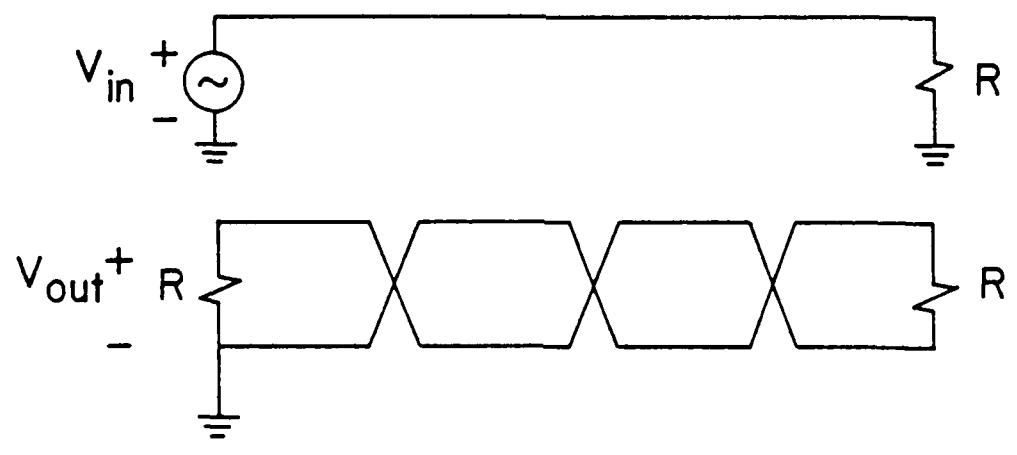


FIGURE 1-7. THE "CLICK" MODEL.



(a) The Unbalanced, Twisted Pair



(b) The "Abrupt-Loop" Model

FIGURE 1-6. (a) THE TWP. (b) THE "ABRUPT-LOOP" MODEL.

The "abrupt-loop" model represents the TWP as a sequence of vertical loops with wires alternating positions suddenly between loops (Figure 1-6). Although the overall line is still nonuniform, each loop is uniform. The voltages and currents at the ends of the entire line can then be determined by combining the chain parameter matrices of the loops. These chain parameter matrices relate the voltages and currents at the ends of the loops, so in combining the matrices, the voltages and currents associated with the matrices must change positions appropriately to account for the wire interchange.

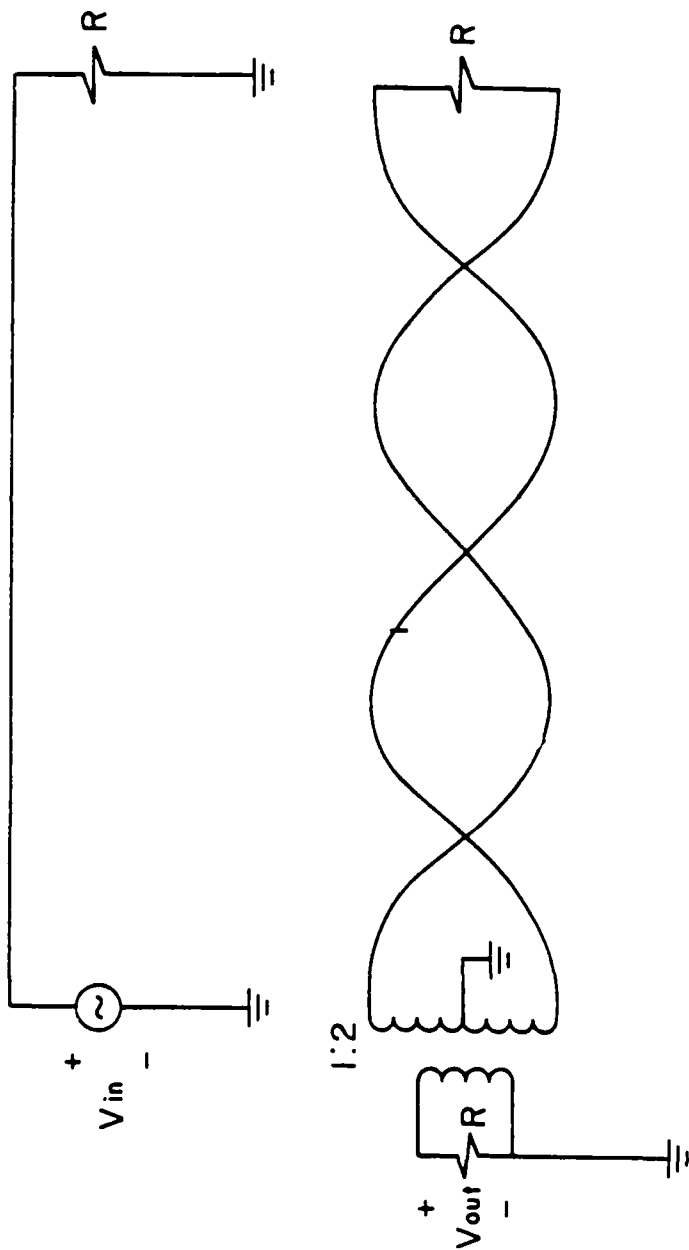
A further refinement of this abrupt-loop model is to somehow approximate the twist of the loops of the TWP. This can be accomplished by representing each loop as a cascade of uniform segments which rotate about the line axis in discrete angular increments (Figure 1-7), [3].

This report will investigate several TWP configurations and will attempt to provide some understanding of the effectiveness of using a TWP. Chapter II will describe the work of C. R. Paul, where he examined the electromagnetic coupling for the special case of three-conductor transmission lines in homogeneous media [13]. In determining the solution of the transmission-line equations, Paul showed that, for sufficiently small frequencies, the crosstalk can be modeled by the sum of inductive-coupling and capacitive-coupling contributions. The concepts developed in this simple low-frequency model will be used in later chapters to explain the

The nonuniformity of the TWP makes it difficult to calculate per-unit-length inductances and capacitances of the line, which are essential to the development of a transmission line model. Perhaps a more important problem with nonuniform lines is that because these per-unit-length parameters are functions of the line axis variable (x), the resulting transmission line differential equations are nonconstant coefficient (e.g., Bessel's equation) and are extremely difficult to solve [1].

One TWP model which has been used modifies the per-unit-length parameters of the SWP to approximate the TWP. The elements of the inductance matrix are determined by averaging the values obtained for a line tilted at an angle θ with the horizontal over angles from 0 to $\pi/2$. A propagation velocity of the TWP is calculated to account for the fact that waves do not travel down the line at the speed of light, but slower than the speed of light due to the helical twisting of the line. This propagation velocity is based on the line pitch (the number of twists per unit of line length), the separation of the wires of the pair and the speed of light. The per-unit-length capacitance matrix can then be determined using the averaged inductance matrix and the velocity of propagation of the line [9].

An approximation to the solution of a nonuniform line is to model the line as a cascade of uniform sections [1,10]. Consider again the case of the TWP receptor wire (Figure 1-3).



(a)

FIGURE 1-5. TWP BALANCED BY MEANS OF A CENTER-TAPPED TRANSFORMER.

Another means of achieving balanced terminal impedances in TWP circuits is through the use of center-tapped transformers (Figure 1-5).

The explanation given previously showed how magnetic field coupling was reduced by using a TWP. However, an electric field is also produced by the generator wire and it too contributes to the crosstalk. If it were possible to determine how parameters such as terminal configurations and physical geometry affect each component of the crosstalk, some qualitative insight could be gained into the effectiveness of TWP's in individual situations. It would be beneficial to have accurate models for predicting the crosstalk to or from TWP's. This would enable a designer to determine, quantitatively, the effectiveness of TWP's when they are used.

Initial attempts to model TWP's were concerned with determining the magnetic field resulting from a current on an infinitely long, isolated TWP [4] - [7]. The usefulness of this model is limited, however, since TWP's are usually in close proximity to other wires as well as structural members such as an aircraft fuselage.

One of the problems in developing a model for TWP's is that most transmission line models assume a uniform line. Lines are said to be uniform if cross-sectional views of the line at every point along the line are identical [8]. The TWP resembles a bifilar helix. Consequently, it is not a uniform line.

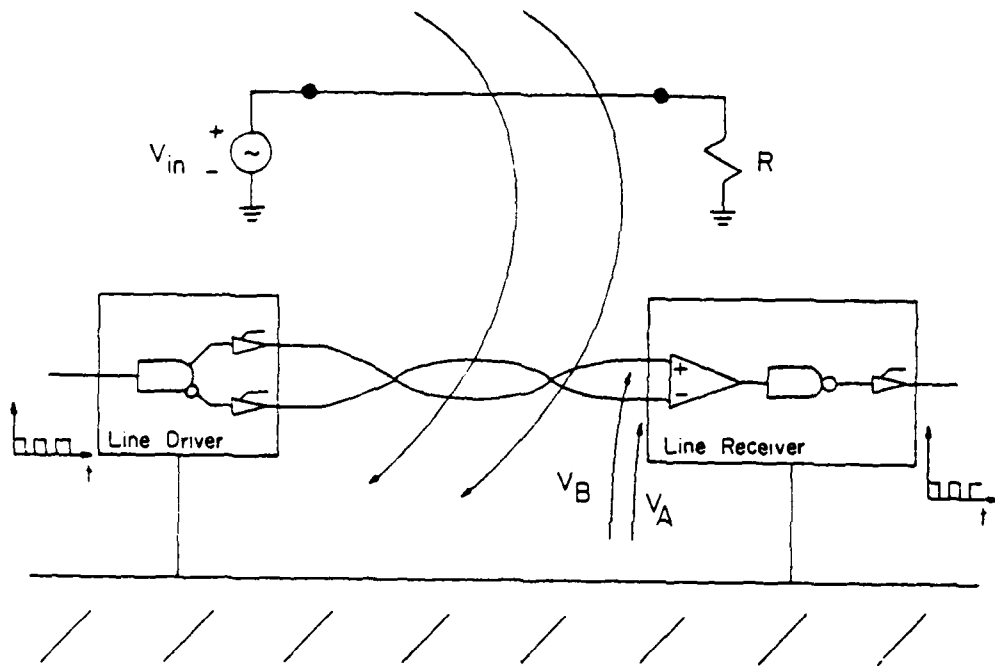


FIGURE 1-4. TWP TERMINATED IN DIFFERENTIAL LINE DRIVERS AND LINE RECEIVERS.

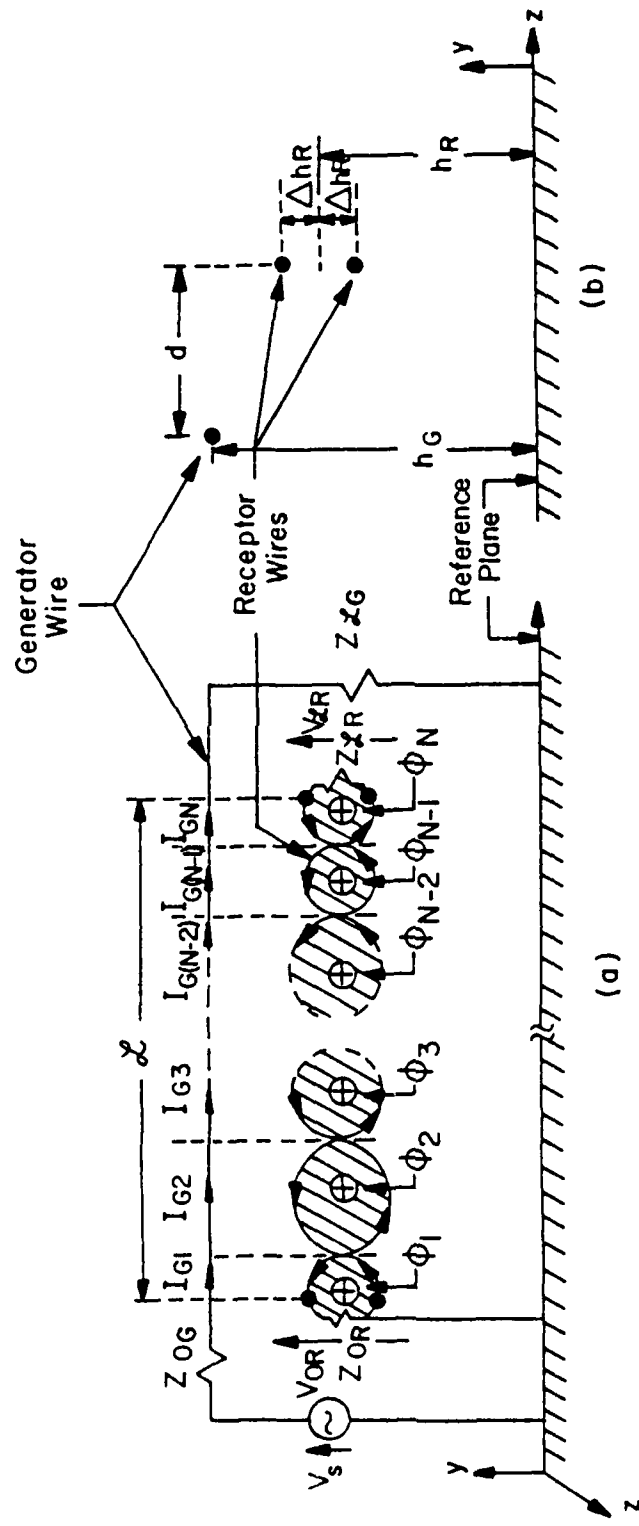


FIGURE 1-3. THE TWP RECEPTOR CONFIGURATION.

and the per-unit-length capacitance matrix is defined by

$$\underline{\underline{C}} = \begin{bmatrix} (c_G + c_m) & -c_m \\ -c_m & (c_R + c_m) \end{bmatrix} \quad (2-2b)$$

The elements of $\underline{\underline{L}}$ can be calculated from the physical characteristics and dimensions of the line. The velocity of propagation in the surrounding media is defined by

$$v = \frac{1}{\sqrt{\mu \epsilon}} \quad (2-3)$$

The entries of $\underline{\underline{C}}$ can then be derived from [8]

$$\underline{\underline{L}} \underline{\underline{C}} = \frac{1}{v^2} \underline{\underline{I}}_2 \quad (2-4)$$

or,

$$\underline{\underline{C}} = \frac{1}{v^2} \underline{\underline{L}}^{-1} \quad (2-5)$$

where $\underline{\underline{I}}_2$ is the identity matrix

$$\underline{\underline{I}}_2 = \begin{bmatrix} 1 & 0 \\ 0 & 1 \end{bmatrix} \quad (2-6)$$

The solution of the transmission line equations is obtained through manipulation of the chain parameter matrices [1,10], which relate the voltages and currents at one end of the line to those at the other end of the line, and through utilization of the terminal conditions of the line. The terminal networks are given by Generalized Thevenin Equivalents [8]:

$$V_G (0) = V_S - Z_{OG} I_G (0) \quad (2-7a)$$

$$V_G (L) = Z_{LG} I_G (L) \quad (2-7b)$$

$$V_R (0) = -Z_{OR} I_R (0) \quad (2-7c)$$

$$V_R (L) = Z_{LR} I_R (L) \quad (2-7d)$$

Paul's solution of the transmission line equations gives exact, literal expressions for $V_R(0)$ and $V_R(L)$ [13].

It is important here, however, to note that if the total line is electrically short and the terminal impedances are frequency-independent, then as the frequency becomes sufficiently small, the exact equations for $V_R(0)$ and $V_R(L)$ can be approximated by

$$V_R(0) = \frac{Z_{OR}}{Z_{OR} + Z_{LR}} (j\omega L_m L) I_{G_{DC}} \quad (2-8a)$$

$$+ \frac{Z_{CR} Z_{LR}}{Z_{OR} + Z_{LR}} (j\omega c_m L) V_{G_{DC}}$$

$$V_R(L) = \frac{-Z_{LR}}{Z_{OR} + Z_{LR}} (j\omega L_m L) I_{G_{DC}}$$

$$+ \frac{Z_{OR} Z_{LR}}{Z_{OR} + Z_{LR}} (j\omega c_m L) V_{G_{DC}} \quad (2-8b)$$

$V_{G_{DC}}$ and $I_{G_{DC}}$ are the zero-frequency (DC) values of the generator wire voltage and current

$$V_{G_{DC}} = \frac{Z_{LG}}{Z_{CG} + Z_{LG}} V_s \quad (2-9a)$$

$$I_{G_{DC}} = \frac{1}{Z_{OG} + Z_{LG}} V_s \quad (2-9b)$$

This is called the low-frequency model because of the criteria that the line is electrically short and that frequency is sufficiently small.

Notice that the equations for the receptor voltages are separated into two parts - one dependent on L_m and the other on c_m . The part of the receptor voltage dependent on the per-unit-length mutual inductance between the two circuits, L_m , is generally termed the inductive-coupling contribution, and the part dependent on the per-unit-length

mutual capacitance between the two circuits, c_m , is the capacitive-coupling contribution. Thus, the equation for $V_R(0)$, for example, can be written

$$V_R(0) = V_R(0)^{IND} + V_R(0)^{CAP} \quad (2-10)$$

where

$$V_R(0)^{IND} = \frac{Z_{OR}}{Z_{OR} + Z_{LR}} (j\omega L_m L) I_{G_{DC}} \quad (2-11a)$$

$$V_R(0)^{CAP} = \frac{Z_{OR} Z_{LR}}{Z_{OR} + Z_{LR}} (j\omega c_m L) V_{G_{DC}} \quad (2-11b)$$

Equation 2-10 (and a similar equation for $V_R(L)$) could also be derived from a low-frequency approximation to the receptor circuit (Figure 2-4), where $V_R(0)$ (or $V_R(L)$) is obtained as the superposition of the effects of the two sources.

The possibility that the contribution from one type of coupling - inductive or capacitive - might be dominant over the contribution from the other type of coupling in the determination of the receptor voltages is evident in Equations (2-10) and (2-11). For "low-impedance" loads the inductive-coupling dominates the capacitive-coupling contribution and for "high-impedance" loads the capacitive-coupling is dominant. An understanding of what is meant

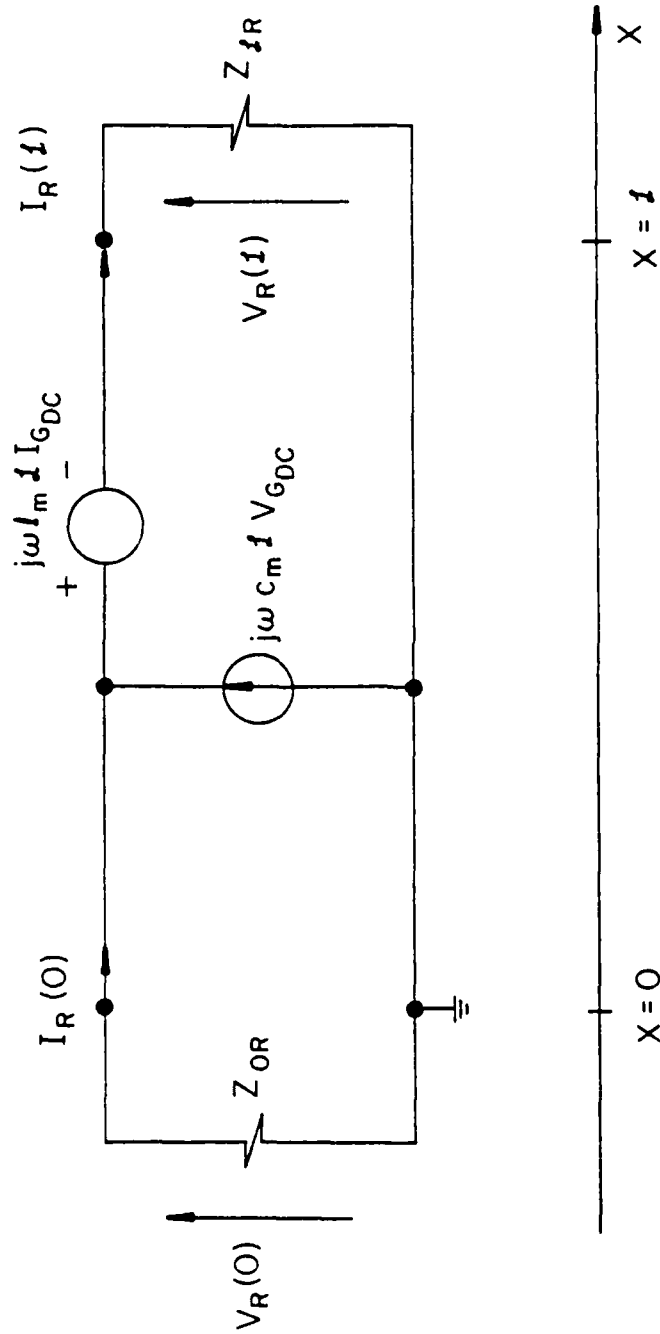


FIGURE 2-4. THE LOW-FREQUENCY APPROXIMATION.

by "low-impedance" or "high-impedance" loads can be gained through examination of Equations (2-8). The inductive-coupling contribution is dominant in $V_R(0)$ when

$$L_m \gg c_m Z_{LR} Z_{LG} \quad (2-12)$$

This can also be expressed as

$$\left(\frac{Z_{LG}}{Z_{cG}} \right) \left(\frac{Z_{LR}}{Z_{cR}} \right) \ll 1 \quad (2-13)$$

where Z_{cG} (Z_{cR}) is generally referred to as the characteristic impedance of the generator (receptor) in the presence of the receptor (generator) circuit [13]. Similarly, the inductive-coupling contribution in $V_R(L)$ is dominant when

$$L_m \gg c_m Z_{OR} Z_{LG} \quad (2-14)$$

or

$$\left(\frac{Z_{LG}}{Z_{cR}} \right) \left(\frac{Z_{OR}}{Z_{cR}} \right) \ll 1 \quad (2-15)$$

Thus, when the above inequalities hold, the configuration is said to have "low-impedance" loads. Capacitive-coupling

is dominant when the above inequalities are reversed. The dominance of one type of coupling over the other can be illustrated graphically (Figure 2-5).

The concept of separating crosstalk into inductive-coupling and capacitive-coupling contributions for sufficiently small frequencies as developed for the simple three-conductor line configuration will be applied to the twisted wire pairs investigated later in the paper. As will become evident, this concept is very important in understanding the mechanism of coupling in TWP's. Also, this separation of the crosstalk allows the simple illustration and calculation of certain crosstalk results for TWP's.

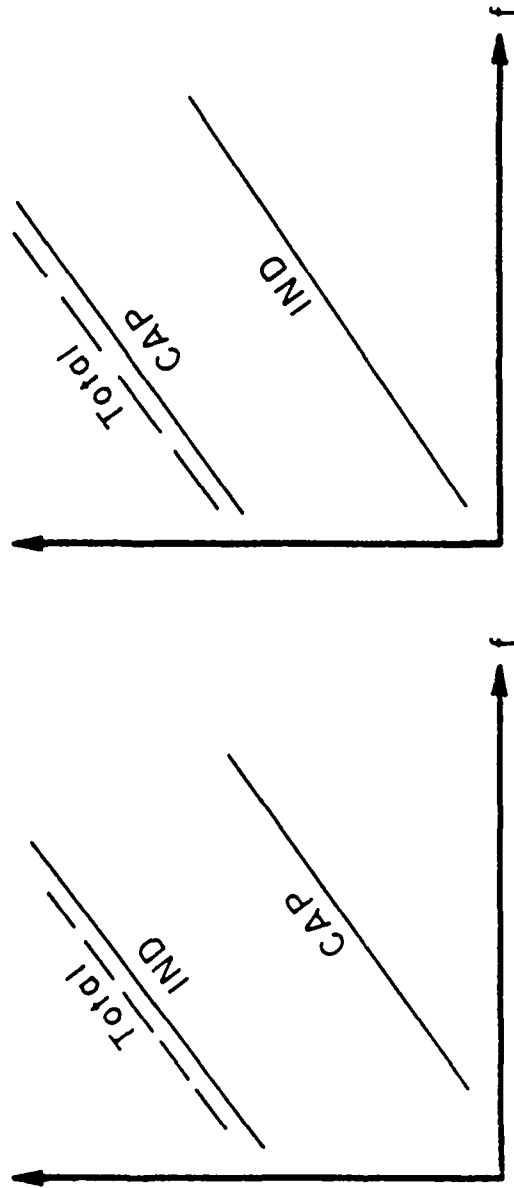


FIGURE 2-5. AN EXPLANATION OF INDUCTIVE-COUPPLING AND CAPACITIVE COUPLING IN THE LOW-FREQUENCY MODEL. (a) LOW-IMPEDANCE LOADS. (b) HIGH-IMPEDANCE LOADS.

CHAPTER III

CROSSTALK IN THE UNBALANCED TWISTED-PAIR CONFIGURATION

The use of twisted wire pairs to reduce crosstalk was described in the Introduction. The purpose of this chapter is to review the works of C. R. Paul and M. B. Jolly [3,12], wherein the configuration investigated was a single wire with ground return as the generator circuit and an unbalanced TWP as the receptor circuit. That work has direct bearing on the coupling investigations of this report. Their work showed that, for certain loads, the crosstalk level of the TWP showed large sensitivity to minor variations in line twist. This sensitivity to line twist, which will be explained later in the chapter, also appears in the TWP line configurations investigated for this report. The application of the theory developed by Paul and Jolly to other TWP configurations will be examined.

The experiment performed by Paul and Jolly is outlined below (see Figure 3-1). The generator wire and the TWP were suspended 2 cm above a 1/8 inch thick aluminum ground plane and were separated from each other by 2 cm. The positions of the generator wire and the TWP were supported above the ground plane by styrofoam blocks placed along the line. The line length was 4.705 m. All wires were #22 gauge, stranded, with polyvinyl chloride insulation approximately 16 mils thick.

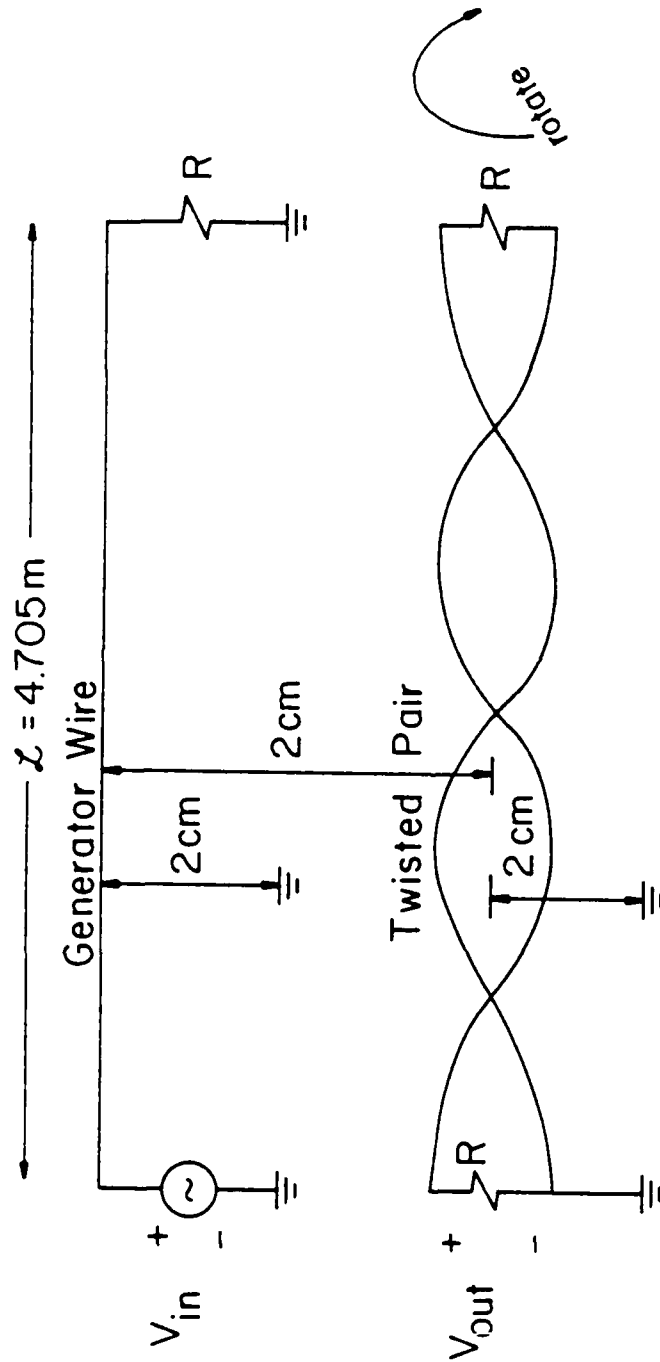


FIGURE 3-1-1. THE SINGLE WIRE TO UNBALANCED TWP EXPERIMENT.

The minimum center - to - center separation between the wires of the TWP was 57.3 mils. The TWP contained approximately 170 full twists, which corresponds to a pitch of about 7 twists per foot.

A sinusoidal generator was connected at the left end of the line between the generator wire and the ground plane. This input voltage was referred to as V_{in} . Identical resistance values were used for all loads. It was not required for all resistances to be equal, but they were chosen equal to facilitate the analysis of the results. During the course of the experiment four resistances were used to terminate both lines, $R = 1\Omega, 3\Omega, 50\Omega$ and $1\text{ k}\Omega$. The TWP was unbalanced with respect to its terminal configurations. The right end of the TWP was ungrounded and one wire at the left end of the TWP was connected to ground. The voltage across the left end termination of the TWP was measured and was referred to as V_{out} . The voltage transfer ratio was then defined by

$$\text{Voltage transfer ratio} = \frac{V_{out}}{V_{in}} \quad (3-1)$$

The voltage transfer ratio was determined for frequencies from 100 Hz to 1 MHz. Within each decade of this frequency range, measurements were taken in steps of 1, 1.5, 2, 2.5, 3, 4, 5, 6, 8, 9. A Hewlett-Packard HP 3550A low frequency vector analyzer was used to measure V_{out} below 15 kHz. For frequencies above 15 kHz an Electrometrics EMC-35 interference

analyzer was used. For $R = 1 \text{ k}\Omega$, a Hewlett-Packard HP 3400A rms voltmeter was used to measure V_{out} at all frequencies. An HP 3400A rms voltmeter was also used to monitor V_{in} for all frequencies and termination resistances.

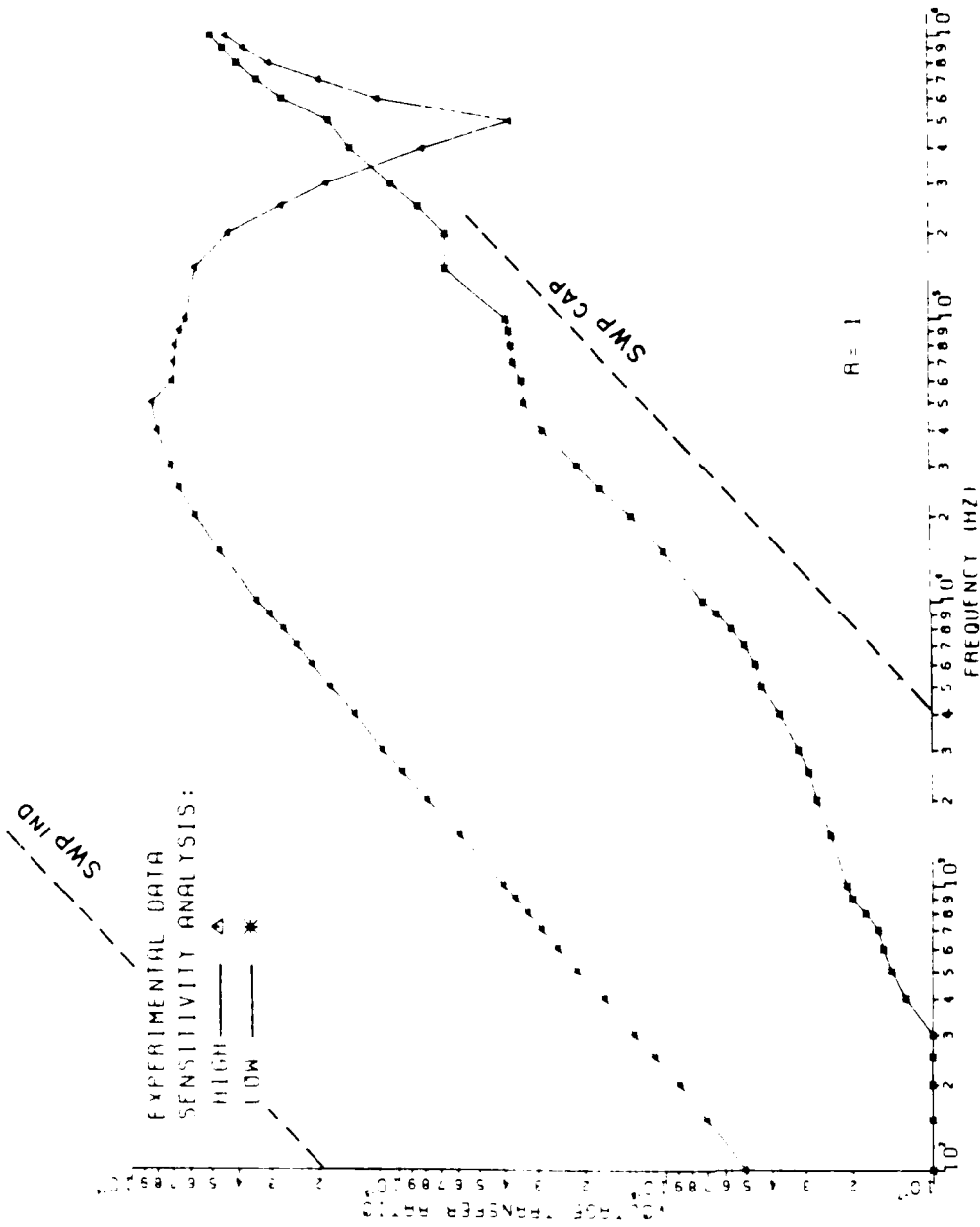
The sensitivity experiment proceeded in the following manner. With load resistances of $R = 1 \Omega$, the EMC-25 was connected to measure V_{out} and was tuned to a frequency of 15 kHz. The right end of the TWP was rotated, no more than 180° , until the maximum reading on the EMC-25 was found. With the TWP fixed at the position of the maximum reading, measurement of the voltage transfer ratio over the entire frequency range was obtained. Then, without disturbing the line, the $R = 1 \Omega$ resistances were removed and replaced with $R = 3 \Omega$ resistances and measurements were again taken over the entire frequency range. The $R = 50 \Omega$ and $R = 1 \text{ k}\Omega$ measurements were taken for the TWP in the position for the maximum reading obtained for $R = 1 \Omega$. It is important to emphasize that the readings for the four different resistance values were obtained without disturbing the TWP from its position of the maximum reading for $R = 1 \Omega$ and $f = 15 \text{ kHz}$. These measurements constitute the high sensitivity readings.

To obtain the low sensitivity readings, the $R = 1 \Omega$ resistances were again attached and the EMC-25 was connected and tuned to 15 kHz. The right end of the TWP was again rotated, no more than 180° , until a minimum response was found on the EMC-25. Measurements for all four impedances, 1Ω , 3Ω , 50Ω

and 1 k Ω , were taken without disturbing the TWP from the position of the minimum reading.

Plots 3-1(a) - 3-1(d) give the experimental results. Note that in Plot 3-1(a), where $R = 1\Omega$, the difference in the voltage transfer ratio between the high readings and the low readings was as large as 35 dB. That is, a slight variation in the line twist - no more than 180° - changed the crosstalk level induced on the TWP by as much as 35 dB! The results for $R = 3$ are given in Plot 3-1(b). For this case, the sensitivity of the line to twist was reduced to a 20 dB difference. Plots 3-1(c) and 3-1(d) give the results for $R = 50\Omega$ and $R = 1k\Omega$, respectively, and show virtually no sensitivity to twist.

In order to provide an explanation for these sensitivity results, let the TWP receptor circuit be replaced by a pair of parallel wires, the straight wire pair or SWP, with terminal configurations remaining the same (Figure 3-2). Assume that the plane containing the two wires of the SWP is parallel to the ground plane, so that both wires are 2 cm above ground the entire length of the line. Like the TWP, assume that the wires of the SWP are separated from each other only by their insulations. Then the per-unit-length inductances between the generator wire and each wire of the SWP, L_{11} and L_{12} , and the per-unit-length capacitances, C_{11} and C_{12} , can be considered [1, 2]. For a sufficiently small frequency, the voltage induced in the SWP due to excitation of the generator



PLOT 3-1(a)

The component of the crosstalk due to electric field coupling to the IWF can be represented by current sources I_1^{HT} and I_2^{HT} . As was the case for the SWP, current sources on the wire which is tied to ground will not contribute to V_{out}^{CAP} . If the IWF is "untwisted", it can be seen that the current sources, I_1^{HT} and I_2^{HT} , tied to the upper wire alternate due to the original twist. These current sources are related to the per-unit-length capacitances of the line by

$$I_1^{HT} = j\omega c_{G1} \ell_{HT} V_{G_{DC}} \quad (3-8a)$$

$$I_2^{HT} = j\omega c_{G2} \ell_{HT} V_{G_{DC}} \quad (3-8b)$$

where ℓ_{HT} is the length of a half-twist of the line. However, since $c_{G1} = c_{G2}$, it follows that $I_1^{HT} = I_2^{HT}$. Then for this configuration, regardless of whether there is an even or an odd number of half-twists,

$$V_{out}^{CAP} = \frac{E_{CR} E_{LR}}{E_{CR} + E_{LR}} j\omega c_{G1} \ell_{HT} N V_{G_{DC}} \quad (3-9)$$

where N is the number of half-twists. Since the total line length L is

$$L = N \ell_{HT} \quad (3-10)$$

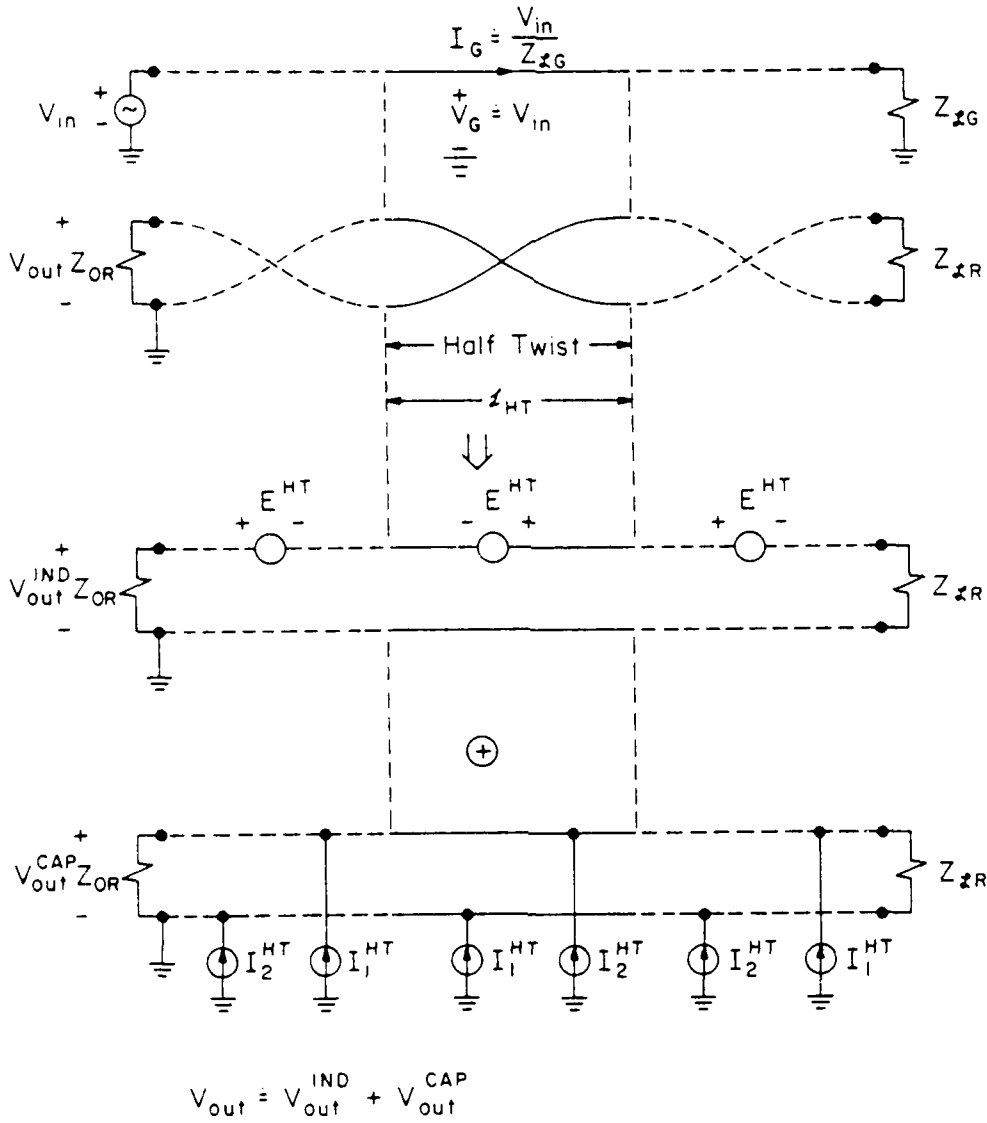


FIGURE 3-4. A-LOW FREQUENCY MODEL OF THE TWISTED PAIR.

the experimental results. This can be seen in Plot 3-2(d), the 1 kHz results.

Now, return to Paul and Jolly's experimental configuration (Figure 3-1), with the TWP as the receptor circuit. A low-frequency model similar to that of the SWP can be obtained (Figure 3-4). E^{HT} represents the EMF induced in a half-twist of the TWP. As mentioned in the Introduction, the EMF is a result of the time rate-of-change of the magnetic flux, Ψ , penetrating the loop. The magnetic flux is produced by the generator wire current. The mutual inductance, \mathcal{L}^{HT} , between the generator wire and the loop can be found by

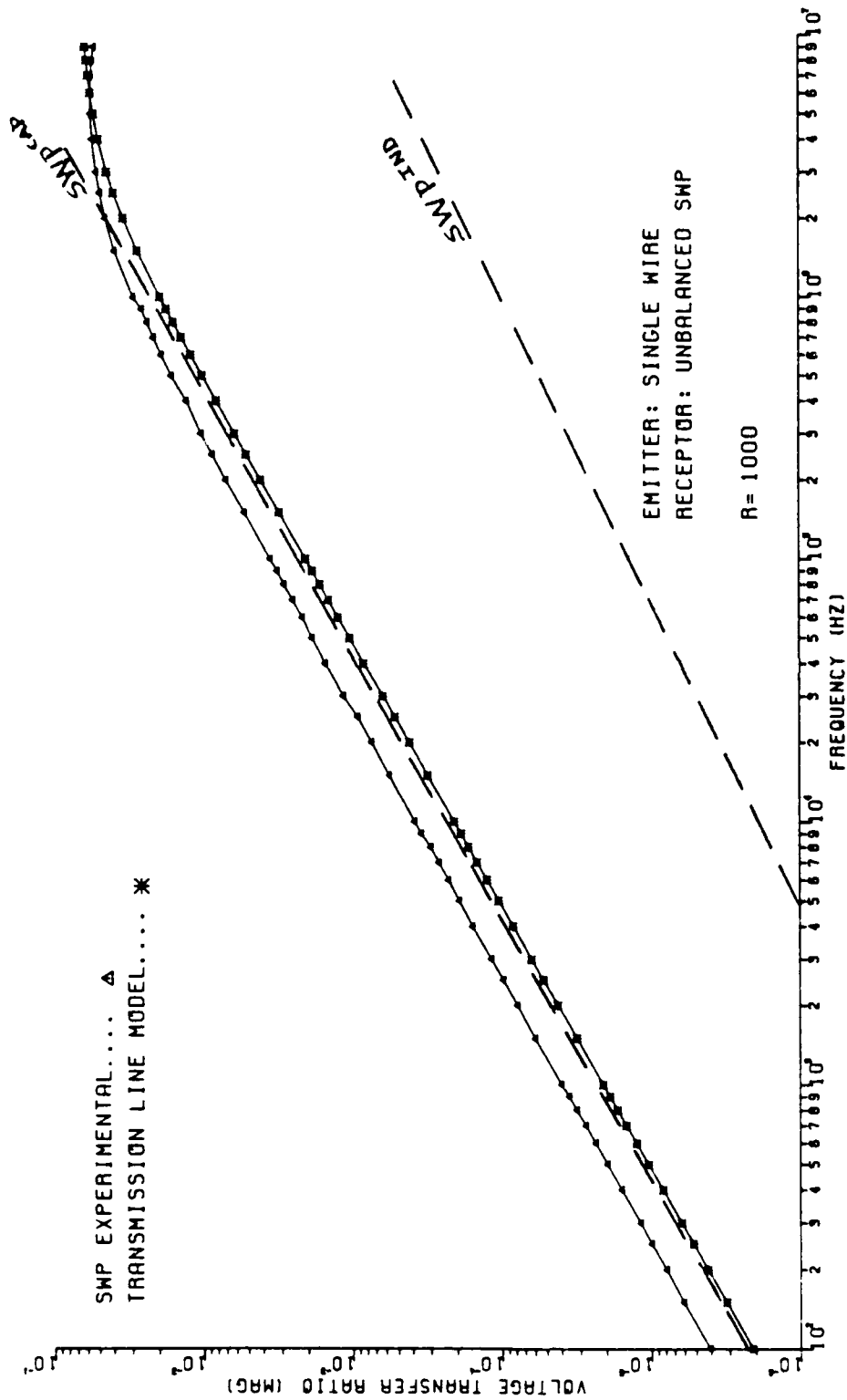
$$\mathcal{L}^{HT} = \frac{\Psi}{I_{G_{DC}}} \quad (3-5)$$

Then E^{HT} is given by

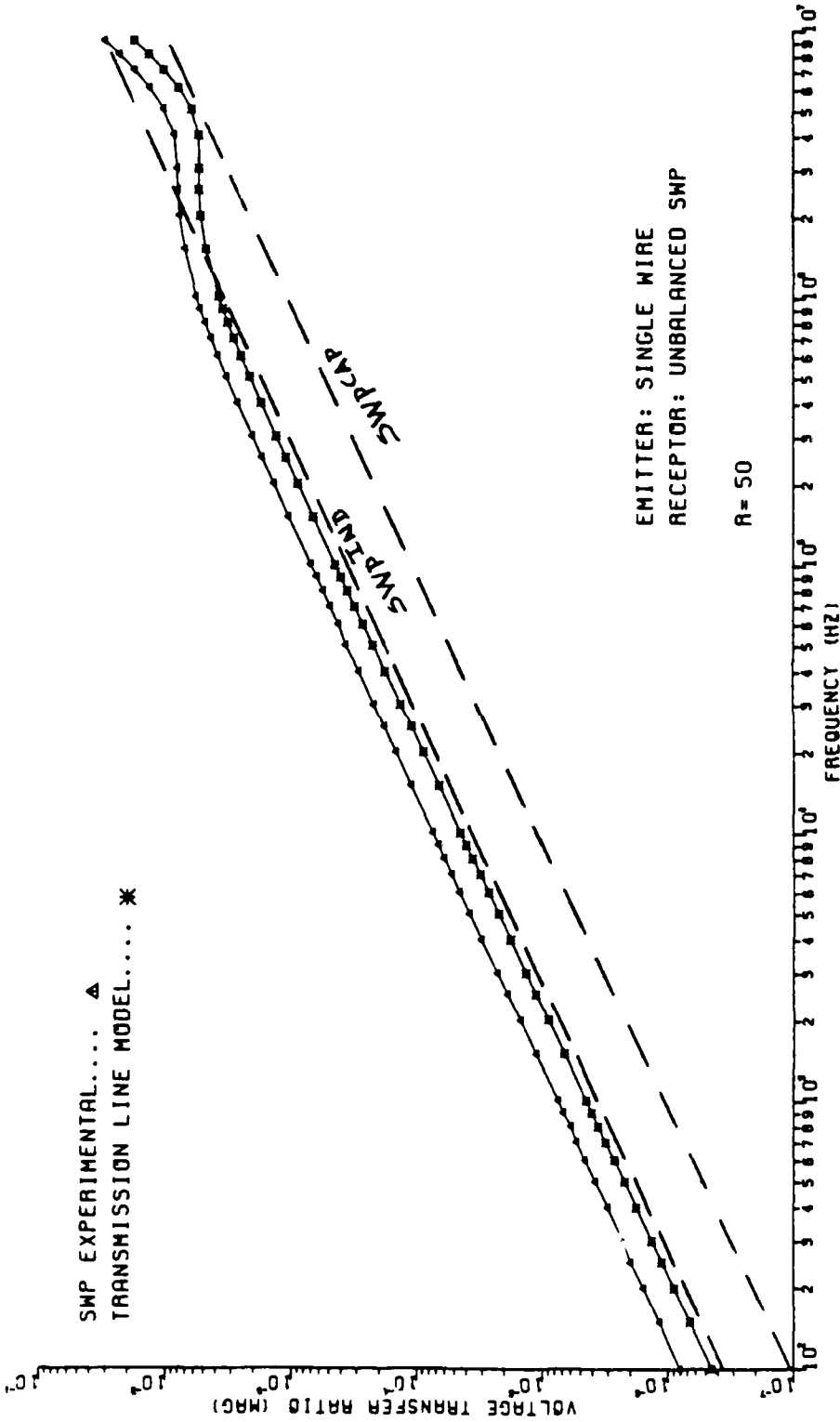
$$E^{HT} = j\omega \mathcal{L}^{HT} I_{G_{DC}} \quad (3-6)$$

Now, "untwist" the TWP (Figure 3-4). If the TWP consists of an even number of loops, the net EMF is zero. That is, V_{out}^{IND} is equal to zero. For an odd number of half-twists, V_{out}^{IND} is given by

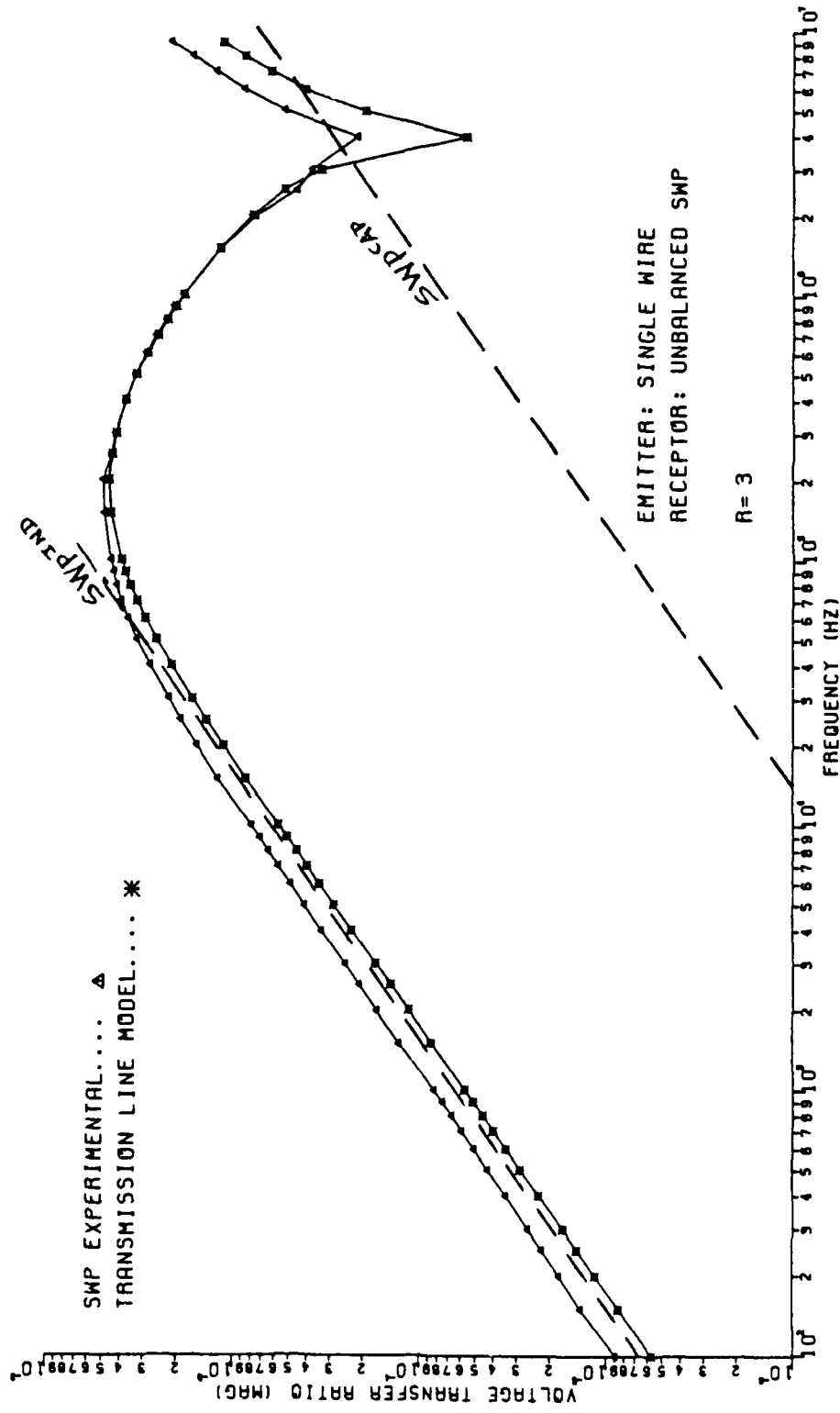
$$V_{out}^{IND} = \frac{\mathcal{E}_{OR}}{\mathcal{E}_{OR} + \mathcal{E}_{LF}} j\omega \mathcal{L}^{HT} I_{G_{DC}} \quad (3-7)$$



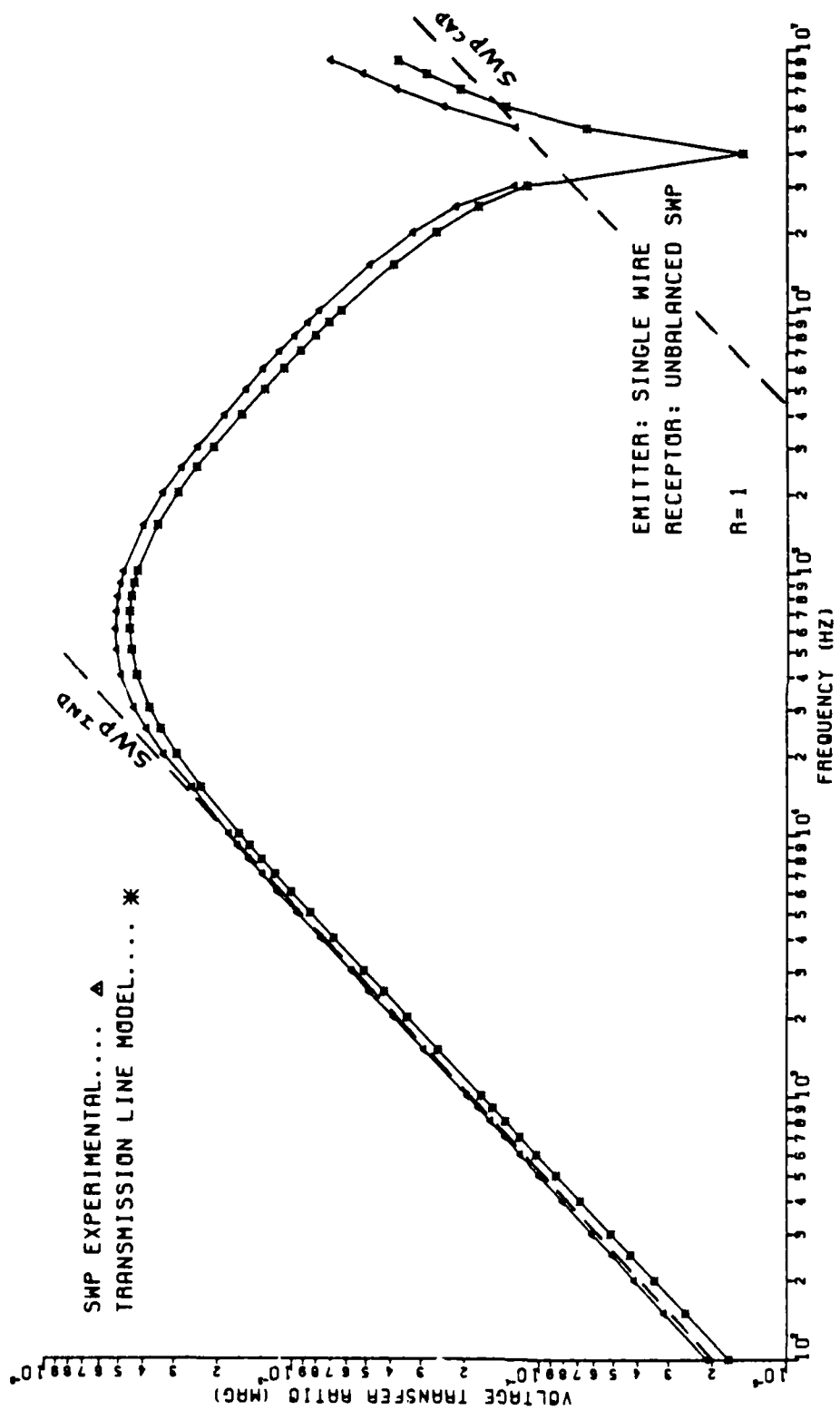
PLOT 3-2(d)



PLOT 3-2(c)



PLOT 3-2(b)



PLOT 3-2(a)

In order to evaluate this low-frequency prediction of the crosstalk, an experiment was performed similar to that of Paul and Jolly's, only an SWP receptor circuit was used instead of a TWP receptor circuit. Also, the line length was 4.674m. The SWP experimental results are given in Plots 3-2(a) - 3-2(d). The values obtained for V_{out}^{IND} and V_{out}^{CAP} as defined by Equations 3-2 through analysis of the low-frequency model have been added to the plots. Also, a computer program was written to calculate the voltage transfer ratio for the SWP via a transmission line model, which does not require that the frequency be small. The transmission line model assumed perfect conductors and neglected the dielectric insulation of the wire. This transmission line model is explained in Appendix A. The results of the transmission line model are given in Plots 3-2(a) - 3-2(d). As can be seen, the low-frequency model and the transmission line model provide adequate predictions of the crosstalk to the SWP. Some error is probably due to the fact that neither model accounts for lossy conductors. This is particularly important for the low impedance case, $R = 1\Omega$. Also, both models assume a homogeneous media. That is, they neglect the presence of the wire insulation. Although the permeability of the wires' insulation is close to that of free space, the permittivity is not. Both models assume the characteristics of free space. Since the relative permittivity of the insulation provides the only significant error in this assumption, it makes sense then when the capacitive-coupling contribution is dominant, the predictions will be less than

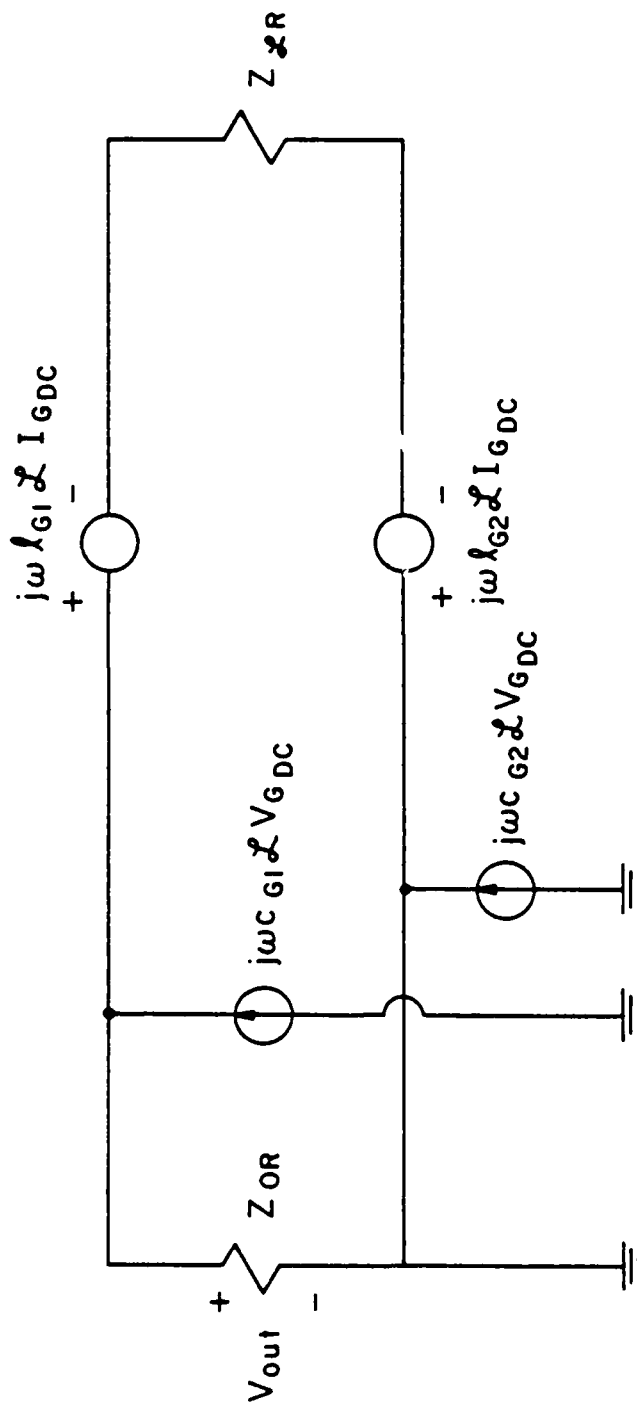


FIGURE 3-3. THE UNBALANCED SWP LOW-FREQUENCY APPROXIMATION.

wire can be separated into inductive- and capacitive-coupling contributions, similar to the three-conductor line case discussed in Chapter 2, and can likewise be represented by a low-frequency circuit (Figure 3-3). Then

$$V_{out}^{IND} = \frac{z_{OR}}{z_{OR} + \frac{z}{L}R} j \omega (\mathcal{L}_{G1} - \mathcal{L}_{G2}) \mathcal{L} I_{G_{DC}} \quad (3-2a)$$

and

$$V_{out}^{CAP} = \frac{z_{OR} \frac{z}{L}R}{z_{OR} + \frac{z}{L}R} j \omega c_{G1} \mathcal{L} V_{G_{DC}} \quad (3-2b)$$

$V_{G_{DC}}$ and $I_{G_{DC}}$ are the dc values of the generator voltage and current:

$$V_{G_{DC}} = V_{in} \quad (3-3a)$$

$$I_{G_{DC}} = \frac{V_{in}}{\frac{z}{L}G} \quad (3-3b)$$

Notice that the current source attached to the grounded wire of the SWP does not affect V_{out}^{CAP} . The output voltage, V_{out} , of the SWP is given by

$$V_{out} = V_{out}^{IND} + V_{out}^{CAP} \quad (3-4)$$

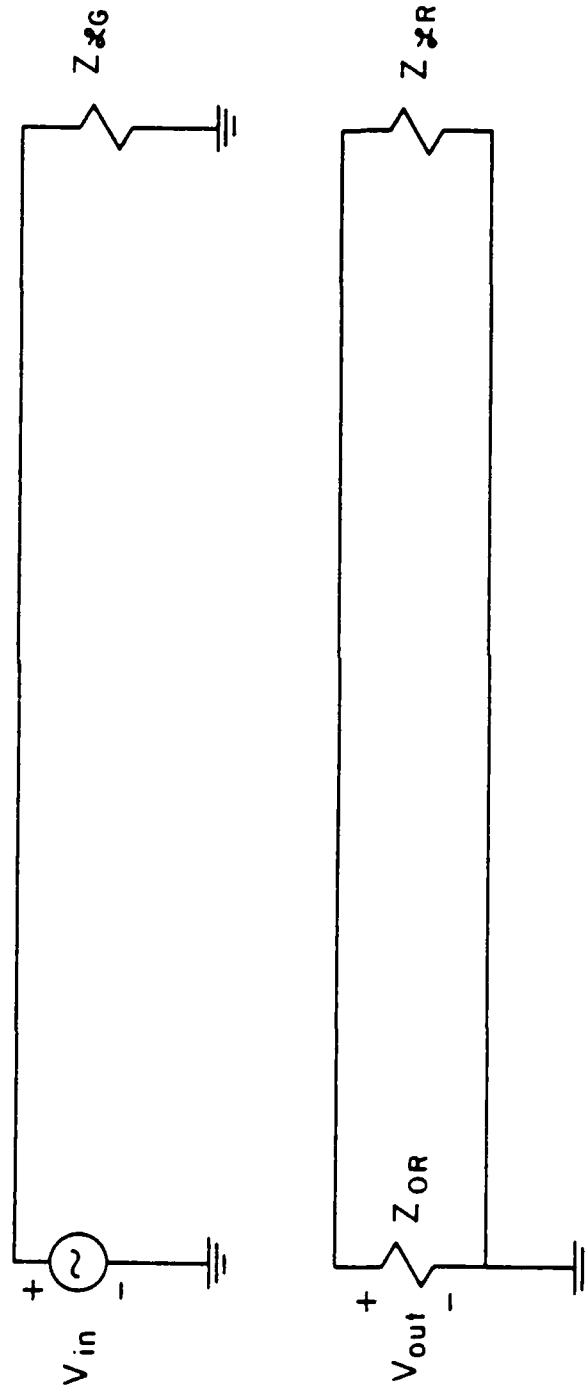
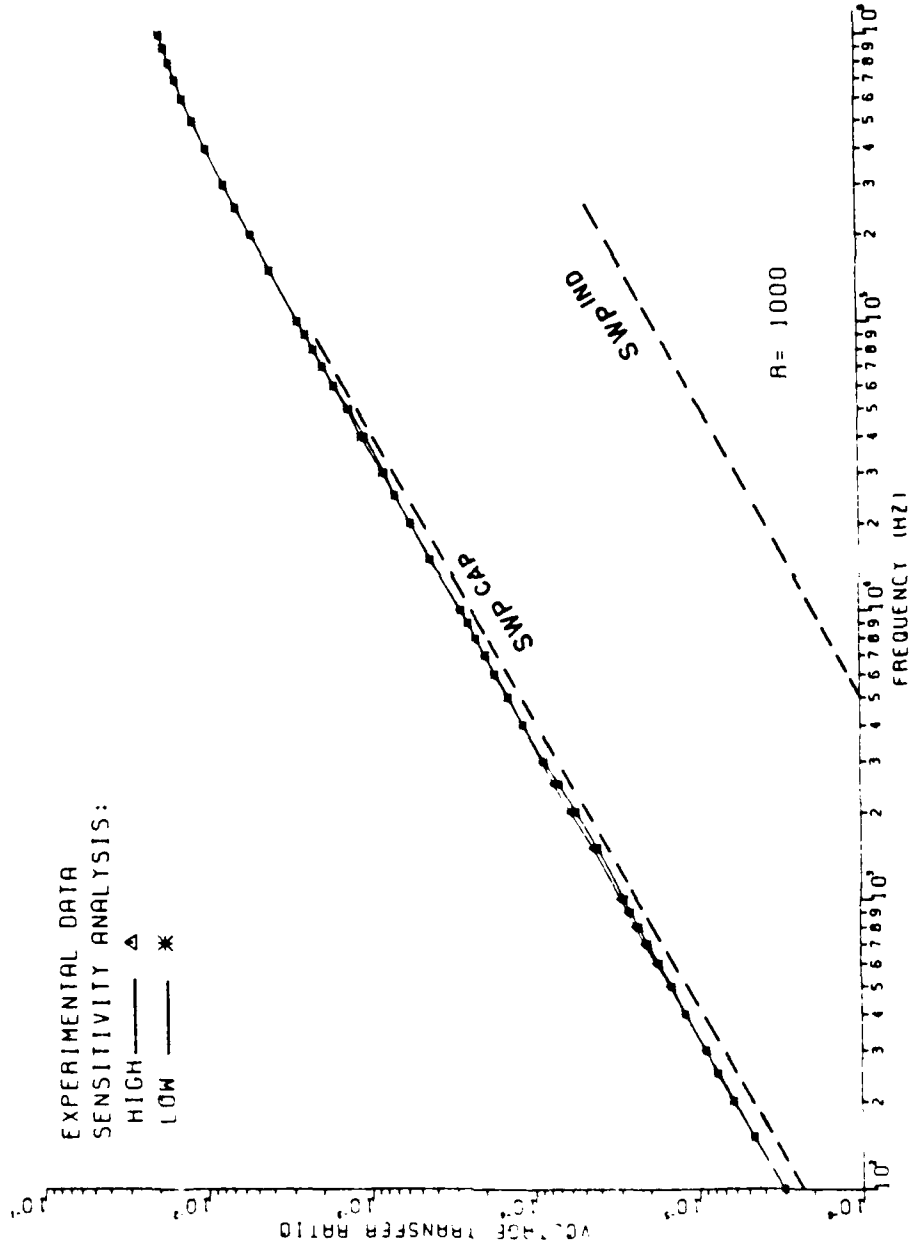
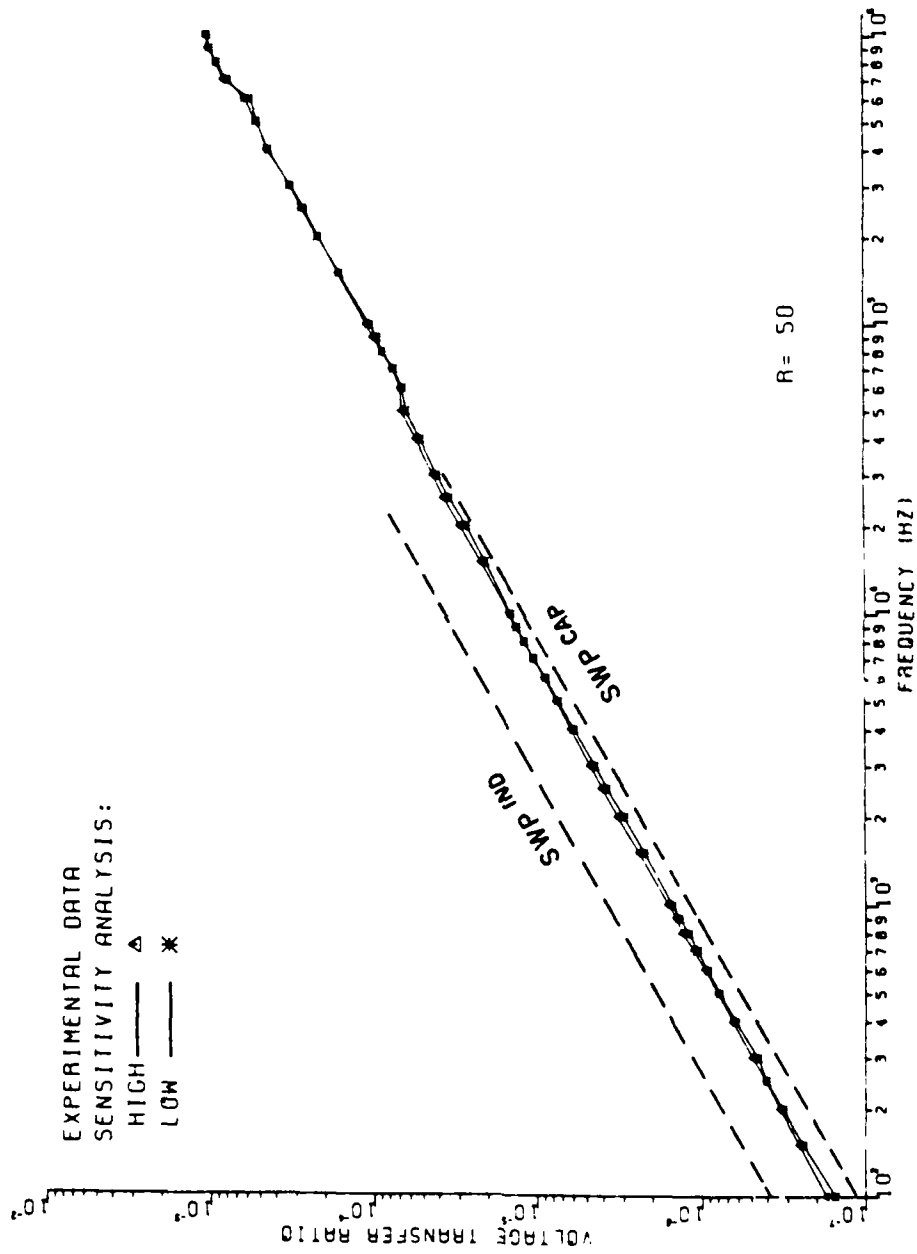


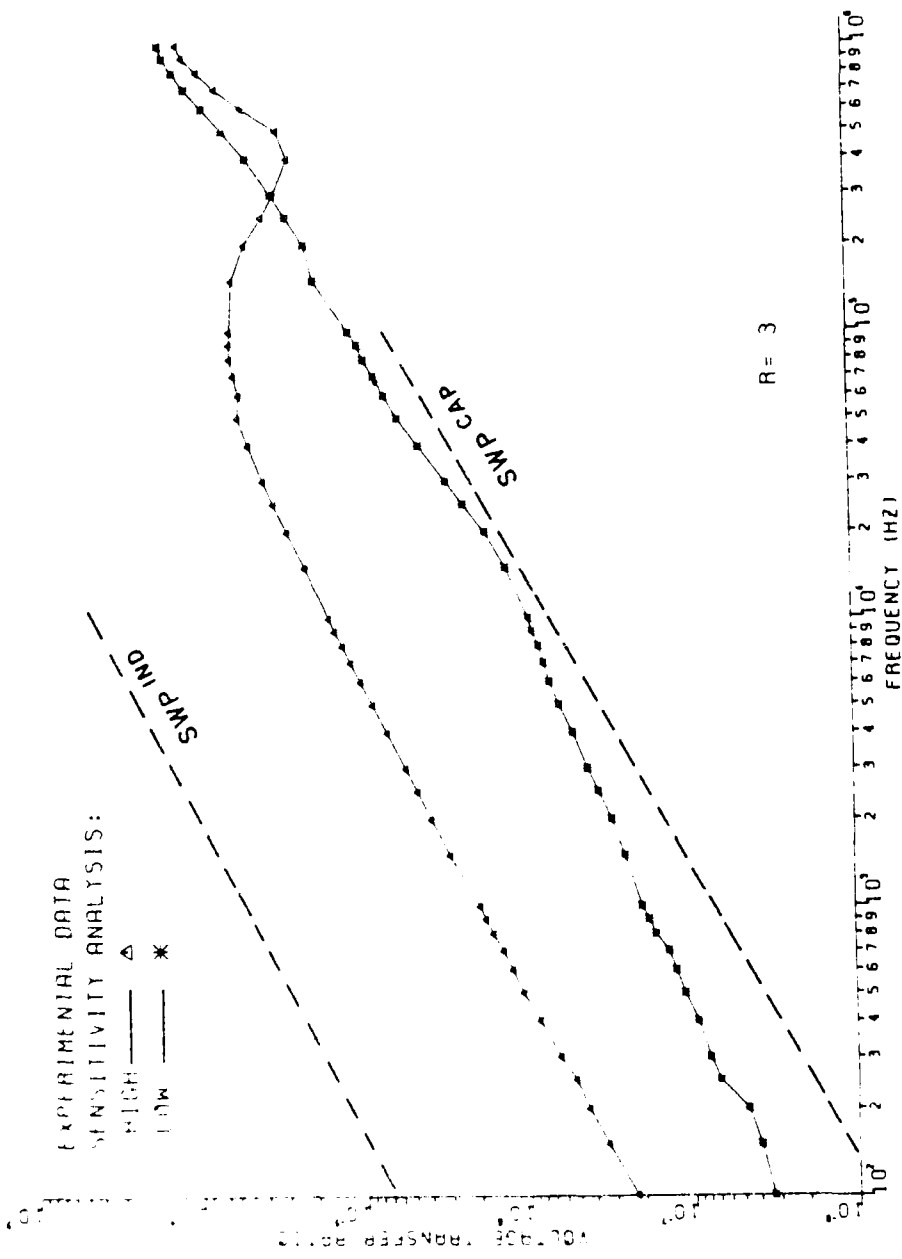
FIGURE 3-2. THE SINGLE WIRE TO UNBALANCED SWP CONFIGURATION.



PLOT 3-1(d)



PLOT 3-1(c)



PLOT 3-1(b)

V_{out}^{CAP} can be written as

$$V_{out}^{CAP} = \frac{E_{OR} E_{LR}}{E_{OR} + E_{LR}} j \omega c_{G1} L V_{GDC} \quad (3-11)$$

which is the same result for capacitive-coupling which was obtained for V_{out}^{CAP} with the SWP as the receptor circuit. The voltage V_{out} is the sum of the inductive-coupling contribution and the capacitive-coupling contribution.

$$V_{out} = V_{out}^{IND} + V_{out}^{CAP} \quad (3-12)$$

In order to differentiate between the SWP and the TWP results, let Equations 3-4 and 3-12 be written, respectively, as

$$SWP = SWP^{IND} + SWP^{CAP} \quad (3-13a)$$

and

$$TWP = TWP^{IND} + TWP^{CAP} \quad (3-13b)$$

From the explanation given above, note that

$$SWP^{IND} \gg TWP^{IND} \quad (3-14a)$$

and

$$SWP^{CAP} = TWP^{CAP} \quad (3-14b)$$

Now, to explain the sensitivity results, note that, for an even number of half-twists, twisting the wires drops the total crosstalk level from the sum of the two SWP coupling contributions to the capacitive-coupling contribution only; the inductive coupling is (ideally) reduced to zero by the twist. For an odd number of half-twists, the TWP crosstalk level is that same capacitive-coupling contribution plus the inductive-coupling contribution due to only one half-twist. Thus for the case of low-impedance loads, such as 1Ω and 3Ω , where $SWP^{IND} \gg SWP^{CAP}$, twisting the wires drops the crosstalk levels significantly. However, since the inductive-coupling contribution of one half-twist of the TWP is, by the above analysis, assumed to be greater than TWP^{CAP} ($=SWP^{CAP}$), the crosstalk level of the line shows a sensitivity to minor variations in line twist due to the changing inductive-coupling contribution. For these low-impedance loads, the low readings are equal to TWP^{CAP} ($=SWP^{CAP}$). The high sensitivity readings are equal to the sum of TWP^{IND} , due to one half-twist, and TWP^{CAP} .

For the case of high-impedance loads, such as $R = 50\Omega$, twisting the wires, for an odd or an even number of half-twists, drops V_{out}^{IND} to such an extent that TWP^{CAP} is greater than TWP^{IND} . Since TWP^{CAP} for this configuration is apparently not dependent on line twist, the crosstalk level, represented by the voltage transfer ratio, will show no sensitivity to variation in line twist. For the very high-impedance loads of $1\text{ k}\Omega$, SWP^{CAP} is greater than SWP^{IND} , so although twisting

the wires drops the inductive-coupling contribution, the crosstalk level remains at that due to SWP^{CAP} . Of course, in this case, there is no sensitivity to line twist.

These concepts of the determination of the crosstalk levels are given graphically in Figure 3-5. Also, the actual values of SWP^{IND} and SWP^{CAP} , calculated using Equations 3-2, have been added to Plots 3-1 to give additional clarity to the concepts described above.

The sensitivity to line twist exhibited by the low-impedance loads in the experiments of Paul and Jolly leads to a problem in the development of a model to predict the crosstalk levels of TWP's. Since, in a practical situation, the fact that there is an even or an odd number of half-twists is not taken into account when installing a TWP, it is not possible to predict the inductive-coupling contribution. It seems that, for the low-impedance loads, the best that could be hoped for would be a model which could determine upper bounds on TWP crosstalk levels.

The theory developed by Paul and Jolly to explain the sensitivity found in their TWP receptor circuit experiment will be applied later in this report when other TWP configurations are investigated. Specifically, the sensitivity to variations in line twist for low-impedance loads is again observed for the case when both receptor and generator circuits are TWP's.

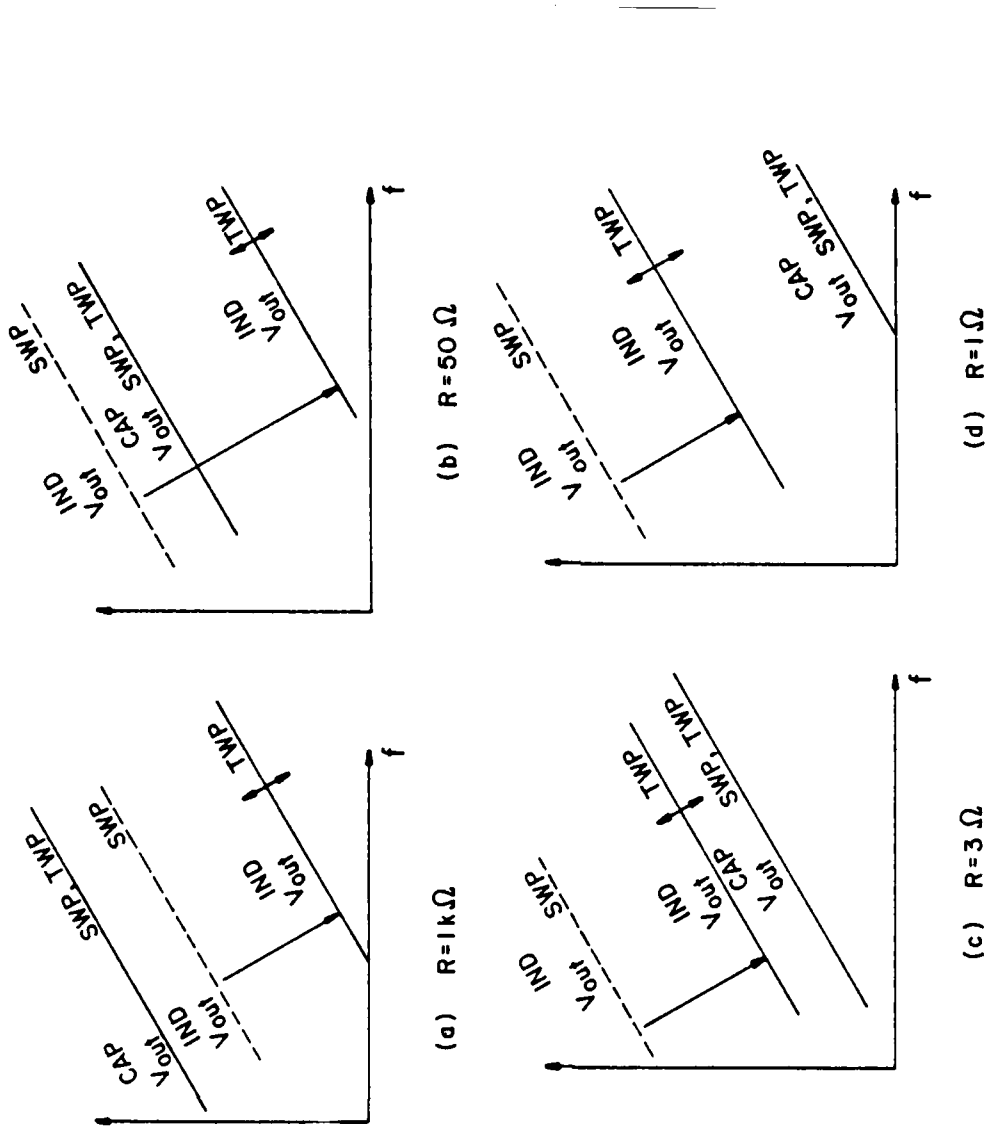


FIGURE 3-5. AN EXPLANATION OF THE SENSITIVITY TO TWIST. SWP DENOTES STRAIGHT WIRE (UNTWISTED) PAIR AND TWP DENOTES THE TWISTED PAIR.

Also, when the case of the single wire generator circuit and balanced TWP receptor circuit is investigated, the sensitivity to line twist is expected for all terminal impedances.

CHAPTER IV

THE UNBALANCED TWISTED-PAIR GENERATOR AND RECEPTOR CIRCUITS

Chapter III described the work of C. R. Paul and M. B. Jolly where they examined the crosstalk into an unbalanced twisted wire pair (TWP) receptor circuit caused by the excitation of a single wire with ground return generator circuit. With this configuration, they found that for certain low impedance loads the crosstalk level in the TWP was very sensitive to slight variations in line twist. This sensitivity was explained through the concept that inductive coupling is dependent on the amount of twist in the line whereas the capacitive coupling appeared to be insensitive to twist because of the terminal configurations. In this chapter, the configuration which consists of an unbalanced TWP as the generator circuit as well as an unbalanced TWP as the receptor circuit is examined. It is expected that this configuration will show a similar sensitivity to variation in the receptor TWP twist.

The experiment which was performed in order to analyze this TWP to TWP crosstalk was identical to the experiment conducted by Paul and Jolly [12] as much as possible. For the TWP to TWP experiment (Figure 4-1), the receptor and generator circuits were suspended 2 cm above an aluminum ground plane and were separated from each other by 2 cm. The wire positions were held constant through the use of

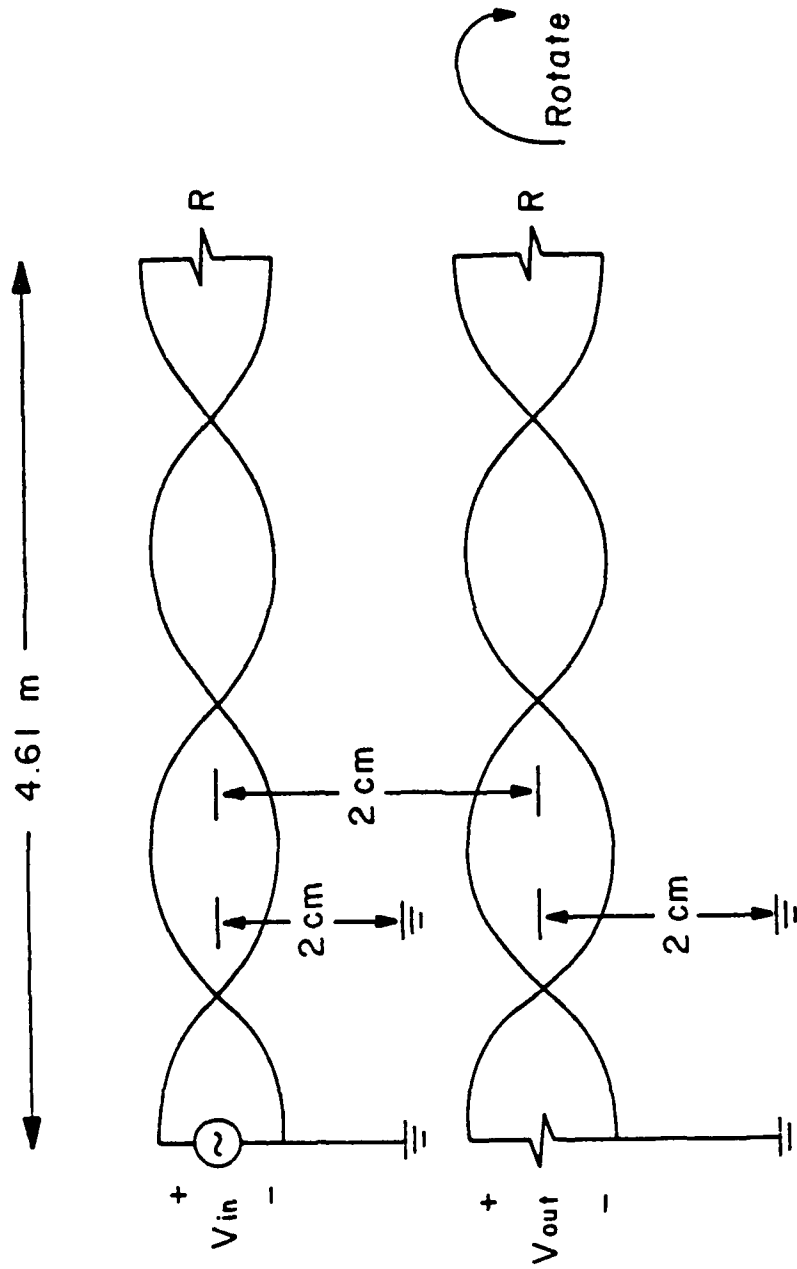


FIGURE 4-1. THE TWP TO TWP EXPERIMENT.

styrofoam blocks. All wires were #22 gauge, stranded, so that the minimum center-to-center separation of the wires of either generator or receptor TWP was 57.3 mils. The line length for this experiment was 4.61 m. The generator TWP contained 95 full twists and the receptor TWP contained 100 full twists.

As was the case for Paul and Jolly's experiment, identical resistances were used for all loads and the experiment was conducted for four values of resistance; $R = 1\ \Omega$, $3\ \Omega$, $50\ \Omega$ and $1\ k\Omega$. However, in this experiment both generator and receptor circuits were TWP's which were unbalanced with respect to their terminal configurations. A sinusoidal generator was attached between the two wires of the generator TWP at the left end of the line and was denoted V_{in} . One wire at the left end of the generator circuit was connected to ground. The right end of the generator circuit was ungrounded. The right end of the receptor circuit was also ungrounded and one wire at the left end of the receptor TWP was connected to ground. The voltage across the left end termination of the receptor TWP was referred to as V_{out} . The voltage transfer ratio was again defined by

$$\text{voltage transfer ratio} = \frac{V_{out}}{V_{in}} \quad (4-1)$$

Measurements were taken in the frequency range of 1 kHz to 100 kHz in steps of 1, 1.5, 2, 2.5, 3, 4, 5, 6, 7,

8, 9, for each decade of frequency. The measurement equipment and technique was the same as that of Paul and Jolly as described in Chapter III except that an HP3400A rms voltmeter was used to measure V_{out} whenever the signal was large enough in the frequency range 50 kHz to 1 MHz. Also, V_{out} and V_{in} were both determined by an HP8405A Vector Voltmeter for all resistance terminations at frequencies above 1 MHz.

The experiment was first performed with both generator and receptor circuits as straight wire pairs (Figure 4-2). The SWP's were placed in a horizontal position, so that the plane containing the four wires was parallel to the ground plane. The two wires of each SWP were separated only by their insulation, so their center-to-center separation, Δ , was 57.3 mils. Measurements of the voltage transfer ratio were taken over the entire frequency range for all four values of resistance. The results are given in Plots 4-1(a) - (d).

For sufficiently small frequencies, the crosstalk induced in the receptor SWP due to excitation of the generator SWP can be modeled using the concepts of inductive-coupling and capacitive-coupling described previously. For this SWP to SWP case, the per-unit-length inductance matrix is

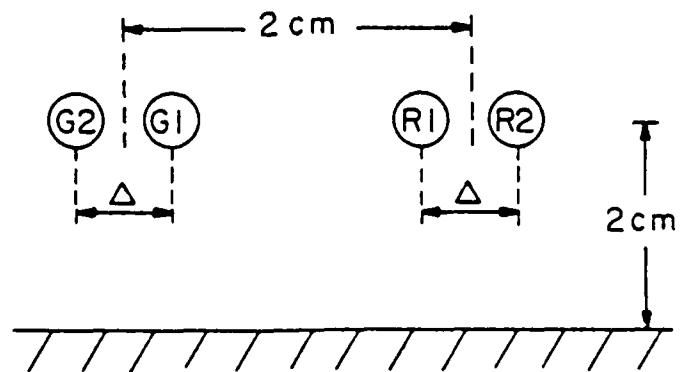
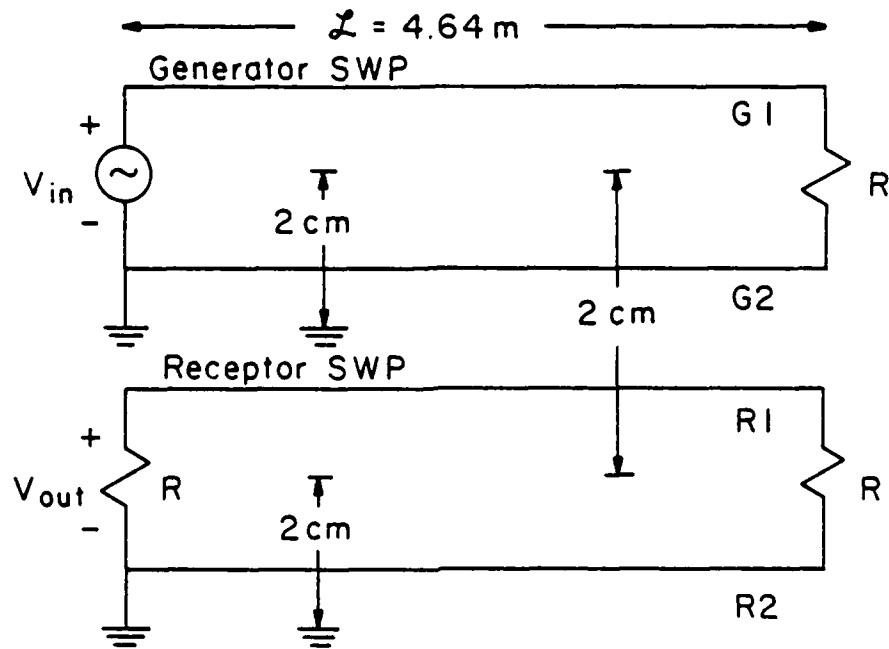
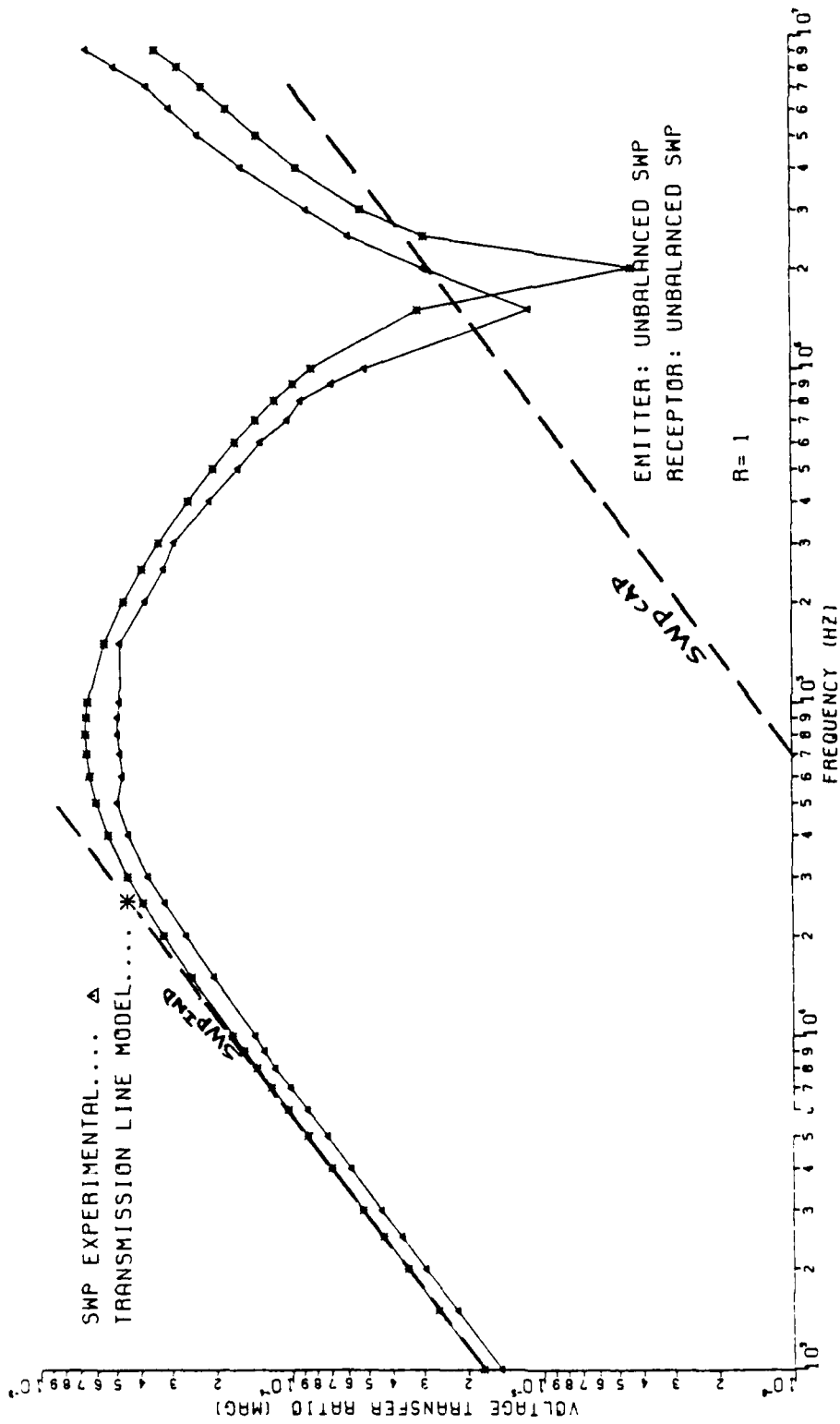
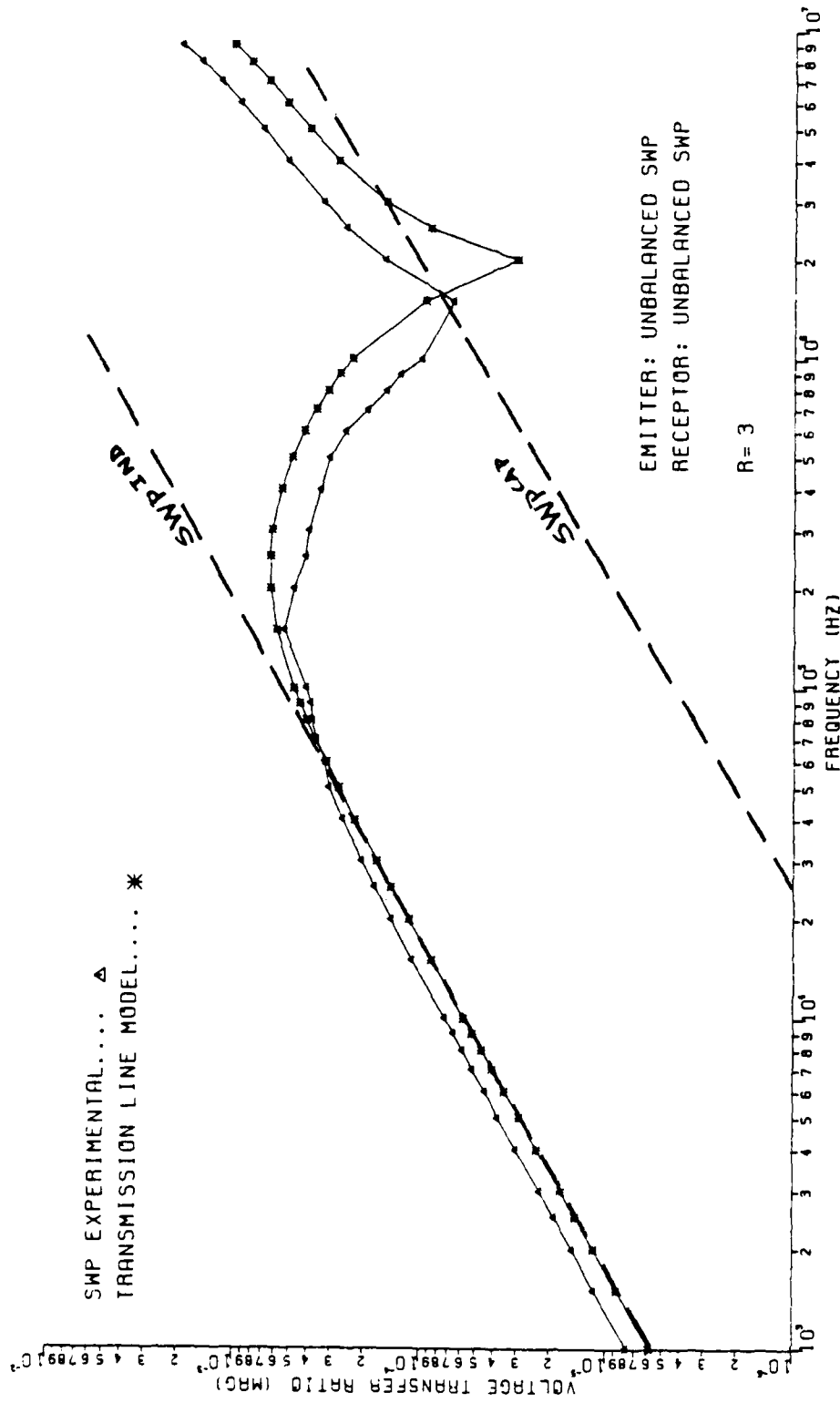


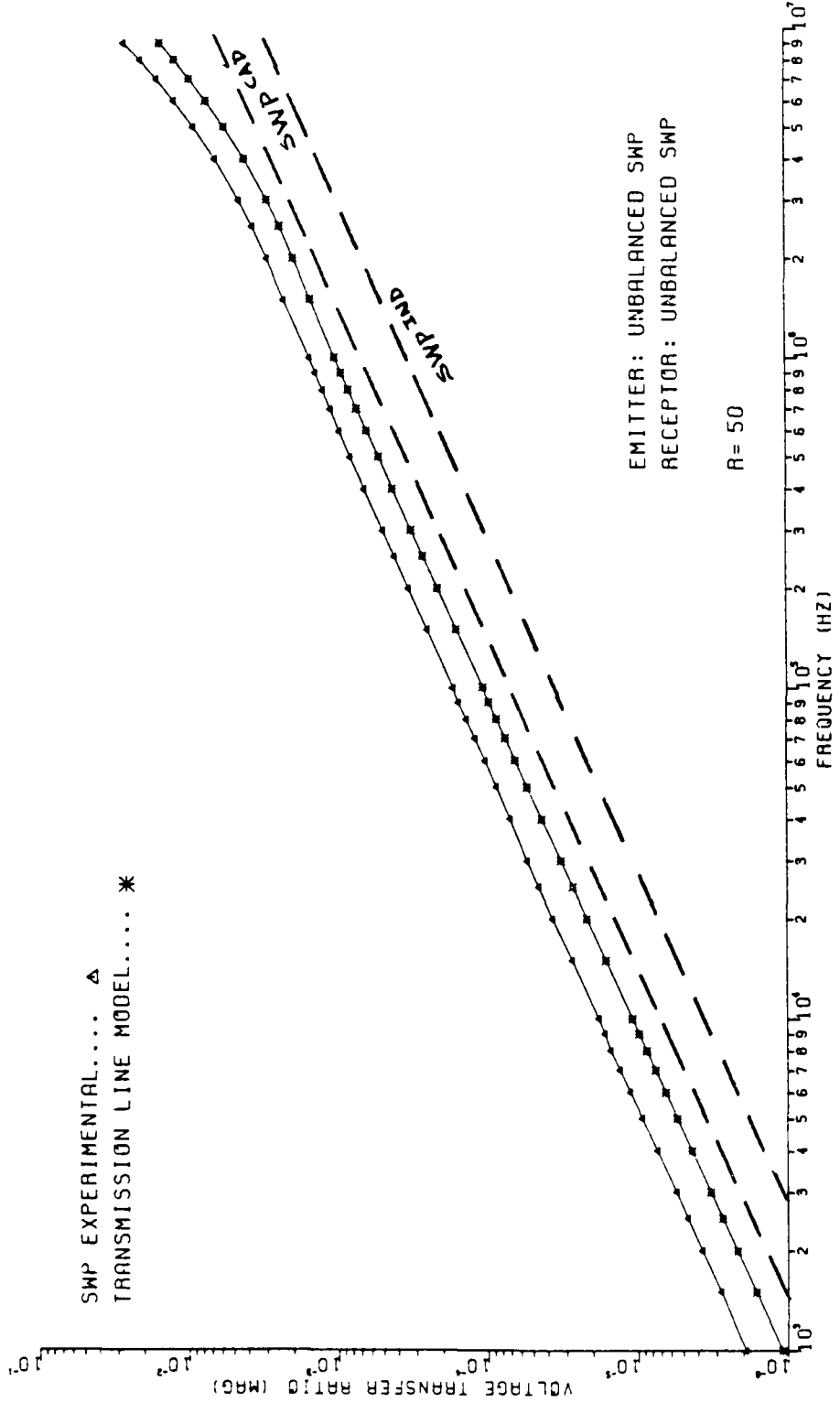
FIGURE 4-2. THE SWP TO SWP EXPERIMENT.
(a) LONGITUDINAL VIEW.
(b) CROSS-SECTIONAL VIEW.



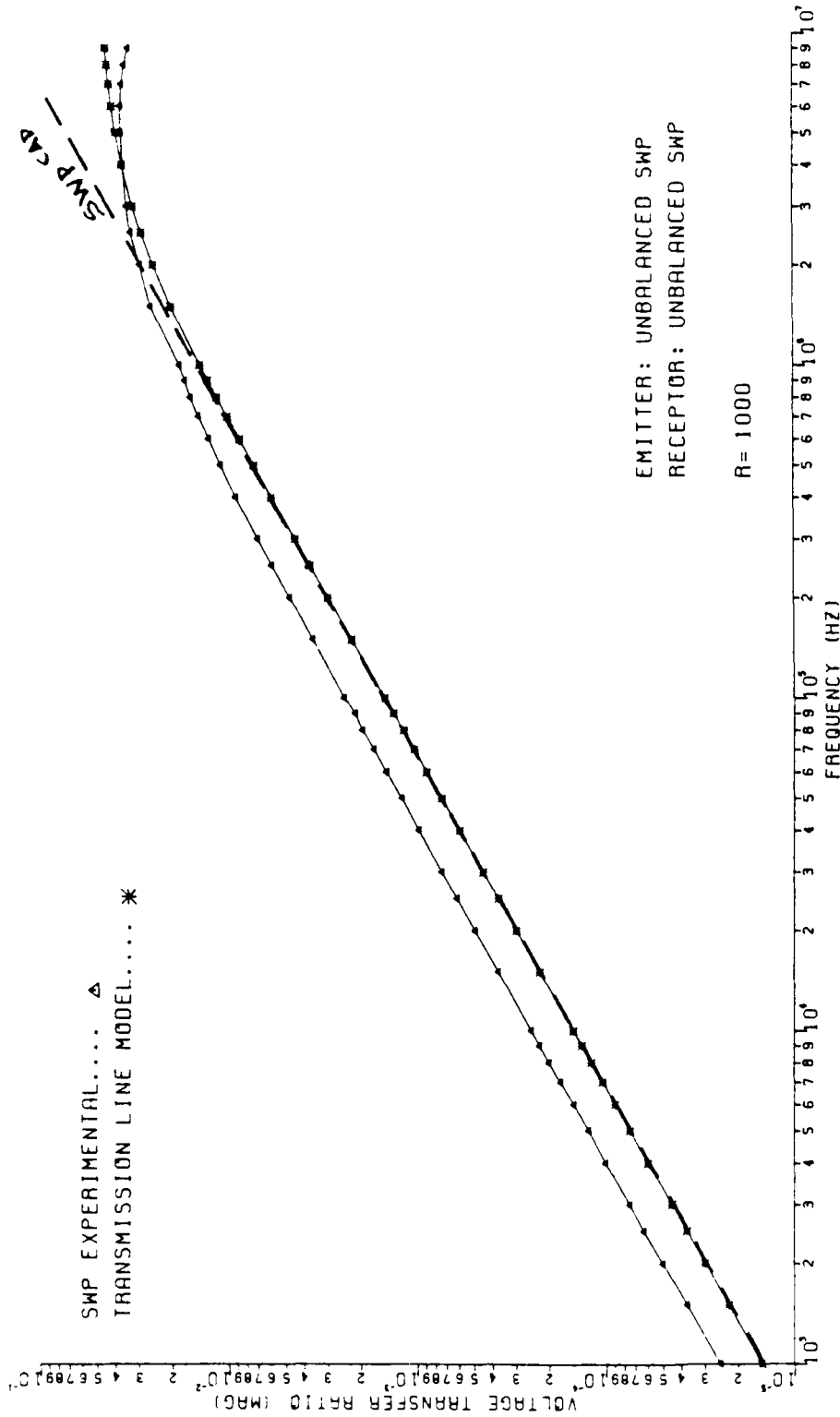
PLOT 4-1(a)



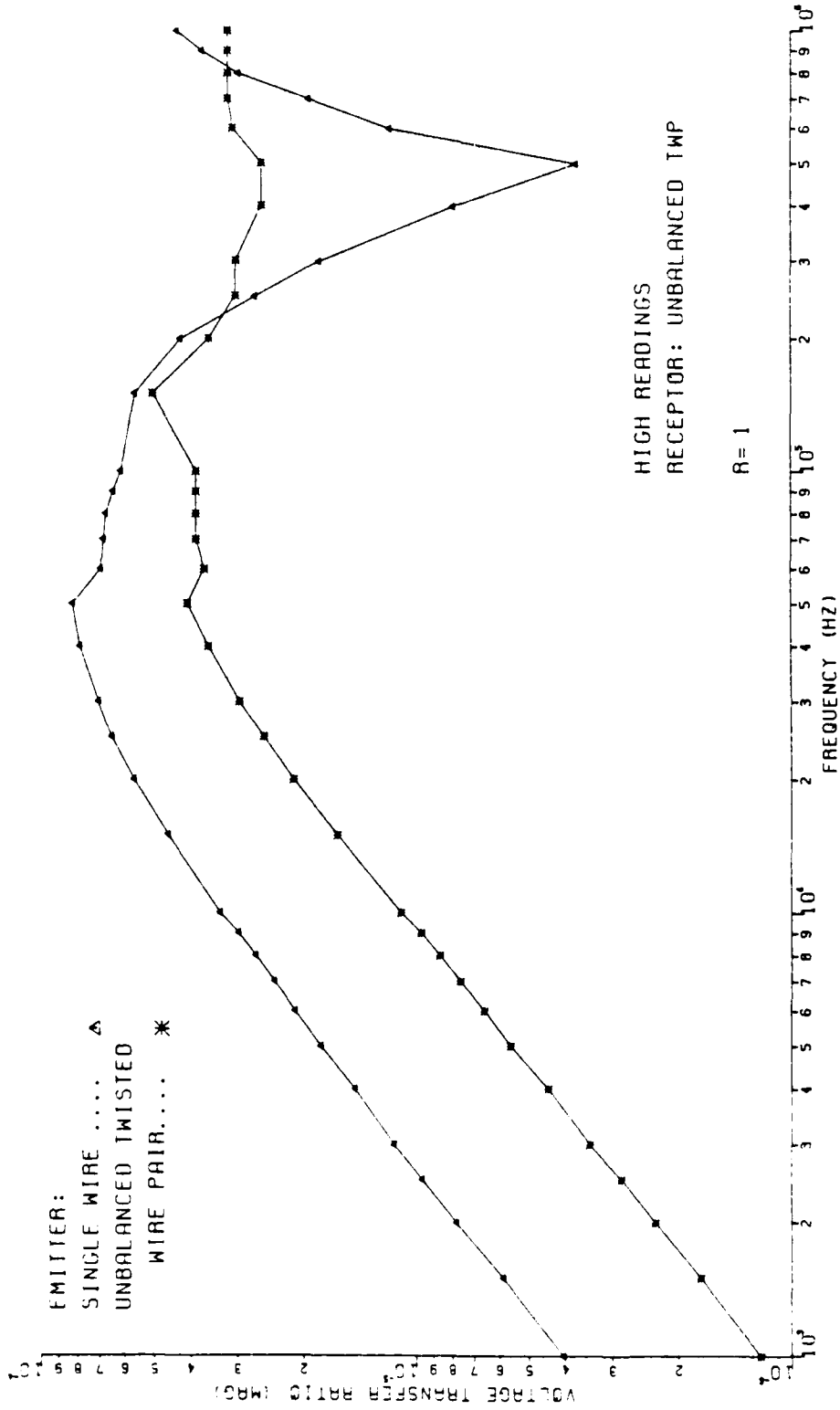
PLOT 4-1(b)



PLOT 4-1(c)



PLOT 4-1(d)



PLOT 4-3(a)

In order to emphasize the concepts explained above, the results of Equations 4-4, which define SWP^{IND} and SWP^{CAP} , have been added to Plots 4-2. It should be noted that it was very difficult to find the minimum response for $R = 1\Omega$. Subsequently, the experiment was set up again and the minimum response was again found. Readings were taken and it was found that these minimum readings were better predicted by the capacitive-coupling floor. However, in order that the line be exactly the same as for the maximum readings (except for the slight variation in line twist) the original minimum readings are the ones plotted.

In an effort to evaluate the effectiveness of using a TWP generator circuit, the experimental measurements of this chapter have been plotted against those of Paul and Jolly's experiment. The comparison of the high readings is given in Plots 4-3(a) - 4-3(d). The low readings are given in Plots 4-4(a) - 4-4(d). Although the results obtained using a TWP emitter were for the most part lower than those obtained using a single wire with ground return, there was not a significant reduction in crosstalk.

This lack of a significant reduction in crosstalk is somewhat surprising. From an intuitive point of view, it would seem that the use of the SWP generator circuit, where the return generator current travels along a wire in close proximity to the wire on which the current was sent, would provide a greater reduction in inductive-coupling than when

The sensitivity results can be explained in the following manner. For the low-impedance loads, $R = 1\Omega$ and $R = 3\Omega$, SWP^{IND} is greater than SWP^{CAP} . When the receptor and generator wires are twisted, the inductive-coupling contribution is dropped to TWP^{IND} . Thus for an even number of half-twists, where $TWP^{IND} = 0$, the total crosstalk level is determined by TWP^{CAP} ($=SWP^{CAP}$). For an odd number of half-twists, the crosstalk level is the sum of TWP^{IND} , which is determined by one half-twist of the line only, and TWP^{CAP} ($=SWP^{CAP}$). So if TWP^{IND} is greater than or equal to TWP^{CAP} ($=SWP^{CAP}$), it would be sensible to assume that the high sensitivity readings were taken when the TWP consisted of an odd number of half-twists. The low sensitivity readings would then have been taken when the TWP consisted of an even number of half-twists, so that the crosstalk level was determined by the capacitive-coupling floor.

For the case of the high-impedance loads, $R = 50\Omega$ and $R = 1\text{ k}\Omega$, notice that SWP^{CAP} is greater than SWP^{IND} . The output voltage for the SWP is effectively determined by SWP^{CAP} for both of these impedances. Twisting the wires further reduces the inductive-coupling contribution to the point where it is very much less than the capacitive-coupling contribution to the output voltage of the TWP. Since the capacitive-coupling for this configuration is assumed to be insensitive to the amount of twist in the line, these high-impedance loads show no sensitivity to line twist.

receptor TWP, V_{out}^{IND} is equal to zero. For an odd number of loops in the receptor TWP, V_{out}^{IND} is equal to the amount of inductive coupling to one half-twist of the line only. Therefore, if V_{out}^{IND} for the TWP configuration is written TWP^{IND} ,

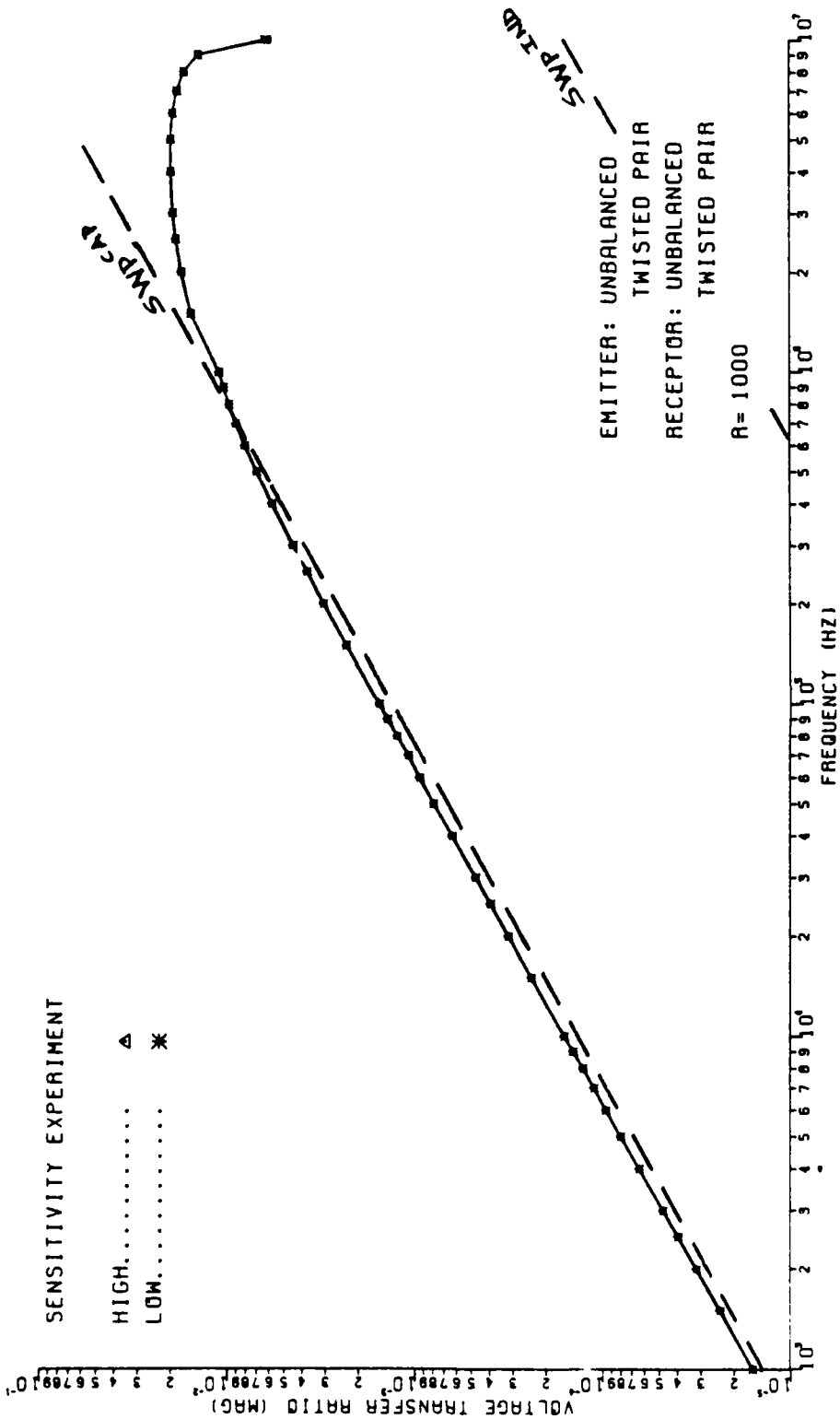
$$SWP^{IND} \gg TWP^{IND} \quad (4-7)$$

The capacitive-coupling contribution of the TWP to TWP configuration is approximately the same as that for the SWP to SWP configuration. Since R2 is grounded, any current sources attached to R2 will not affect TWP^{CAP} (or SWP^{CAP}). Also, V_{G2} is equal to zero, so any current source dependent on V_{G2} does not affect TWP^{CAP} (or SWP^{CAP}). Therefore, if the TWP is "untwisted", it is found that the current sources which determine TWP^{CAP} alternate with each half-twist between that dependent on c_{G1R1} and c_{G1R2} . Since c_{G1R1} is approximately equal to c_{G1R2} , then the capacitive-coupling contribution to the crosstalk for the TWP is approximately the same as that for the SWP (Equation 4-4 b), so

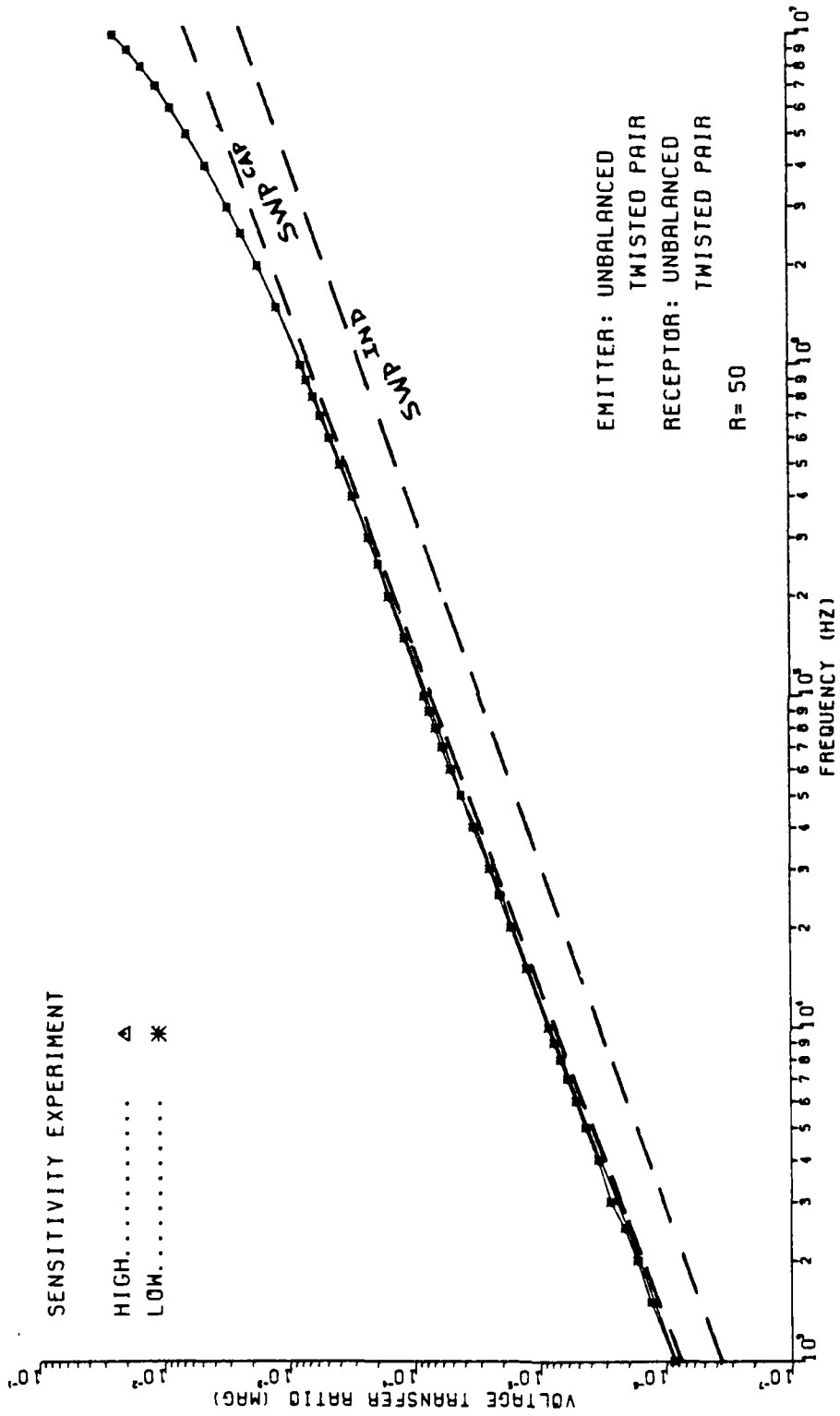
$$SWP^{CAP} \doteq TWP^{CAP} \quad (4-8)$$

The output voltage for the receptor TWP is given by

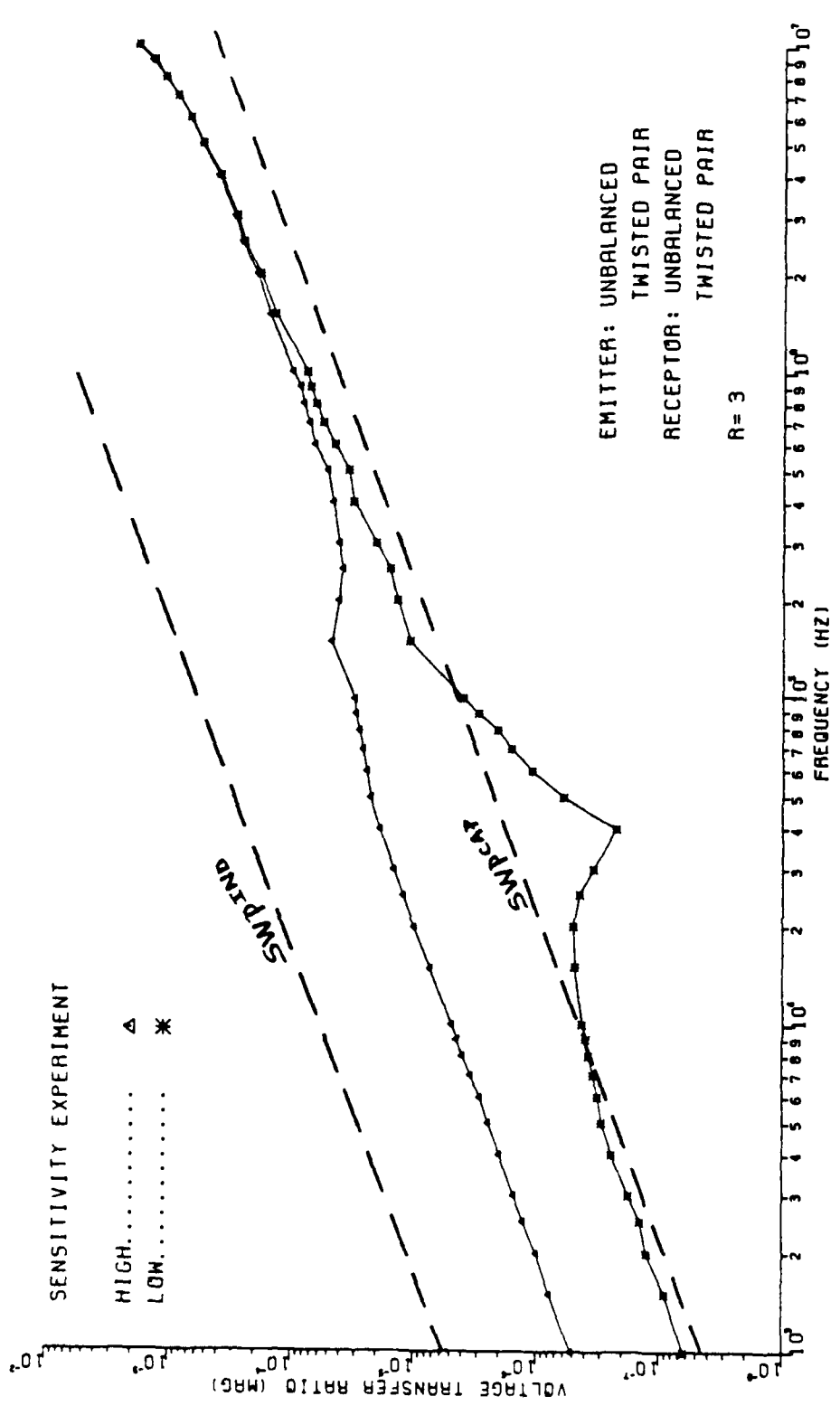
$$TWP = TWP^{IND} + TWP^{CAP} \quad (4-9)$$



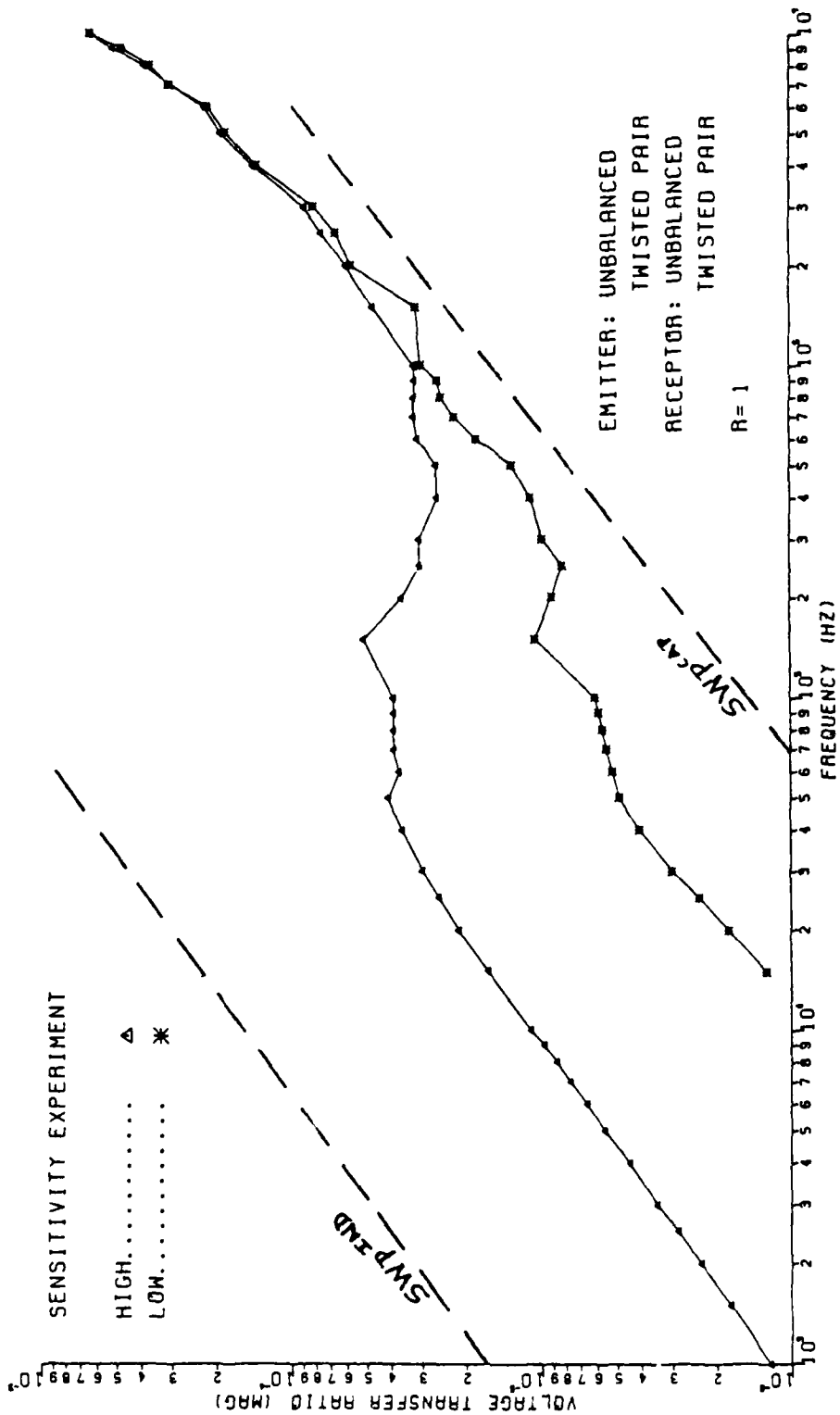
PLOT 4-2(d)



PLOT 4-2(c)



PLOT 4-2(b)



PLOT 4-2(a)

occurs in this situation, the experiment was performed in the following manner. With load resistances of $R = 1 \Omega$, the EMC-25 was attached to measure V_{out} and was tuned to 15 kHz. The right end of the receptor TWP was rotated - no more than 180° - until a maximum response for V_{out} was obtained. With the TWP in the position of this maximum reading, measurements of the voltage transfer ratio were taken for all four impedance values. These measurements constitute the high sensitivity readings for this configuration. Again, with load resistances of $R = 1 \Omega$, the EMC-25 was attached to measure V_{out} and was tuned to 15 kHz. The right end of the receptor TWP was rotated this time until a minimum response was found. These low sensitivity readings were taken for all four impedance values with the TWP in the position of this minimum reading for $R = 1 \Omega$.

The results of the sensitivity experiment are given in Plots 4-2(a) - 4-2(d). Notice that the crosstalk level measured for the low impedance loads, $R = 1 \Omega$ and $R = 3 \Omega$, showed a large sensitivity to variations in line twist. For the high impedance loads, $R = 50 \Omega$ and $R = 1 \text{ k}\Omega$, the line showed virtually no sensitivity to variations in line twist.

The theory developed by Paul and Jolly as described in Chapter III can be used to explain these sensitivity results. First examine the inductive-coupling contribution. If the twists of the generator TWP and the receptor TWP are assumed to be aligned, then for an even number of half-twists in the

effects of c_{G2R1} and c_{G2R2} . The output voltage, V_{out} , of the SWP is

$$V_{out} = V_{out}^{IND} + V_{out}^{CAP} \quad (4-5)$$

In order to differentiate the SWP to SWP crosstalk from the TWP to TWP crosstalk to be discussed later in this chapter, Equation 4-5 is rewritten as

$$SWP = SWP^{IND} + SWP^{CAP} \quad (4-6)$$

The results of the low-frequency analysis of the SWP to SWP configuration as described above have been added to Plots 4-1(a) - 4-1(d). Also, the transmission line model outlined in Appendix A was adapted to calculate the voltage transfer ratio of this SWP to SWP configuration and those results have been added to Plots 4-1(a) - 4-1(d). Notice that for the lower frequencies, the low-frequency model and the transmission line model yield virtually the same results. As the frequency increases, however, the transmission line model continues to provide adequate predictions of the experiments results, but the low-frequency model does not.

After measurements of the SWP to SWP configuration were taken for all four impedance values, the TWP to TWP configuration was constructed. In an effort to determine whether the sensitivity that Paul and Jolly observed in their work also

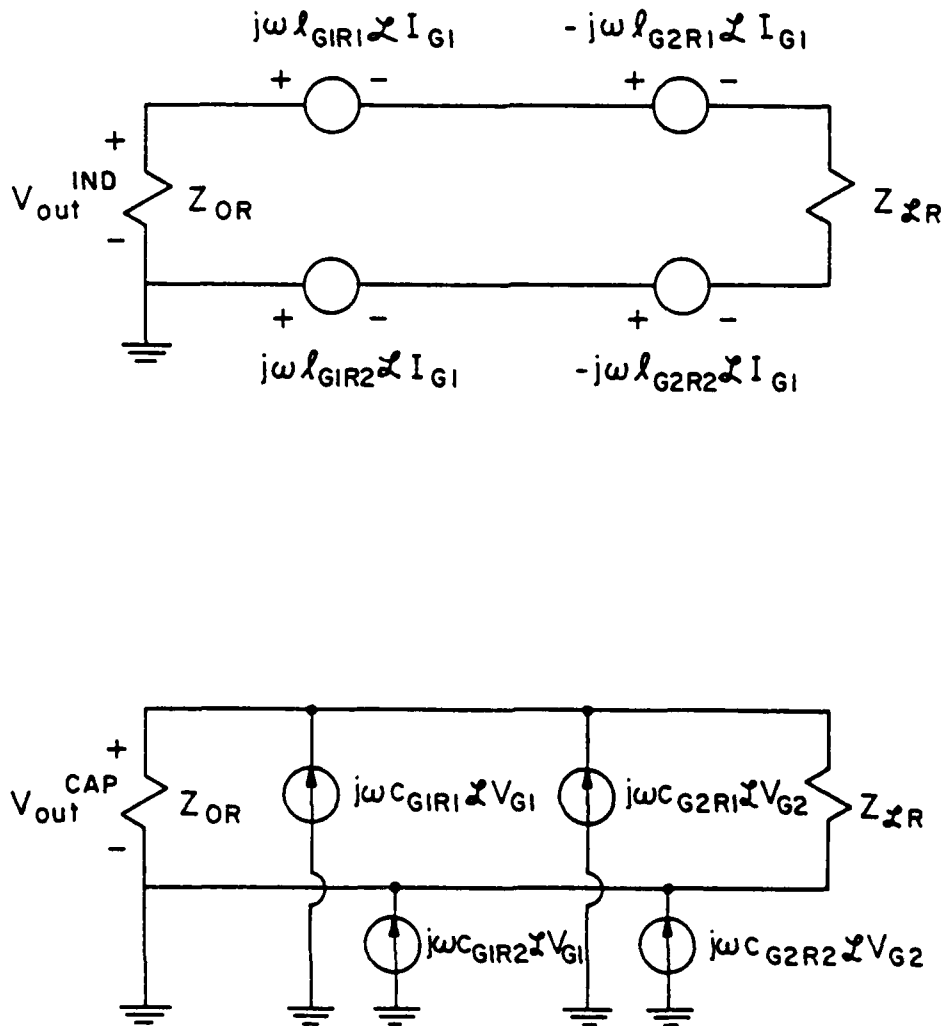


FIGURE 4-4. THE LOW-FREQUENCY APPROXIMATION.
(a) INDUCTIVE-COUPLING.
(b) CAPACITIVE-COUPLING.

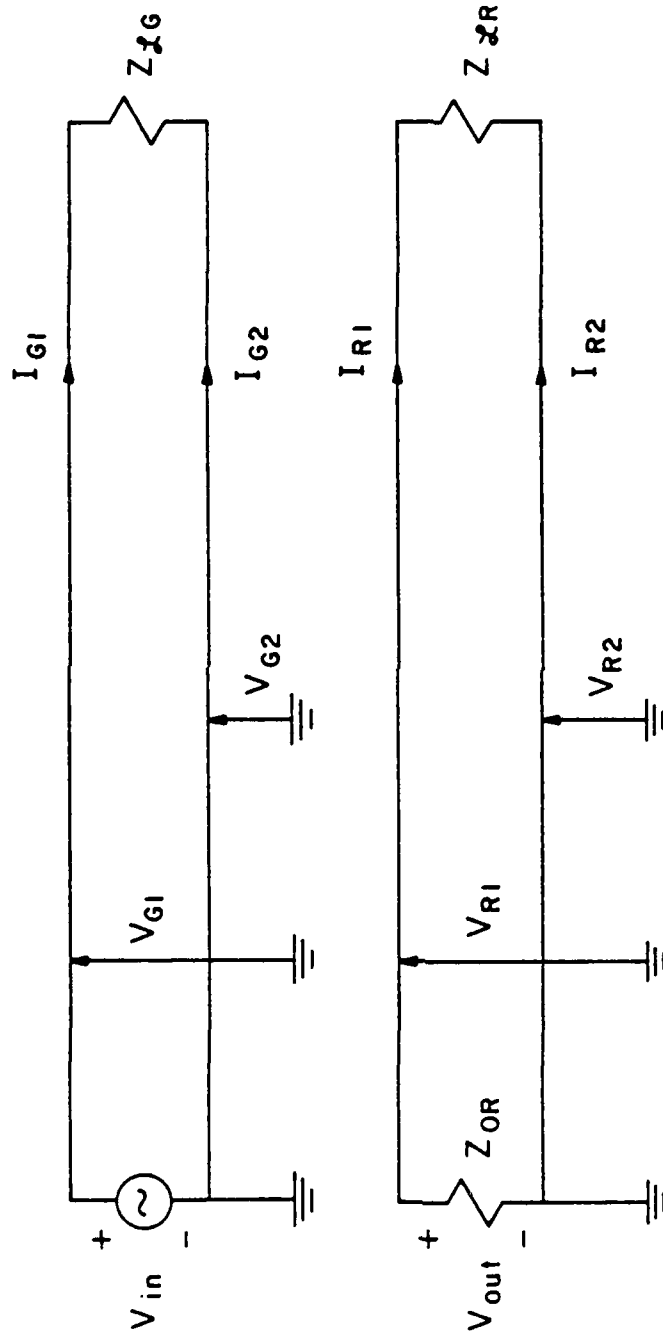


FIGURE 4-3. THE LOW-FREQUENCY UNBALANCED SWP TO UNBALANCED SWP CONFIGURATION.

The d c voltages and currents of the generator wires (Figure 4-3) are given by

$$V_{G1} = V_{in} \quad (4-3a)$$

$$V_{G2} = 0 \quad (4-3b)$$

$$I_{G1} = \frac{V_{in}}{Z_{LG}} \quad (4-3c)$$

$$I_{G2} = -I_{G1} \quad (4-3d)$$

Low-frequency circuits can be derived to represent the inductive-coupling contribution (Figure 4-4(a)) and the capacitive-coupling contribution (Figure 4-4(b)) in the receptor circuit. Then

$$V_{out}^{IND} = \frac{Z_{OR}}{Z_{OR} + Z_{LR}} j \omega (\mathcal{L}_{G1R1} - \mathcal{L}_{G2R1} - \mathcal{L}_{G1R2} + \mathcal{L}_{G2R2}) I_{G1} \quad (4-4a)$$

and

$$V_{out}^{CAP} = \frac{Z_{OR} Z_{LR}}{Z_{OR} + Z_{LR}} j \omega c_{G1R1} I_{G1} \quad (4-4b)$$

Notice that in the determination of V_{out}^{CAP} , the only per-unit-length capacitance value needed is c_{G1R1} . This is because the current sources attached to the grounded receptor wire, R2, do not affect V_{out}^{CAP} and because $V_{G2} = 0$, eliminating the

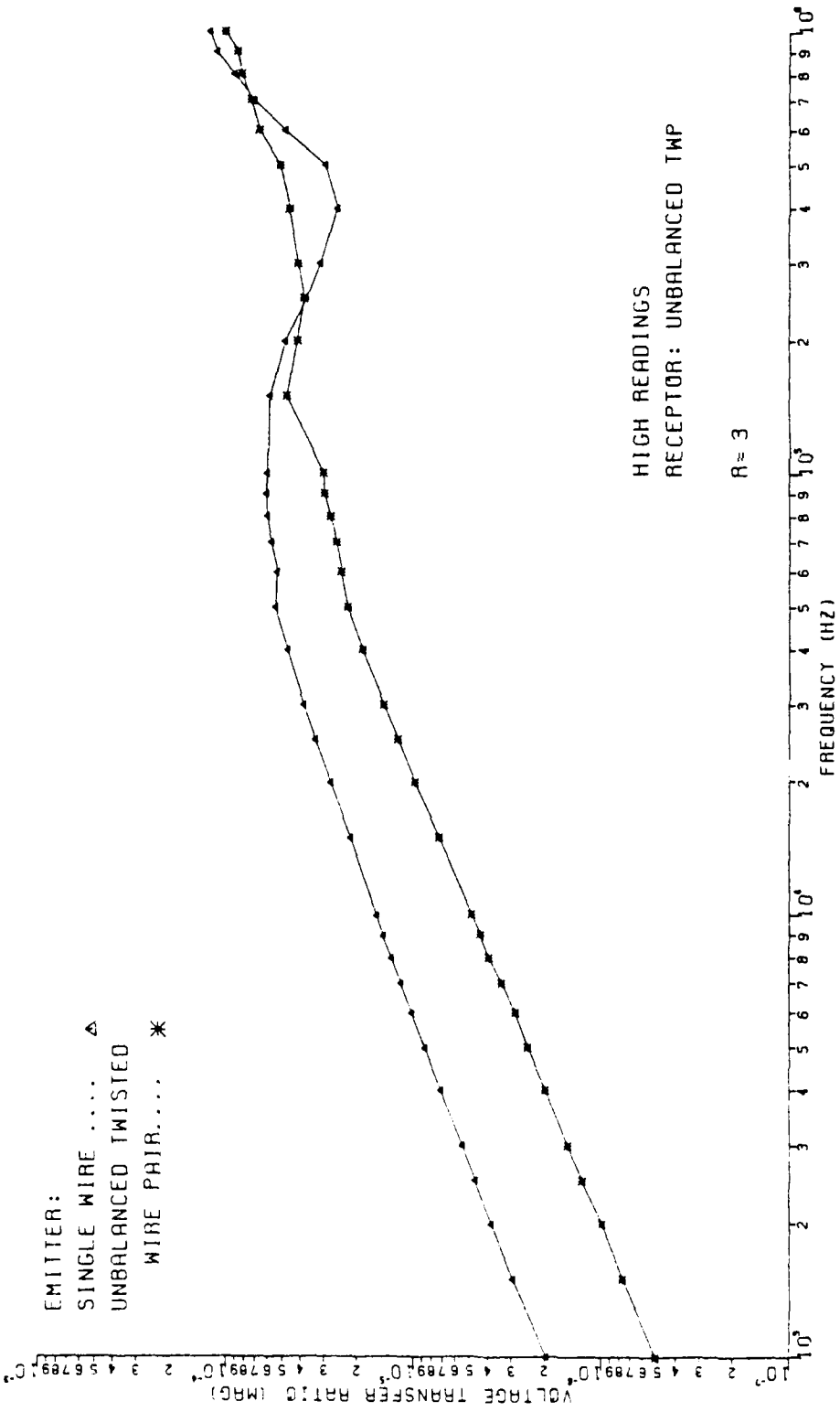
$$\underline{\underline{L}} = \begin{bmatrix} \mathcal{L}_{G1G1} & \mathcal{L}_{G1G2} & \mathcal{L}_{G1R1} & \mathcal{L}_{G1R2} \\ \mathcal{L}_{G2G1} & \mathcal{L}_{G2G2} & \mathcal{L}_{G2R1} & \mathcal{L}_{G2R2} \\ \mathcal{L}_{R1G1} & \mathcal{L}_{R1G2} & \mathcal{L}_{R1R1} & \mathcal{L}_{R1R2} \\ \mathcal{L}_{R2G1} & \mathcal{L}_{R2G2} & \mathcal{L}_{R2R1} & \mathcal{L}_{R2R2} \end{bmatrix} \quad (4-2a)$$

and the per-unit-length capacitance matrix is found by

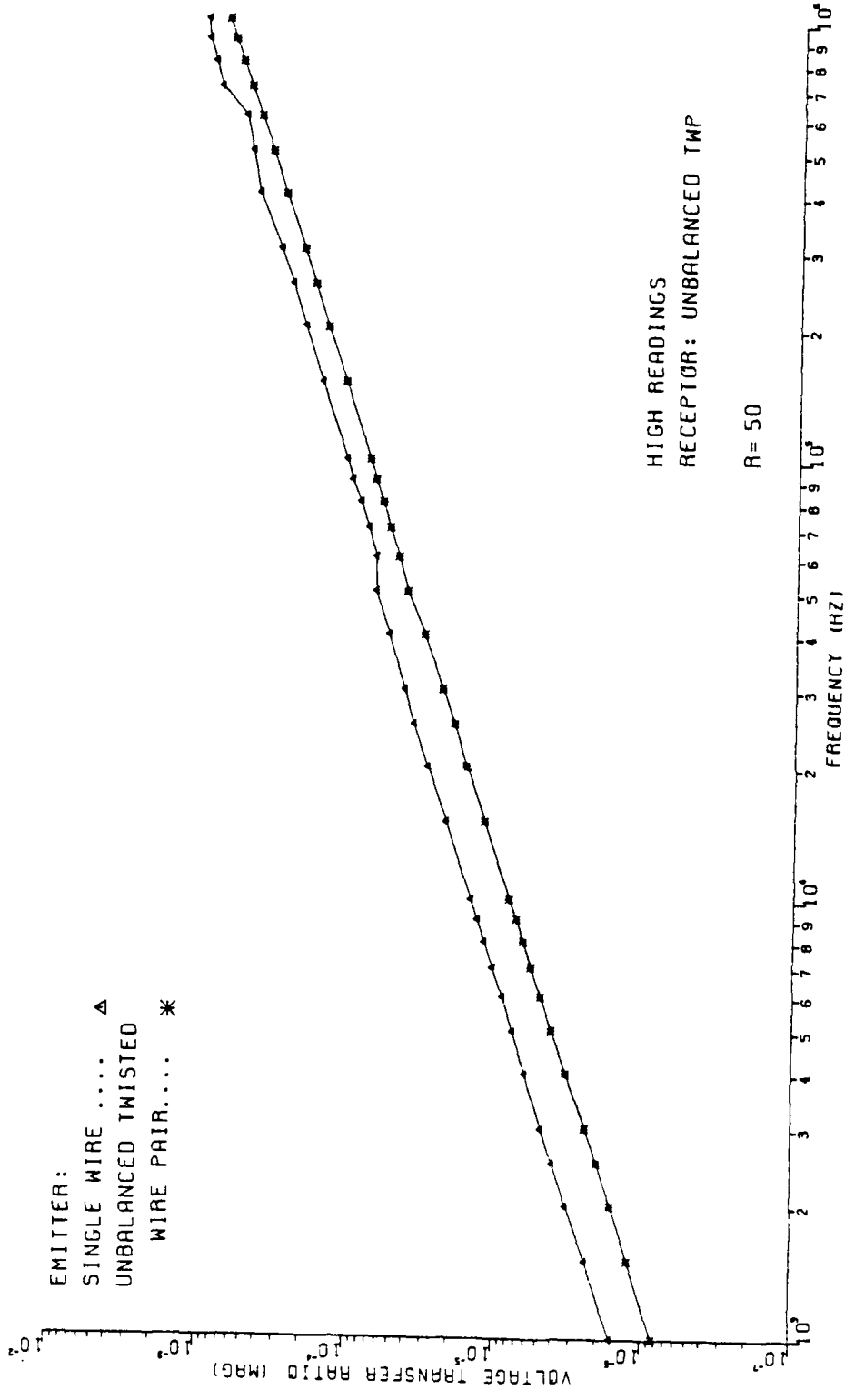
$$\underline{\underline{C}} = \frac{1}{v^2} \underline{\underline{L}}^{-1}$$

$$= \begin{bmatrix} (c_{G1G1} + c_{G1G2} + c_{G1R1} + c_{G1R2}) & -c_{G1G2} \\ -c_{G2G1} & (c_{G2G1} + c_{G2G2} + c_{G2R1} + c_{G2R2}) \\ -c_{R1G1} & -c_{R1G2} \\ -c_{R2G1} & -c_{R2G2} \\ -c_{G1R1} & -c_{G1R2} \\ -c_{G2R1} & -c_{G2R2} \\ (c_{R1G1} + c_{R1G2} + c_{R1R1} + c_{R1R2}) & -c_{R1R2} \\ -c_{R2R1} & (c_{R2G1} + c_{R2G2} + c_{R2R1} + c_{R1R1}) \end{bmatrix} \quad (4-2b)$$

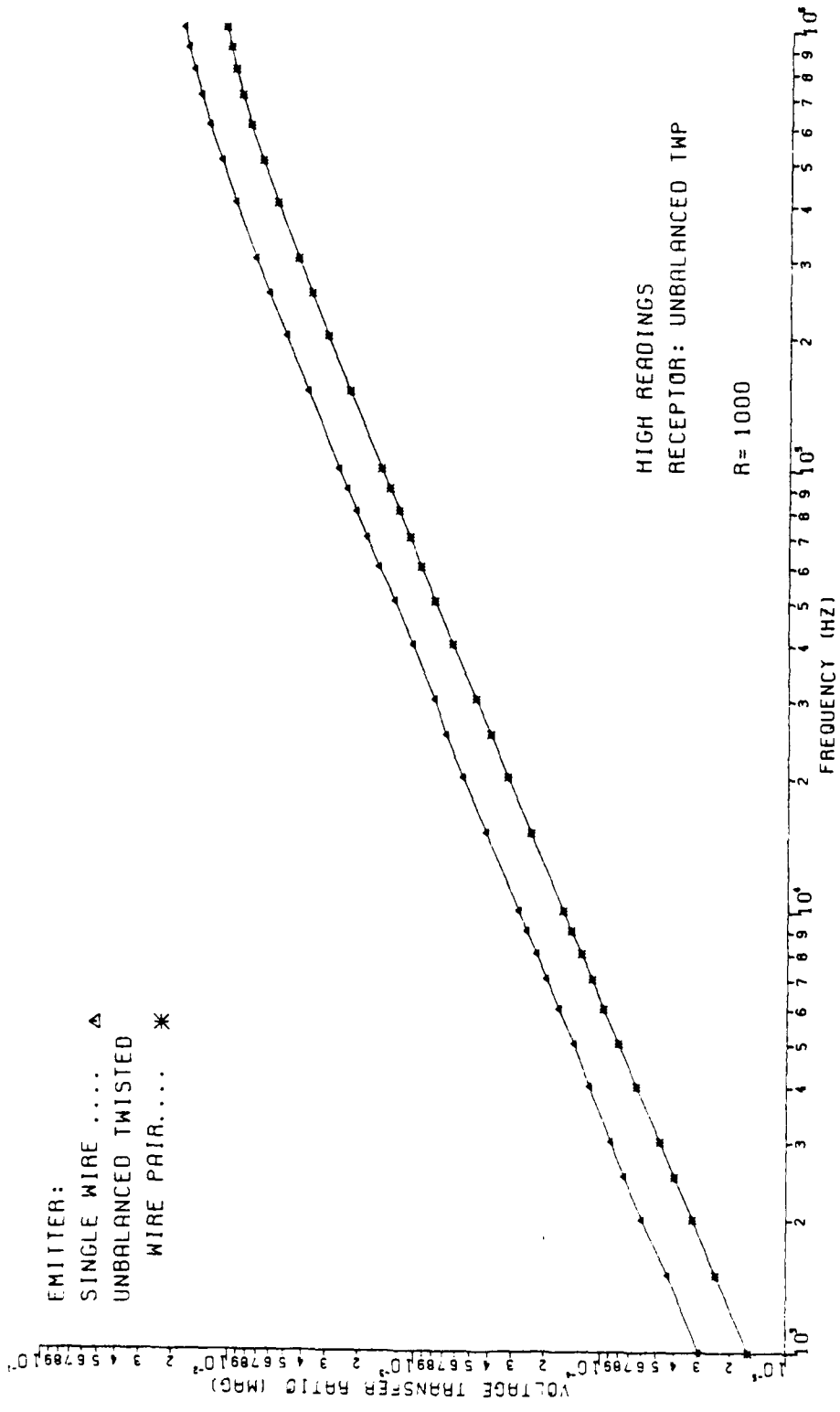
where v is the velocity of propagation in the surrounding (assumed homogeneous) medium, i.e., $v = 3 \times 10^8$ m/s.



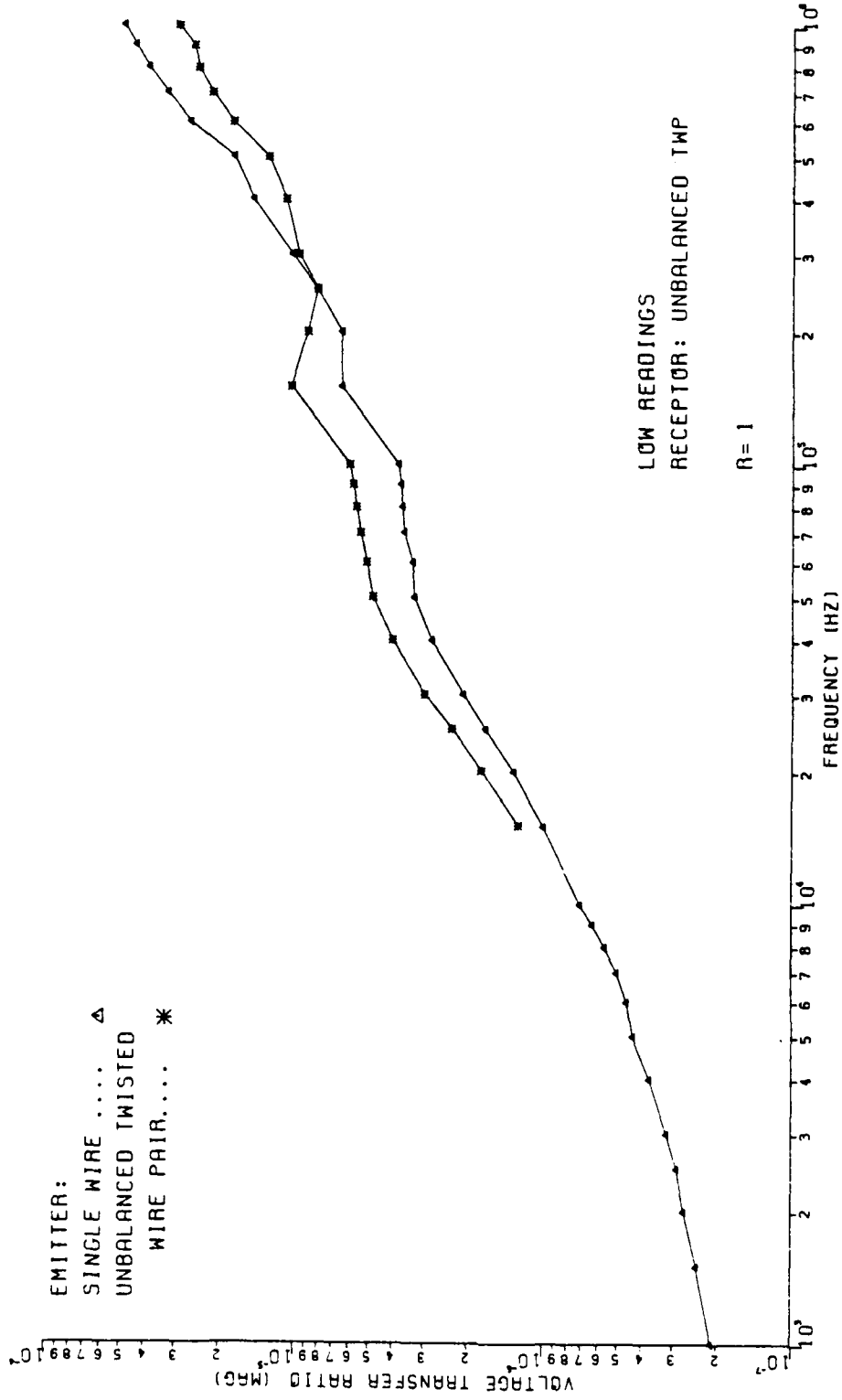
PLOT 4-3(b)



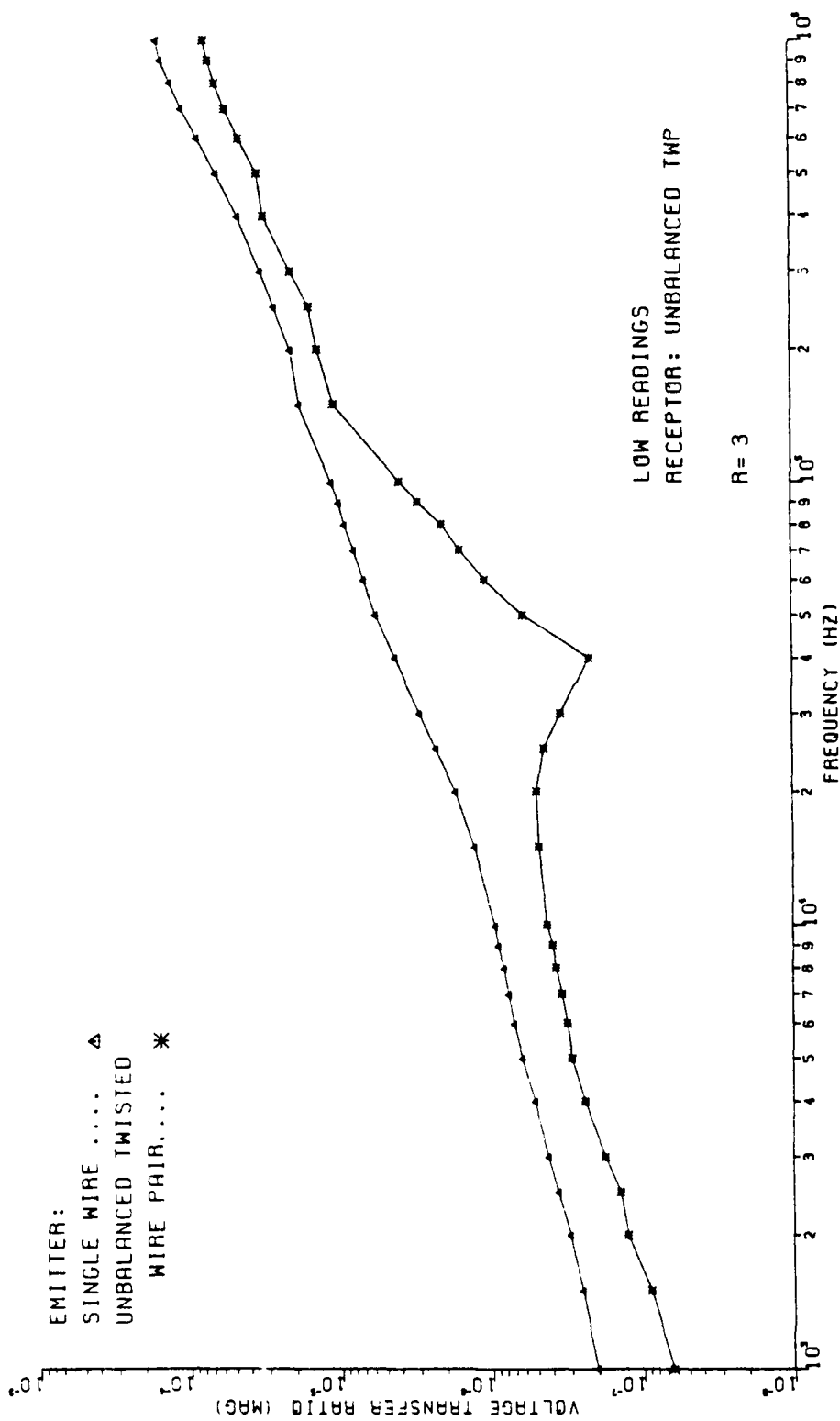
PLOT 4-3(c)



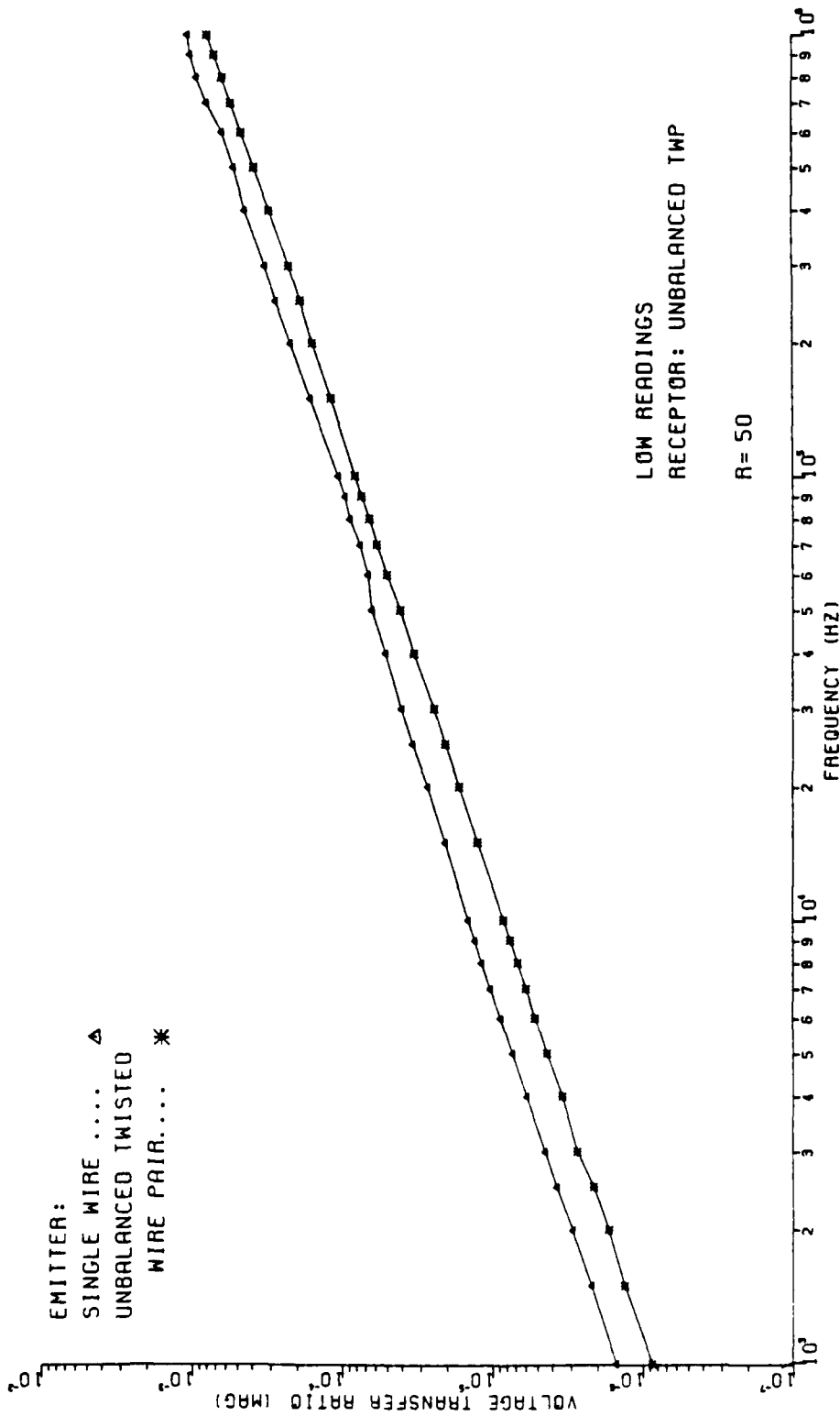
PLOT 4-3(d)



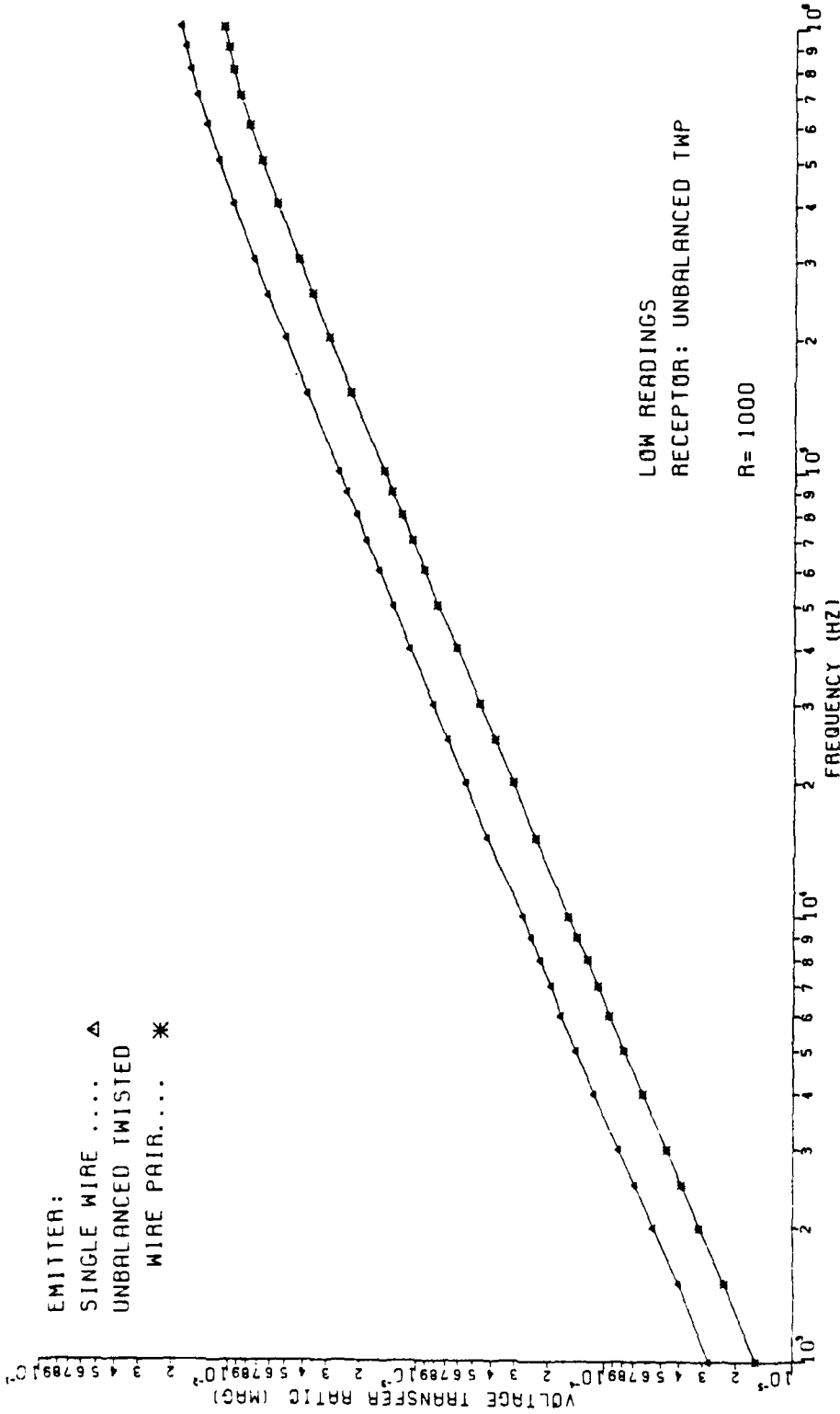
PLOT 4-4(a)



PLOT 4-4(b)



PLOT 4-4(c)



the generator circuit used was a single wire with ground return. However, if the low-frequency expressions for SWP^{IND} are examined, Equation 3-2a, which pertains to a single wire with ground return generator circuit, yields a mutual inductance value of $L_m = 1.3 \times 10^{-9}$ H/m. Equation 4-4 a , which gives SWP^{IND} for the SWP generator circuit configuration, yields a mutual inductance of $L_m = 1.218 \times 10^{-9}$ H/m. Thus, for the SWP configurations, no significant reduction in inductive-coupling is achieved through use of an SWP generator circuit instead of a single wire with ground return generator circuit.

Plots 4-3(a) and 4-3(b), which give a comparison of the high TWP readings for $R = 1\Omega$ and $R = 3\Omega$, show a 10 dB difference in the two configurations. Recall that the high readings for these low-impedance loads are assumed to be due to the inductive-coupling of only one loop of the receptor TWP. There is evidence to suggest, however, that the inductive-coupling of the high readings is very dependent on the nonuniformity of the twist along the TWP. Although it was attempted to construct the two experiments identically, the nonuniformity of the TWP's could obviously not be reproduced. It is expected that the 10 dB difference in the two configurations, shown in Plots 4-3(a) and 4-3(b), is due to the difference in the nonuniformity of the twist in the two experiments.

When capacitive-coupling is dominant ($R = 50\Omega$ and $R = 1\text{ k}\Omega$ in the high readings of Plots 4-3(c) and 4-3(d) and for all values of load impedance in the low readings of Plots 4-4) a reduction of about 3 dB in the crosstalk level occurs by using the TWP generator circuit instead of a single wire with ground return. Recall that wire G2 (see Figure 4-1) of the generator TWP was grounded. Because wire G2 was much nearer to wire G1 than the ground plane was to the single generator wire, more electric field lines could terminate on G2 of the TWP configuration than the ground plane of the single wire configuration. Thus fewer electric field lines would be available to terminate on the wires of the receptor TWP. Therefore the mutual capacitance when the generator circuit was a TWP would be less than when the generator circuit was a single wire with ground return. Equation 3-2b, which pertains to the single wire with ground return generator circuit, shows that c_{G1} is 1.59 pF/m. Equation 4-4b, which gives SWP^{CAP} for the SWP generator circuit, shows a dependence on c_{G1R1} , which has a value of 1.02 pF/m. Thus, the simple low-frequency models demonstrate a reduction in capacitive-coupling of about 4 dB by using the SWP generator circuit.

Overall, a comparison of these two specific configurations indicates that no significant reduction in crosstalk is gained by using a TWP generator circuit over a single wire with ground return, whether inductive- or capacitive-coupling is dominant. These conclusions, of course, apply only to the cross-sectional

configuration which was investigated. For other cross-sectional configurations, such as the generator and receptor circuits being closer together, these conclusions may be different.

As was expected, the unbalanced TWP to unbalanced TWP configuration showed large sensitivity of crosstalk to minor variations in line twist when low-impedance loads were used to terminate the line. This was again explainable in terms of low-frequency models based on the superposition of inductive- and capacitive-coupling. Also, this supported the explanations given by Paul and Jolly of the sensitivity which they uncovered. As was the case for the configuration investigated by Paul and Jolly, for those impedances where this sensitivity is observed, the prediction of the crosstalk level is not possible. This is because it is impossible to determine or insure either the number of half-twists in a TWP or the alignment of those half-twists in a practical installation.

In the previous investigations, the capacitive-coupling floor caused by the unbalance of the load configurations prevented the full realization of reduction in coupling. This was more evident for the high-impedance loads, $R = 50\Omega$ and $R = 1\text{ k}\Omega$, than for the low-impedance loads, $R = 1\Omega$ and $R = 3\Omega$. In the next chapter the effect of balancing the loads of the receptor circuit will be investigated to determine whether this situation is improved by removing (or at least substantially lowering) this capacitive-coupling floor.

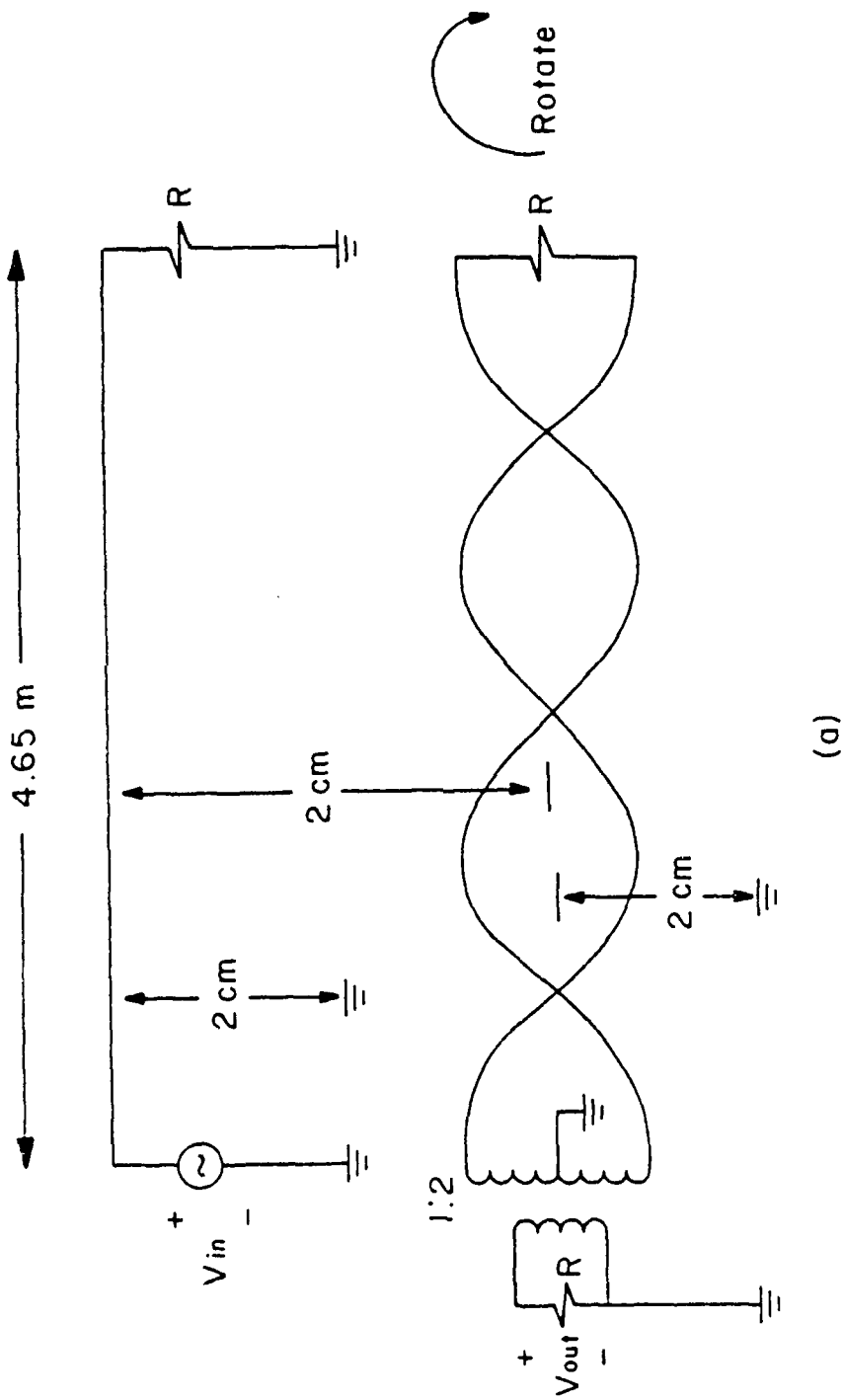
CHAPTER V

CROSSTALK IN THE BALANCED TWISTED-PAIR

The previous two chapters discussed the crosstalk in configurations which were unbalanced with respect to their terminal configurations. It was shown that for certain low-impedance loads the use of twisted wire pair (TWP) receptor circuits resulted in a significant reduction in the crosstalk level of the receptor circuit. Also, for the low-impedance loads, it was found that the crosstalk induced in the TWP receptor circuit was very dependent on minor variations in the line twist. When high-impedance loads were used in those unbalanced configurations, the TWP did not provide a significant reduction in crosstalk, nor did the crosstalk level appear to be influenced by variations in line twist. This was explained using the concepts of inductive-coupling and capacitive-coupling. This chapter will investigate the crosstalk from a single wire with ground return generator circuit to a balanced TWP (and SWP) receptor circuit. For this case, the balancing of the terminal configurations is believed to reduce the capacitive-coupling so that a significant reduction in crosstalk should be found for both low-impedance loads and high-impedance loads when the TWP receptor circuit is used.

The experiment for the single wire with ground return generator circuit and balanced TWP receptor circuit (see Figure 5-1) was constructed like the experiments in Chapter III and Chapter IV as much as possible. As was the case in those chapters, the receptor and generator circuits were suspended 2 cm above an aluminum ground plane and were separated from each other by 2 cm. Their positions were held constant with styrofoam blocks placed along the length of the line. Again, all wires were #22 gauge, stranded, so the minimum separation of the wires of the TWP (SWP) was 57.3 mils. The line length of this experiment was 4.65 m. The receptor TWP contained 80 full twists. Figures 5-2 through 5-5 are photographs of the actual experiment.

The experiment was performed for four values of load impedance; 1Ω , 3Ω , 50Ω , and $1\text{ K}\Omega$. The generator circuit was a single wire above a ground plane return. A sinusoidal generator was attached at the left end of the line between the generator wire and the ground. This voltage was referred to as V_{in} . The receptor circuit was a balanced (with respect to its terminal configurations) TWP. The right end of the receptor TWP was ungrounded. The left end of the TWP was balanced by connecting it across the secondary windings of a center-tapped transformer. The primary windings of the transformer were terminated in one of the impedances listed above and V_{out} was measured across



(a)

FIGURE 5-1. THE UNBALANCED TWP EXPERIMENT.

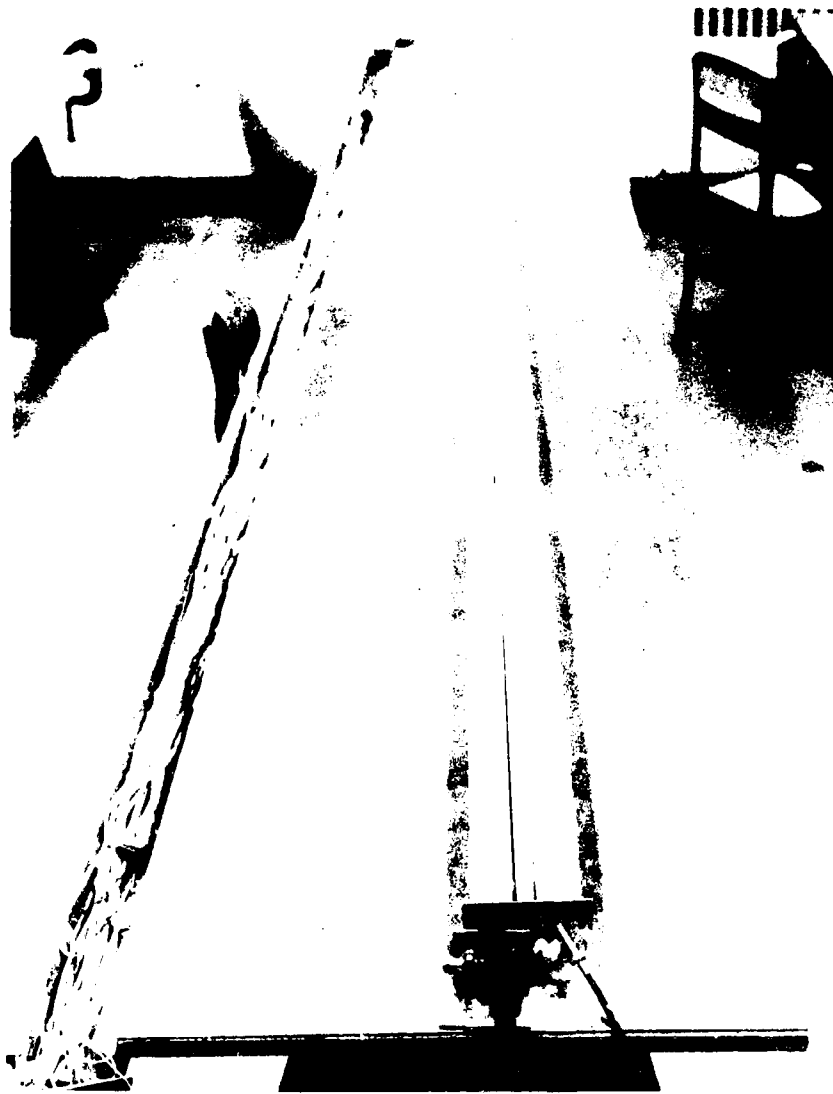
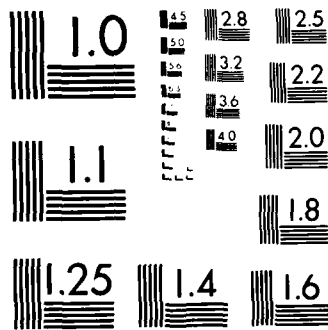


FIGURE 5-2. VIEW OF THE EXPERIMENT.



MICROCOPY RESOLUTION TEST CHART
NATIONAL BUREAU OF STANDARDS-1963-A

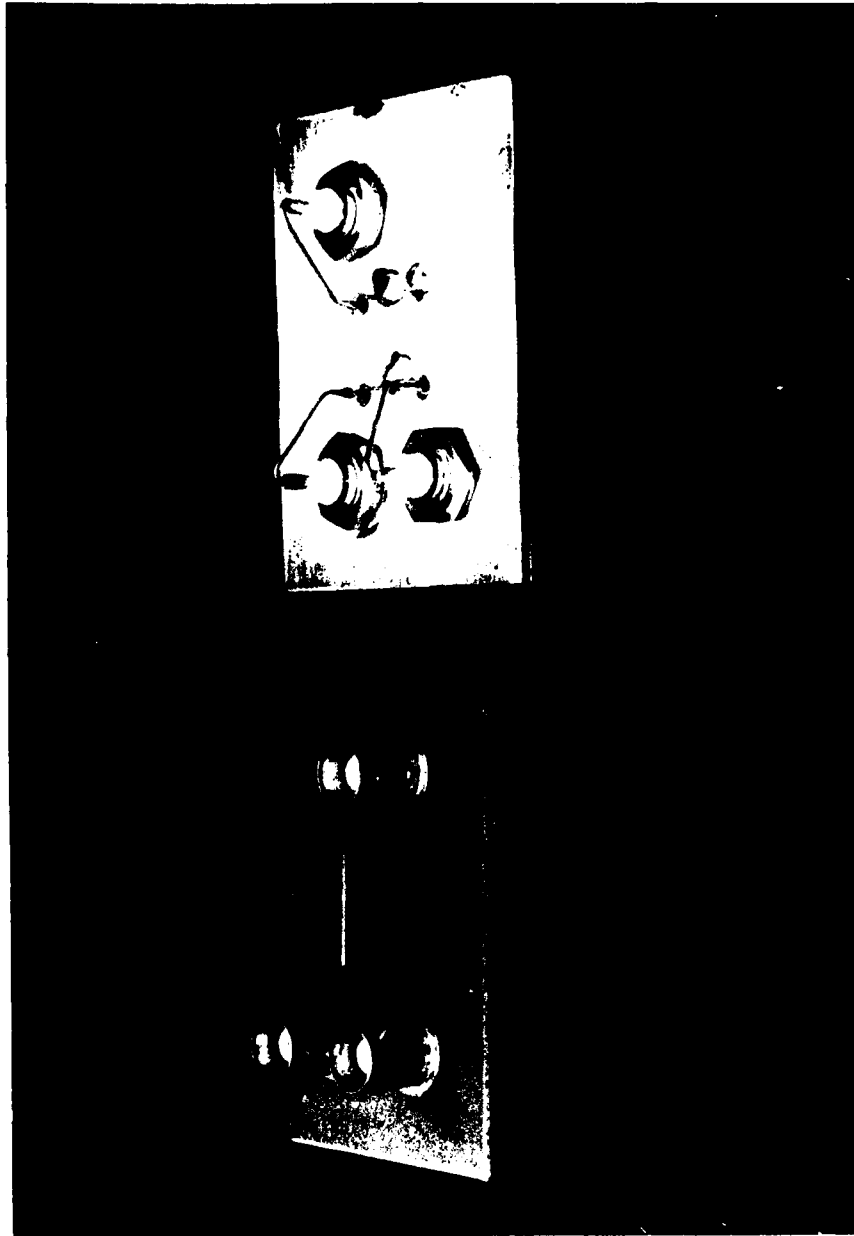


FIGURE 5-3. THE LF-428 TRANSFORMERS.



FIGURE 5-4. VIEW OF THE EXPERIMENT AT $X = 0$.

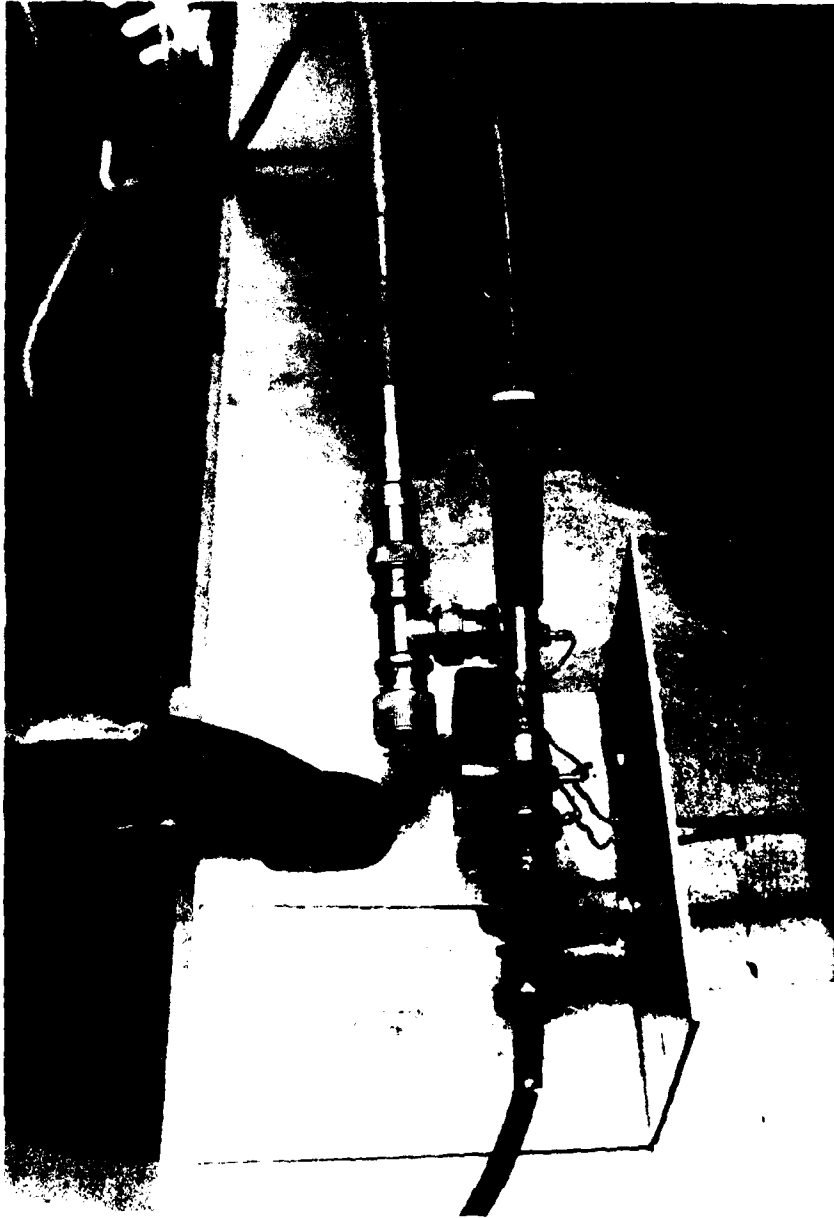


FIGURE 9-5. CROSS-SECTIONAL VIEW AT $X = 0$.

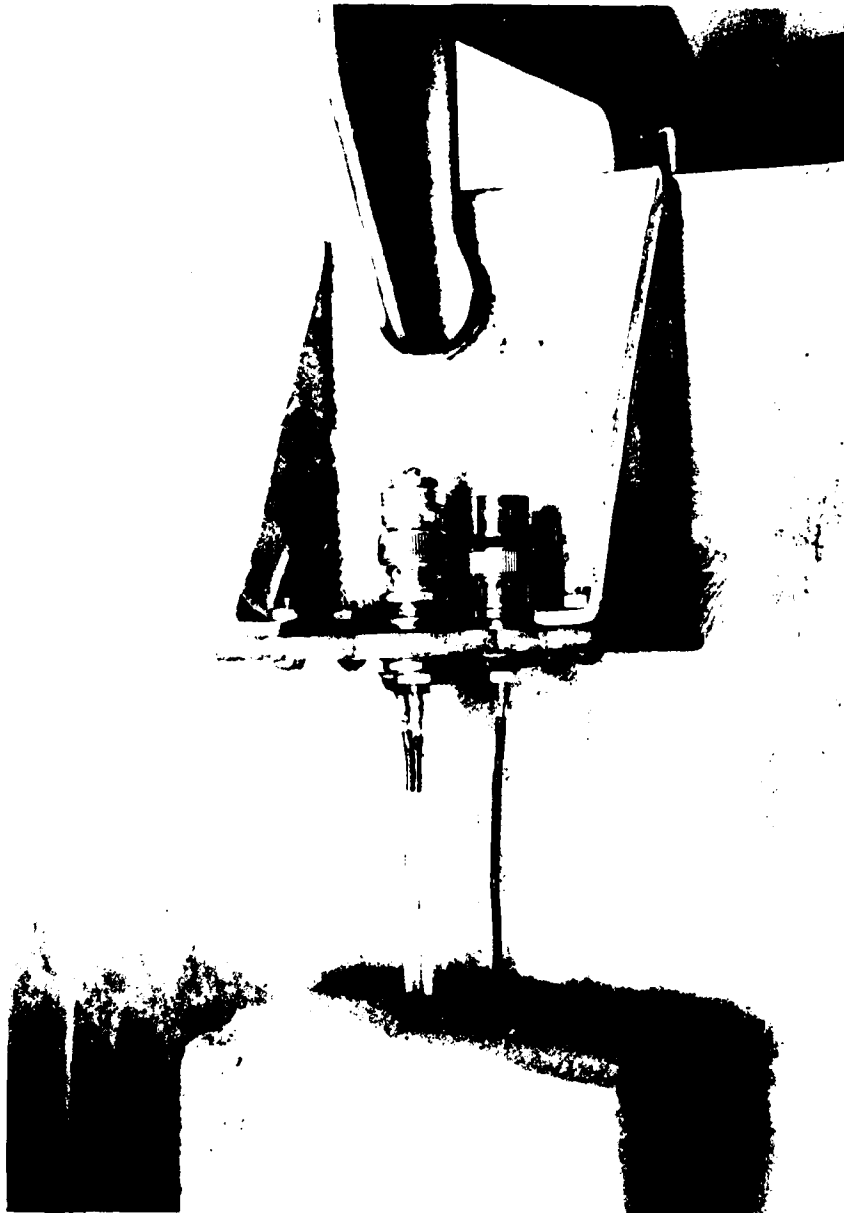


FIGURE 5-6. CROSS-SECTIONAL VIEW AT $X = L$.

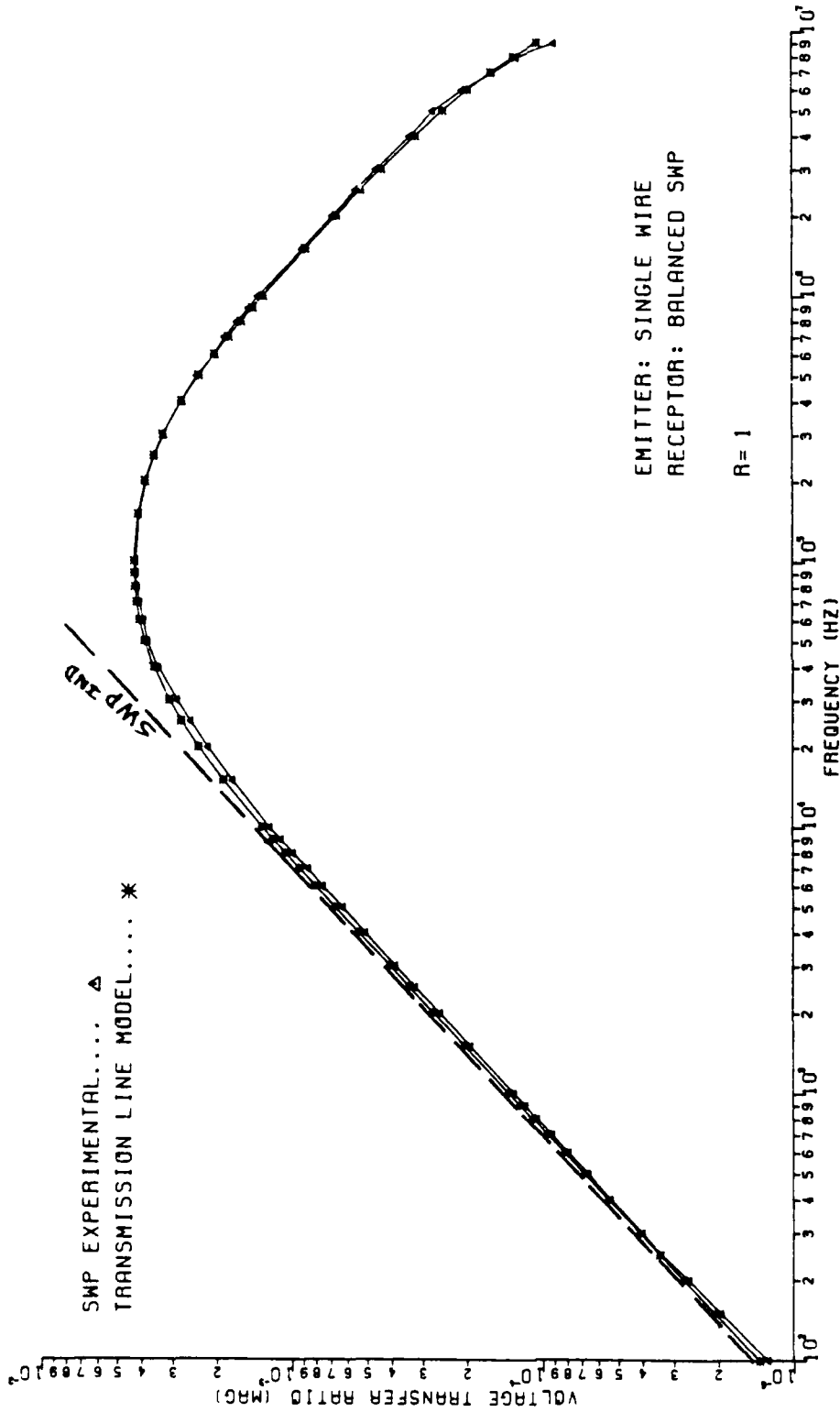
that impedance. The voltage transfer ratio was again defined by

$$\text{voltage transfer ratio} = \frac{V_{\text{out}}}{V_{\text{in}}} \quad (5-1)$$

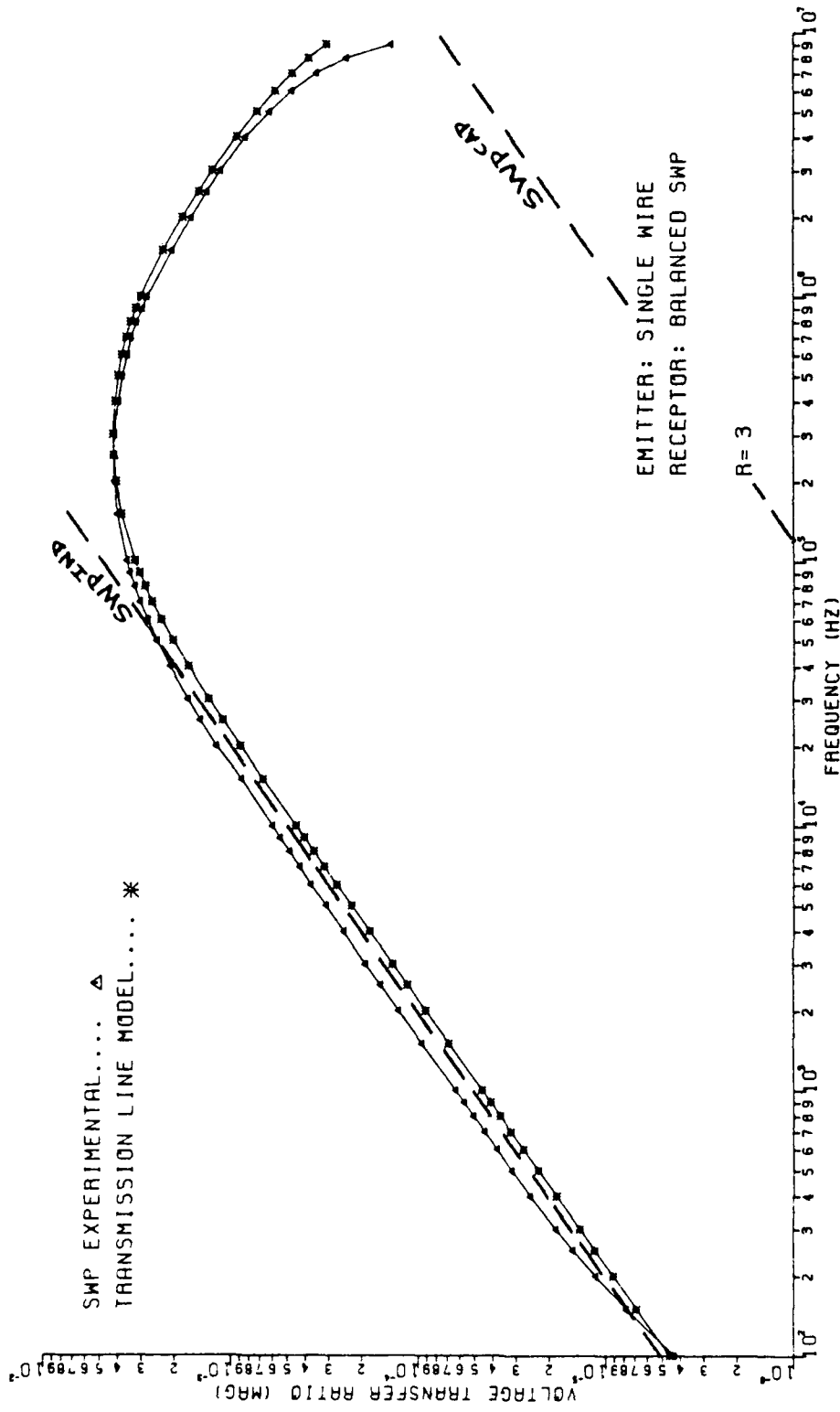
The voltage transfer ratio was measured for frequencies in the range from 100 Hz to 9 MHz. Measurements were taken at frequencies of 1, 1.5, 2, 2.5, 3, 4, 5, 6, 7, 8, 9 in each decade of frequency. The equipment listed in Chapters III and IV was used for this experiment also.

The experiment was first performed for the balanced SWP receptor circuit. The wires of the SWP were horizontal, so that the plane containing the generator wire and the wires of the SWP was parallel to the ground plane. The voltage transfer ratio was measured for all four values of load impedance and the results are given in Plots 5-1(a) - 5-1(d).

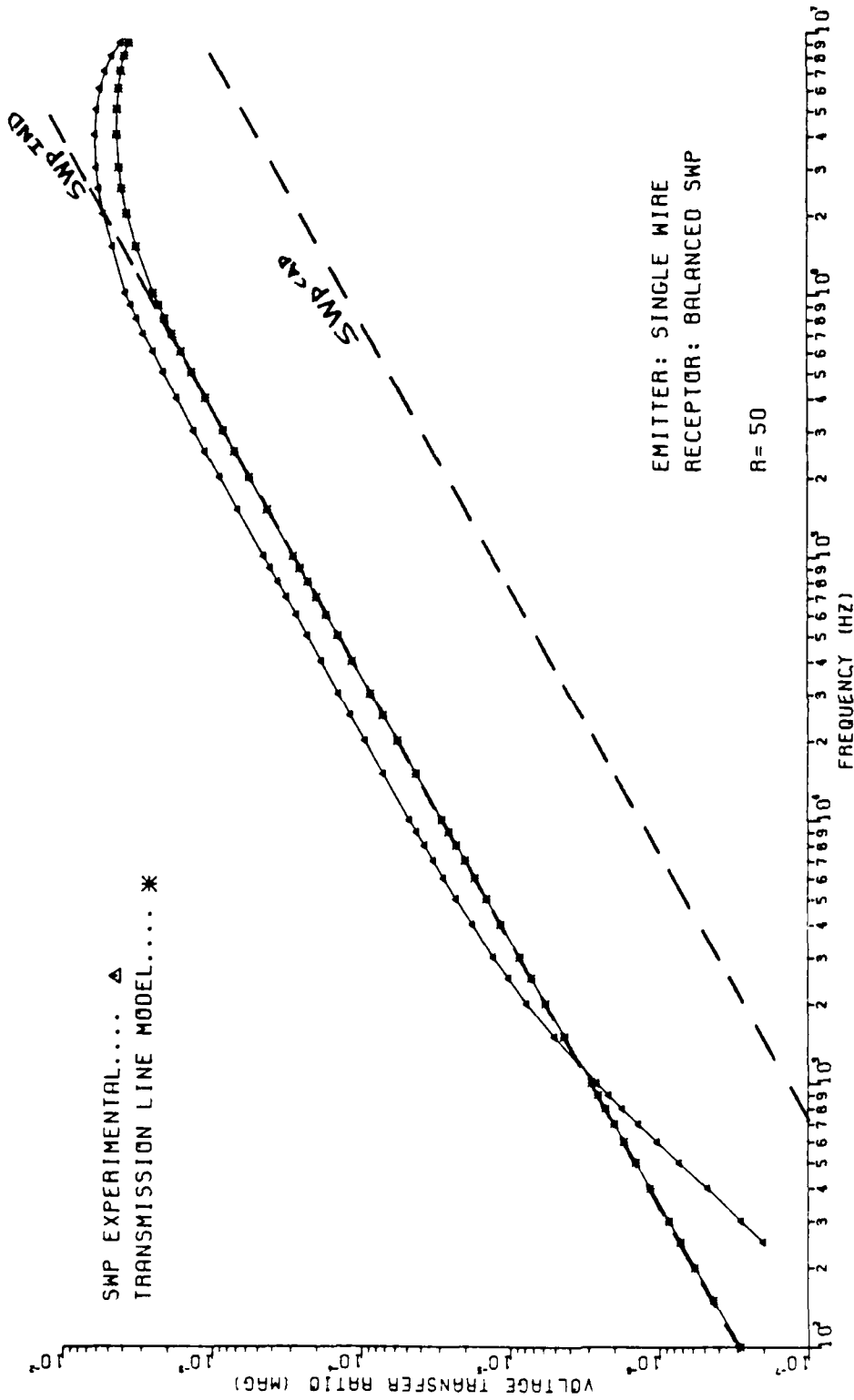
A low-frequency model to predict the SWP voltage transfer ratio can be determined by the superposition of an inductive-coupling and a capacitive-coupling contribution. In the low-frequency circuit of the SWP receptor circuit (Figure 5-6) an equivalent circuit has been used to model the center-tapped transformer. The derivation of this equivalent circuit is explained in Appendix B. The output voltage, V_{out} , needed to calculate the voltage



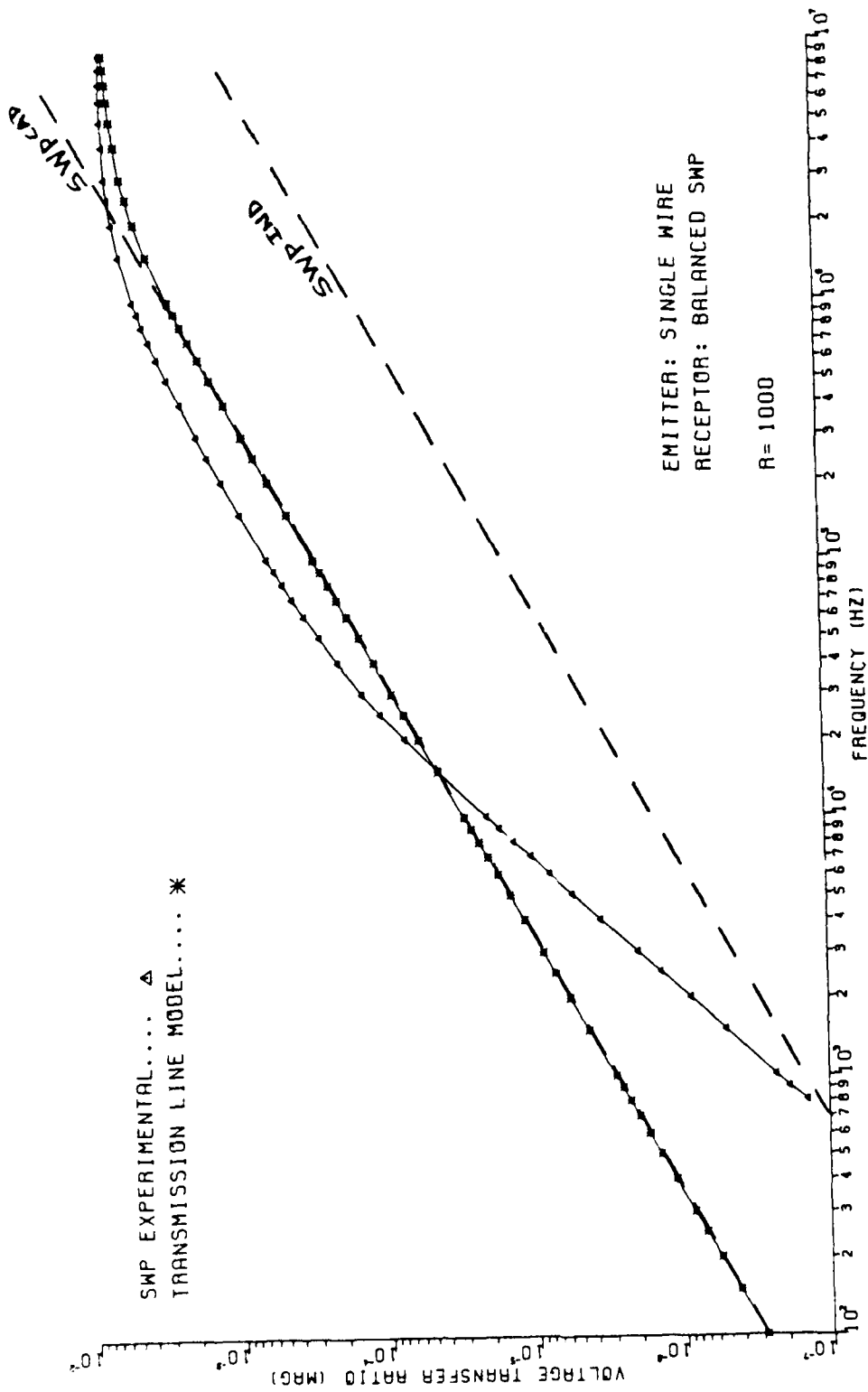
PLOT 5-1(a)



PLOT 5-1(b)



PLOT 5-1(c)



PLOT 5-1(d)

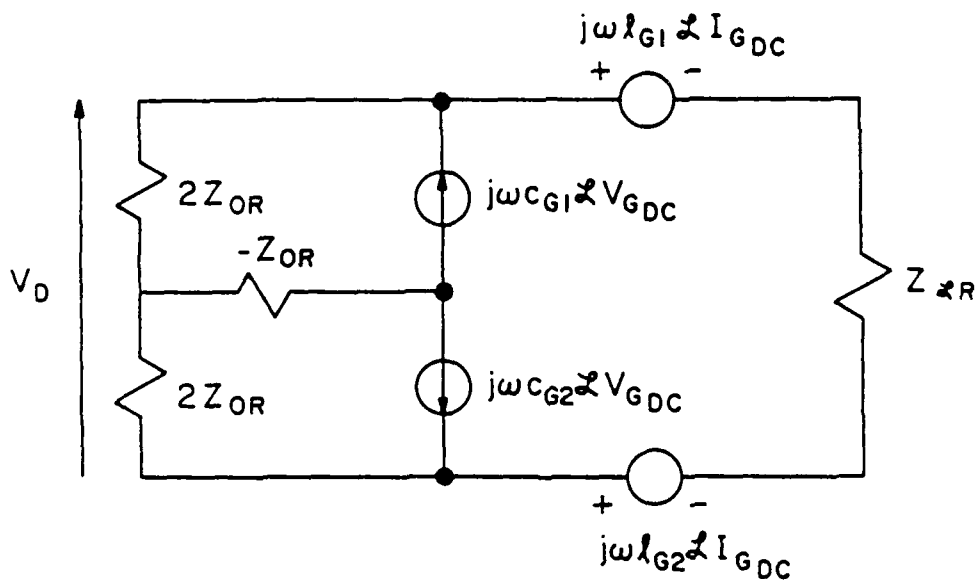


FIGURE 5-7. THE BALANCED SWP LDR-FREQUENCY APPROXIMATION.

transfer ratio is related to this circuit by

$$V_{out} = \frac{1}{2} V_D \quad (5-2)$$

where V_D is the voltage across the transformer secondary.

The per-unit-length inductance matrix, \underline{L} , and capacitance matrix, \underline{C} , are calculated to determine L_{G1} and L_{G2} , the per-unit-length mutual inductances between the generator wire and each wire of the SWP, and C_{G1} and C_{G2} , the corresponding mutual capacitances. Due to the similarity in physical geometry, the inductance and capacitance matrices of this configuration are the same as those of the single wire with ground return generator circuit to unbalanced SWP receptor circuit configuration investigated by Paul and Jolly.

The inductive-coupling and capacitive-coupling contributions to the crosstalk are determined from the low-frequency SWP circuit (Figure 5-6):

$$V_{out}^{IND} = \frac{1}{2} V_D^{IND} = \left(\frac{-\beta_{G1}}{1 + \beta_{G1} + \beta_{G2}} \right) j\omega (L_{G1} - L_{G2}) I_{G_{DC}} \quad (5-3a)$$

$$\begin{aligned} V_{\text{out}}^{\text{CAP}} &= \frac{1}{2} V_D^{\text{CAP}} \\ &= \left(\frac{Z_{\text{OR}}}{Z_{\text{OR}} + Z_{\text{LR}}} \right) j \omega (c_{G1} - c_{G2}) L V_{G_{\text{DC}}} \end{aligned} \quad (5-3b)$$

where

$$V_{G_{\text{DC}}} = V_{\text{in}} \quad (5-4a)$$

$$I_{G_{\text{DC}}} = \frac{V_{\text{in}}}{Z_{\text{LG}}}$$

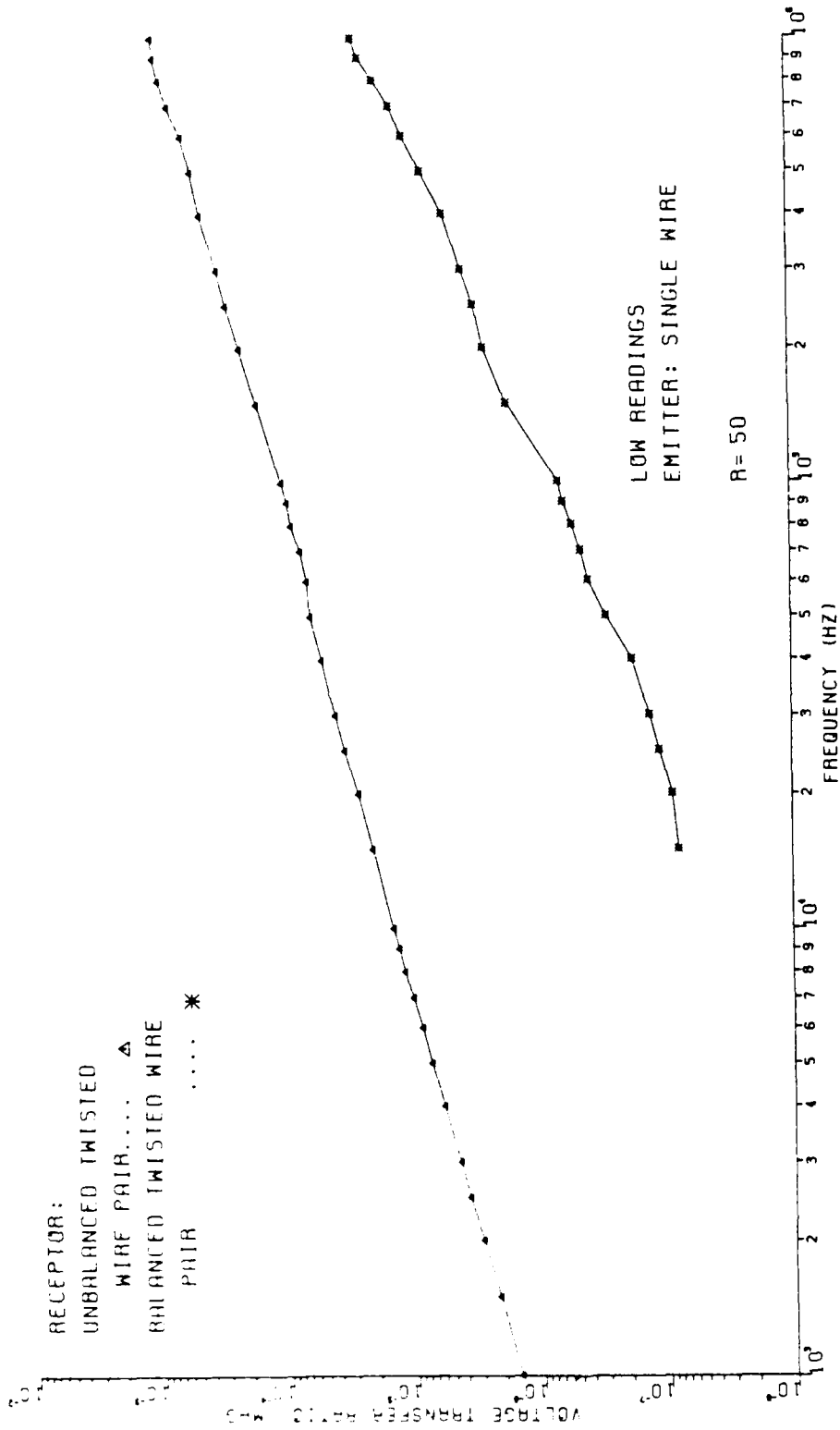
are the DC values of generator voltage and current. Then

$$V_{\text{out}} = V_{\text{out}}^{\text{IND}} + V_{\text{out}}^{\text{CAP}} \quad (5-5a)$$

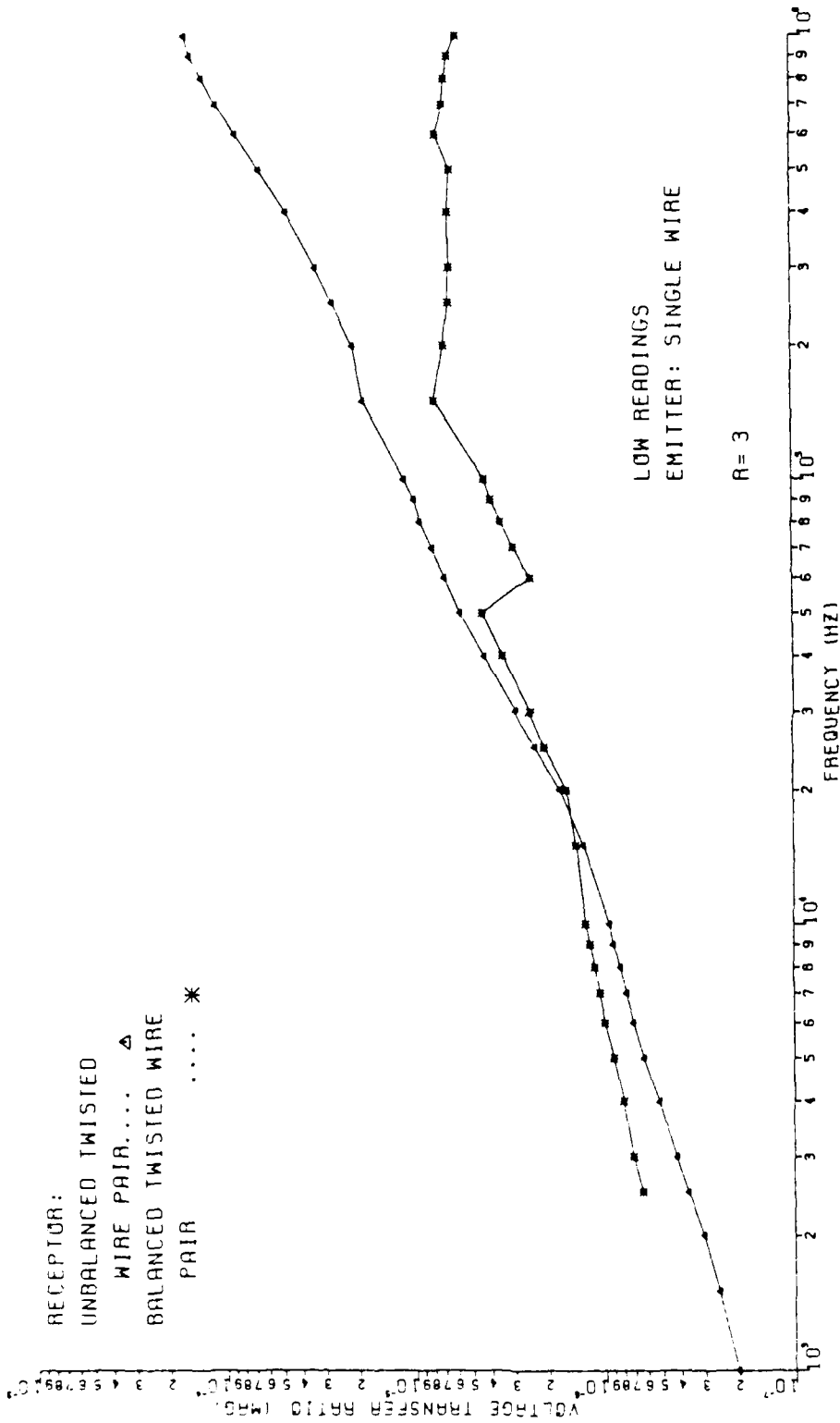
or

$$\text{SWP} = \text{SWP}^{\text{IND}} + \text{SWP}^{\text{CAP}}$$

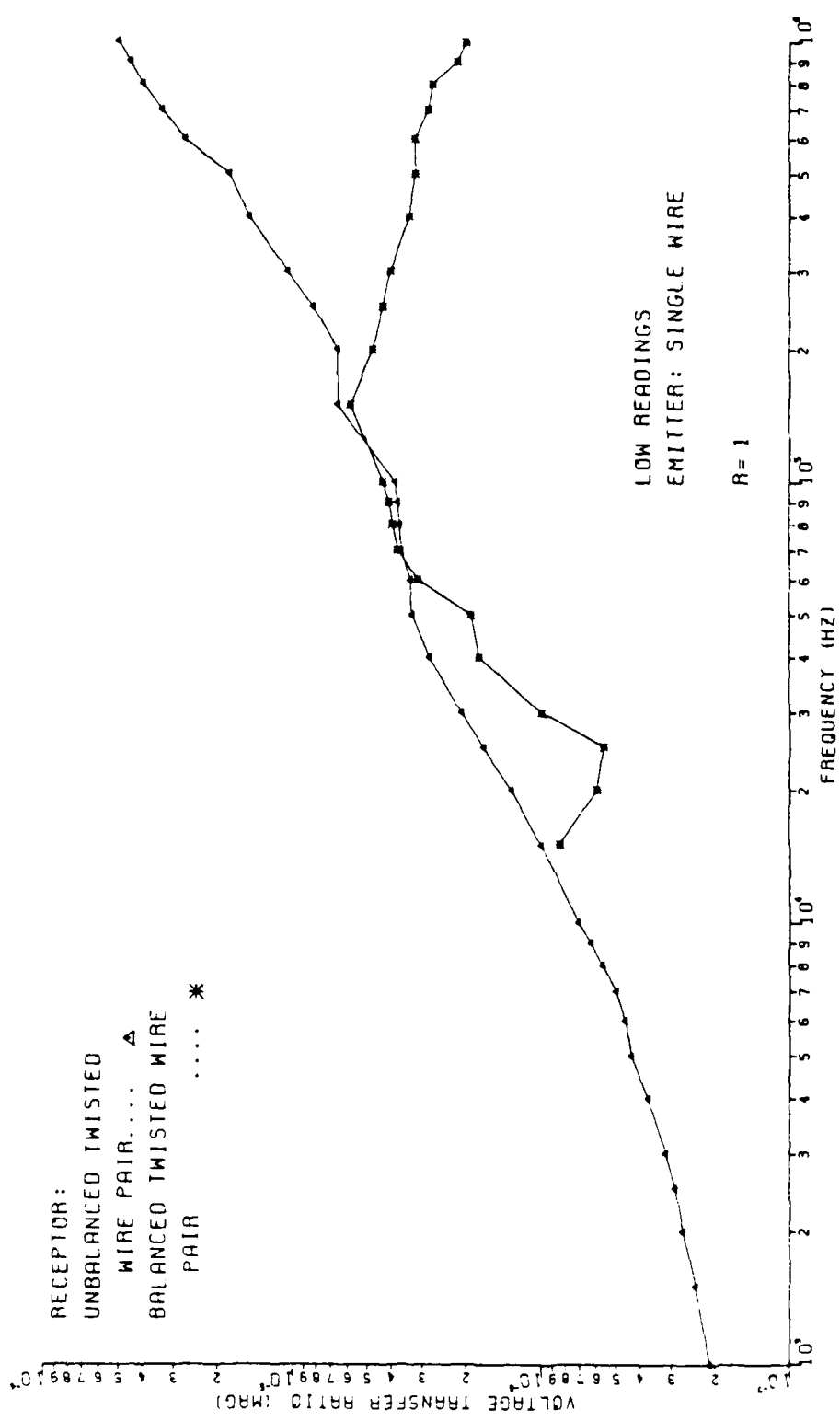
The results of this low-frequency analysis of the crosstalk to the SWP receptor circuit have been added to Plots 5-1. Also, the transmission line model (see Appendix A) was calculated for this configuration and those results are given in Plots 5-1. As expected, at low frequencies, both fields increase linearly with frequency. However,



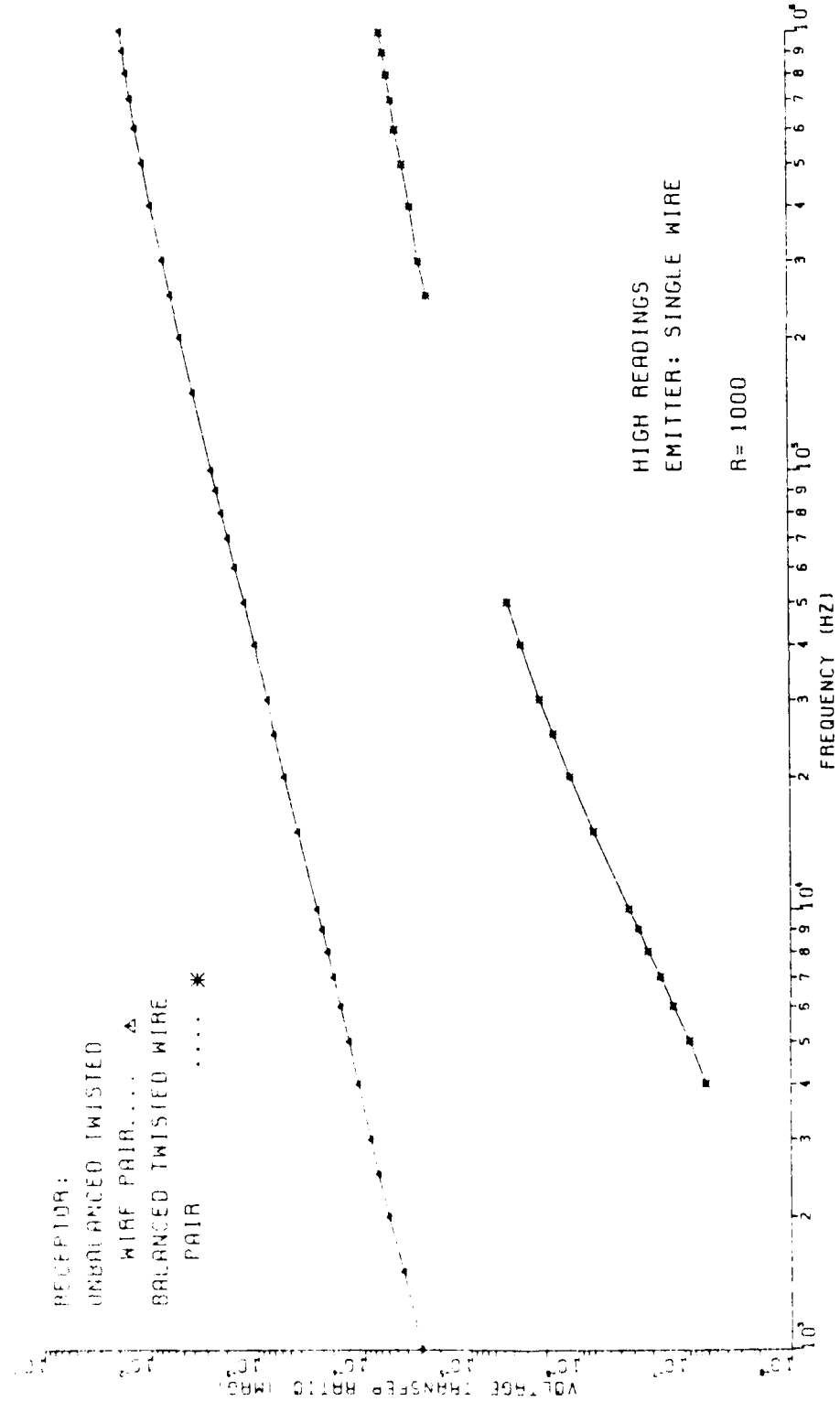
PLOT 5-4(c)



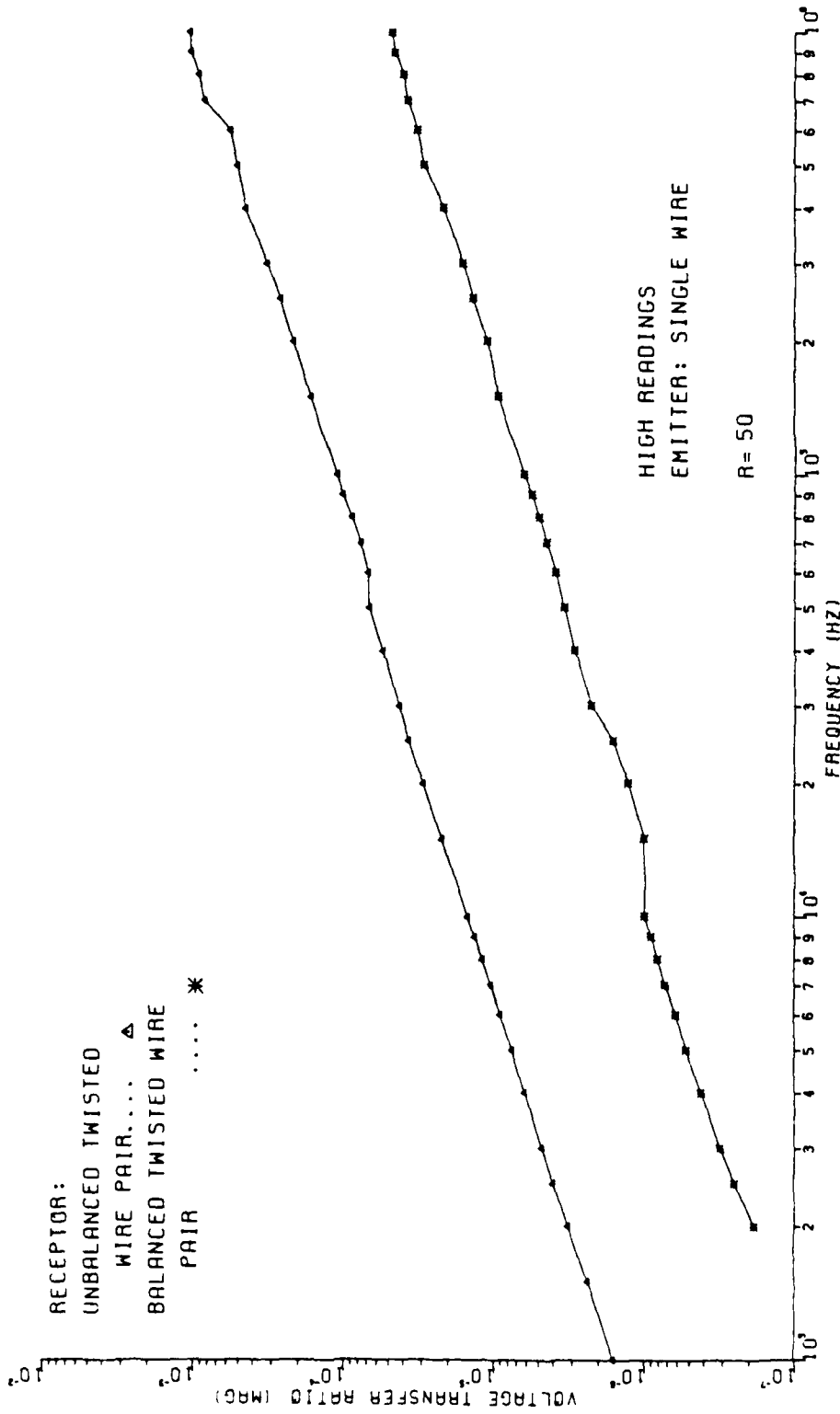
PLOT 5-4(b)



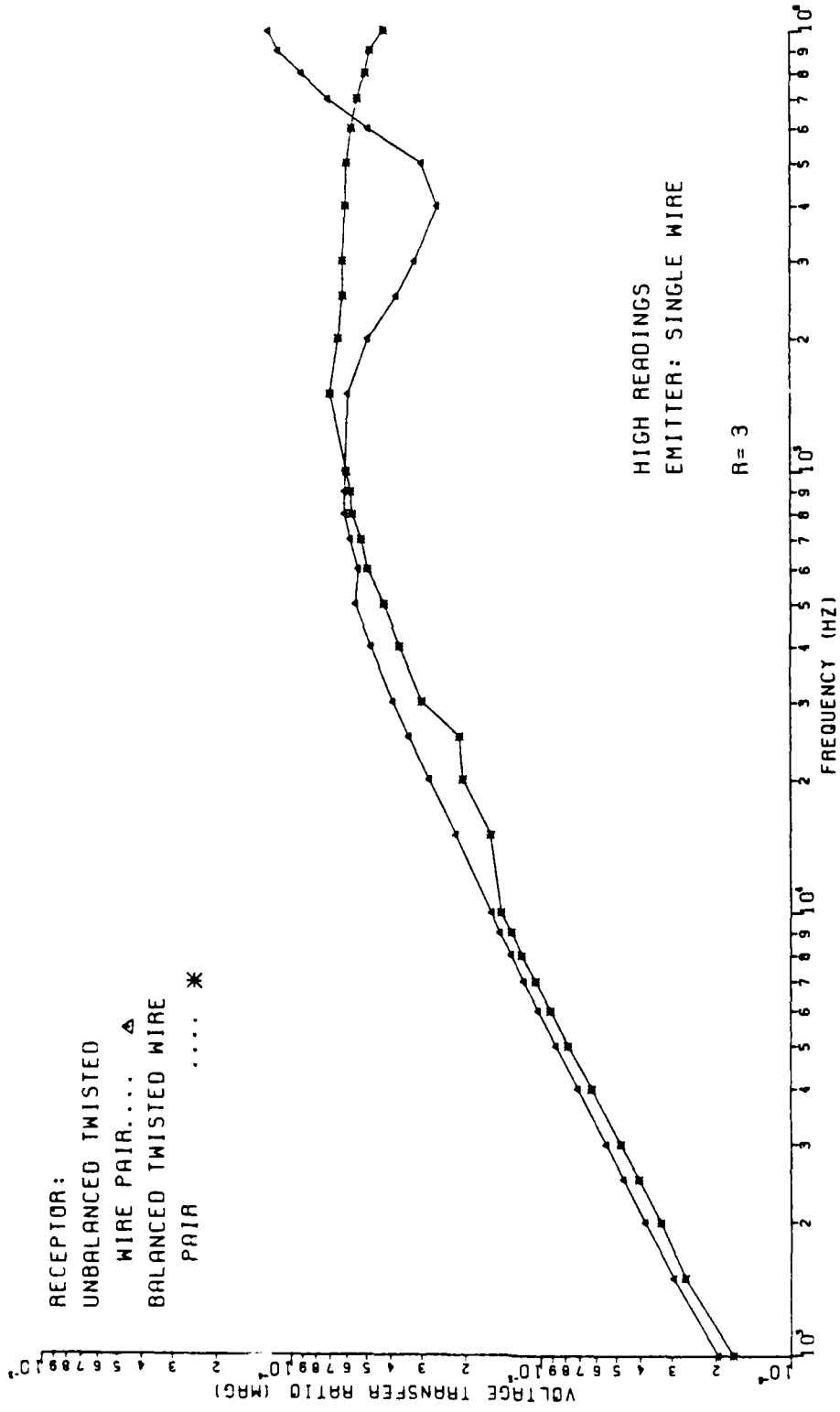
PLOT 5-4 (a)



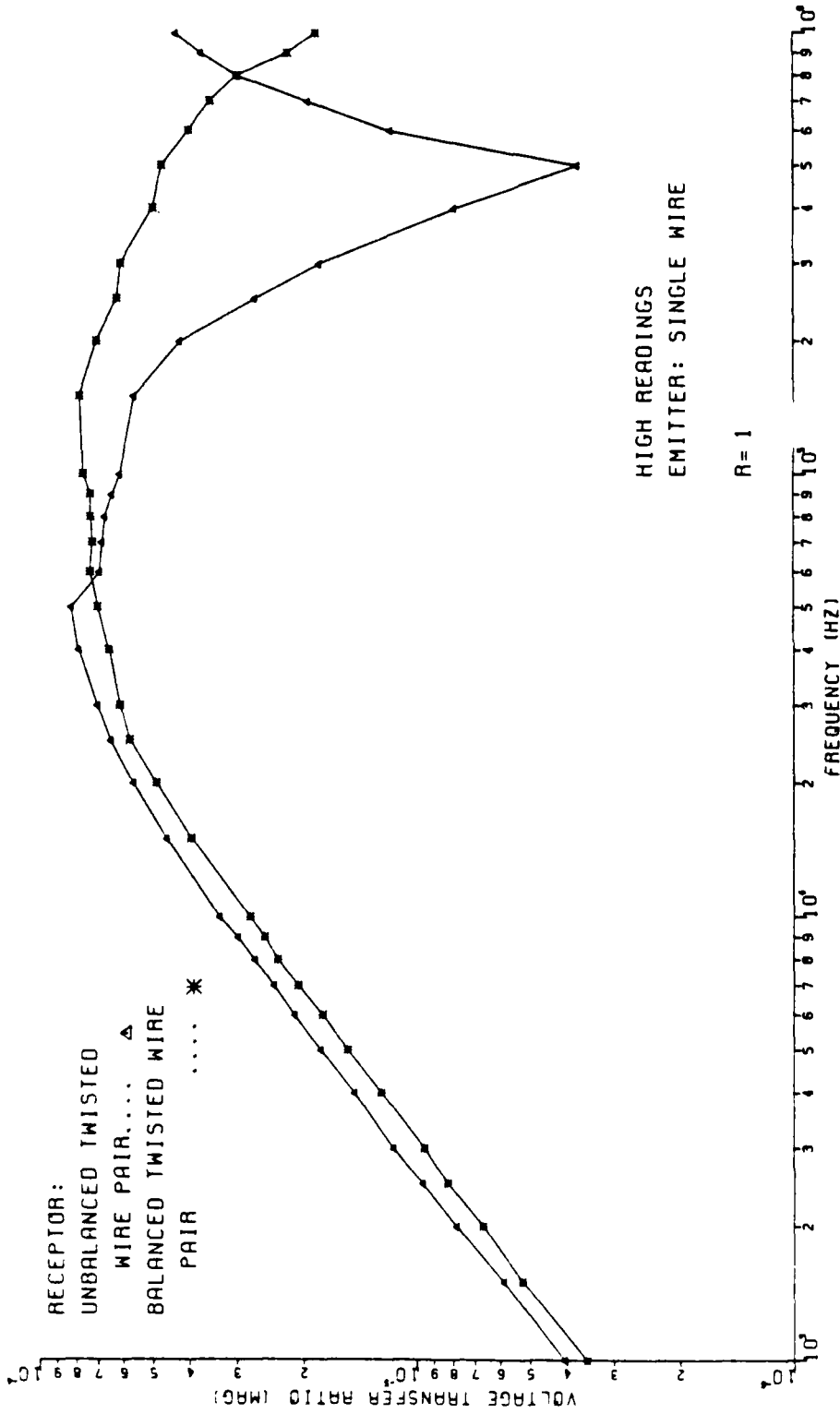
PLOT 5-3(d)



PLOT 5-3(c)



PLOT 5-3(b)

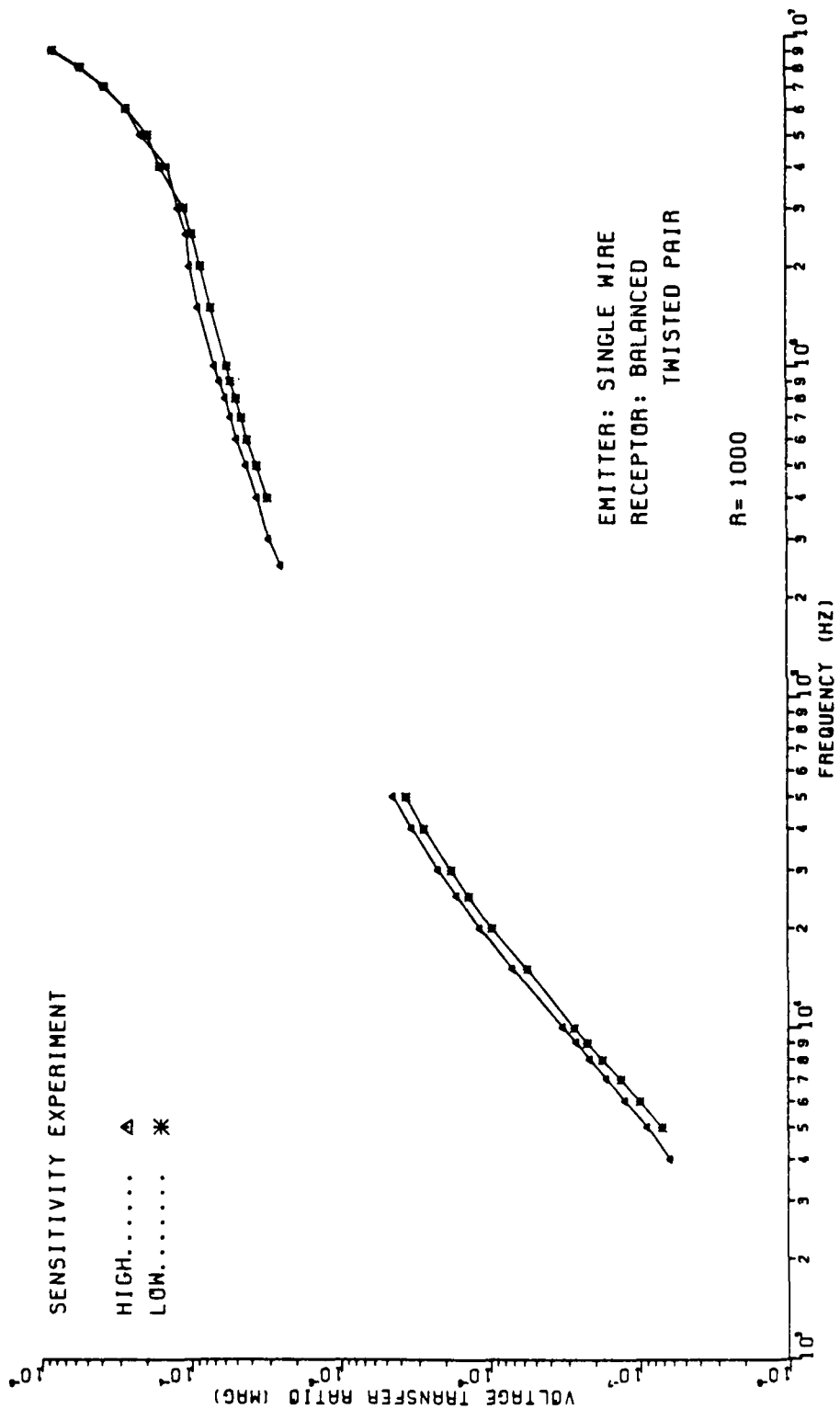


PLOT 5-3(a)

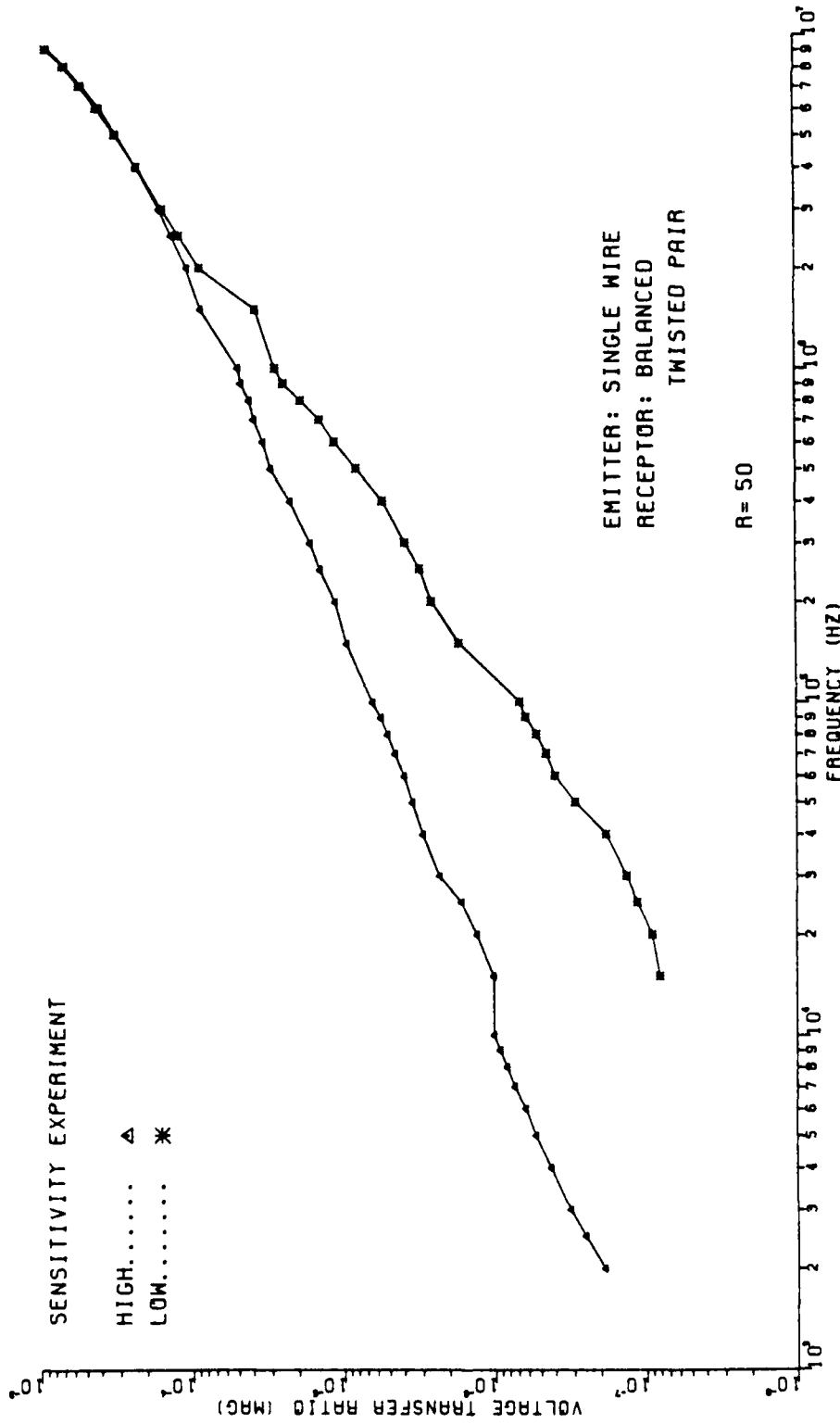
$R = 3\Omega$ results show a difference of about 20 dB.

The $R = 50\Omega$ results of Plot 5-3(c) show a difference between high and low readings of as much as 20 dB. When the receptor TWP was unbalanced, the $R = 50\Omega$ results showed virtually no sensitivity to line twist. The $R = 1\text{ k}\Omega$ results, given in Plots 5-2(d), still show virtually no sensitivity to line twist.

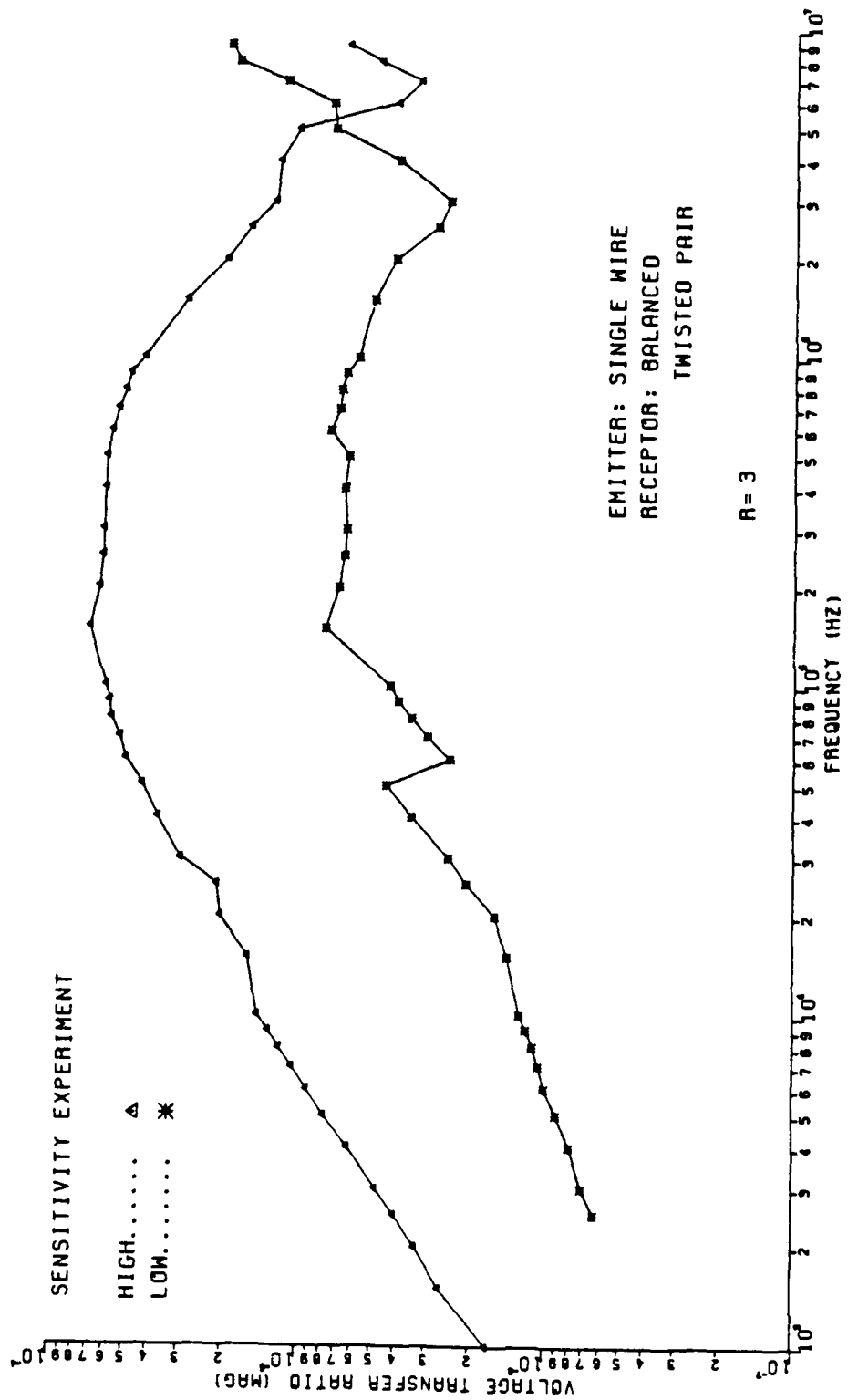
In an effort to demonstrate the effectiveness of balancing the terminal configurations of the receptor circuit TWP, the sensitivity results obtained for the unbalanced TWP receptor have been plotted against those obtained for the balanced TWP receptor. Plots 5-3(a) - 5-3(d) give a comparison of the high sensitivity readings for the two configurations and Plots 5-4(a) - 5-4(d) give a comparison of the low sensitivity readings. The comparisons for the low-impedance loads of 1Ω and 3Ω given in Plots 5-3(a), 5-3(b), 5-4(a) and 5-4(b) show no significant reduction in crosstalk by balancing the loads. The comparisons of the 50Ω results, Plots 5-3(c) and 5-4(c), show that balancing the loads reduces the crosstalk level by at least 20 dB for the high readings and by as much as 40 dB for the low readings. Finally, the comparisons of the $R = 1\text{ k}\Omega$ results of Plots 5-3(d) and 5-4(d) show that balancing the terminal configurations of the receptor TWP reduced the crosstalk level by at least 45 to 50 dB at all times! This is a tremendous reduction in the amount of



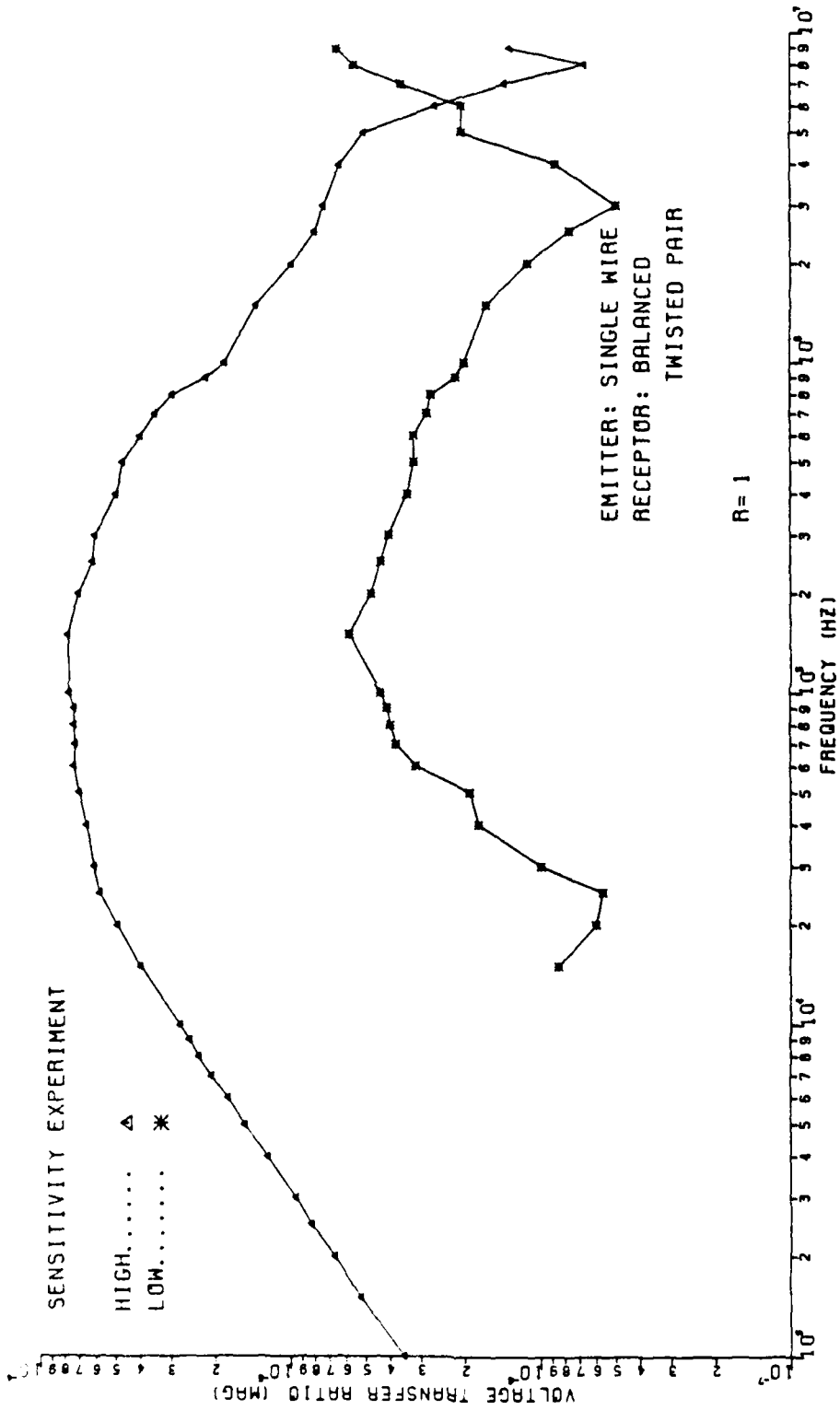
PLOT 5-2(d)



PLOT 5-2(c)



PLOT 5-2(b)



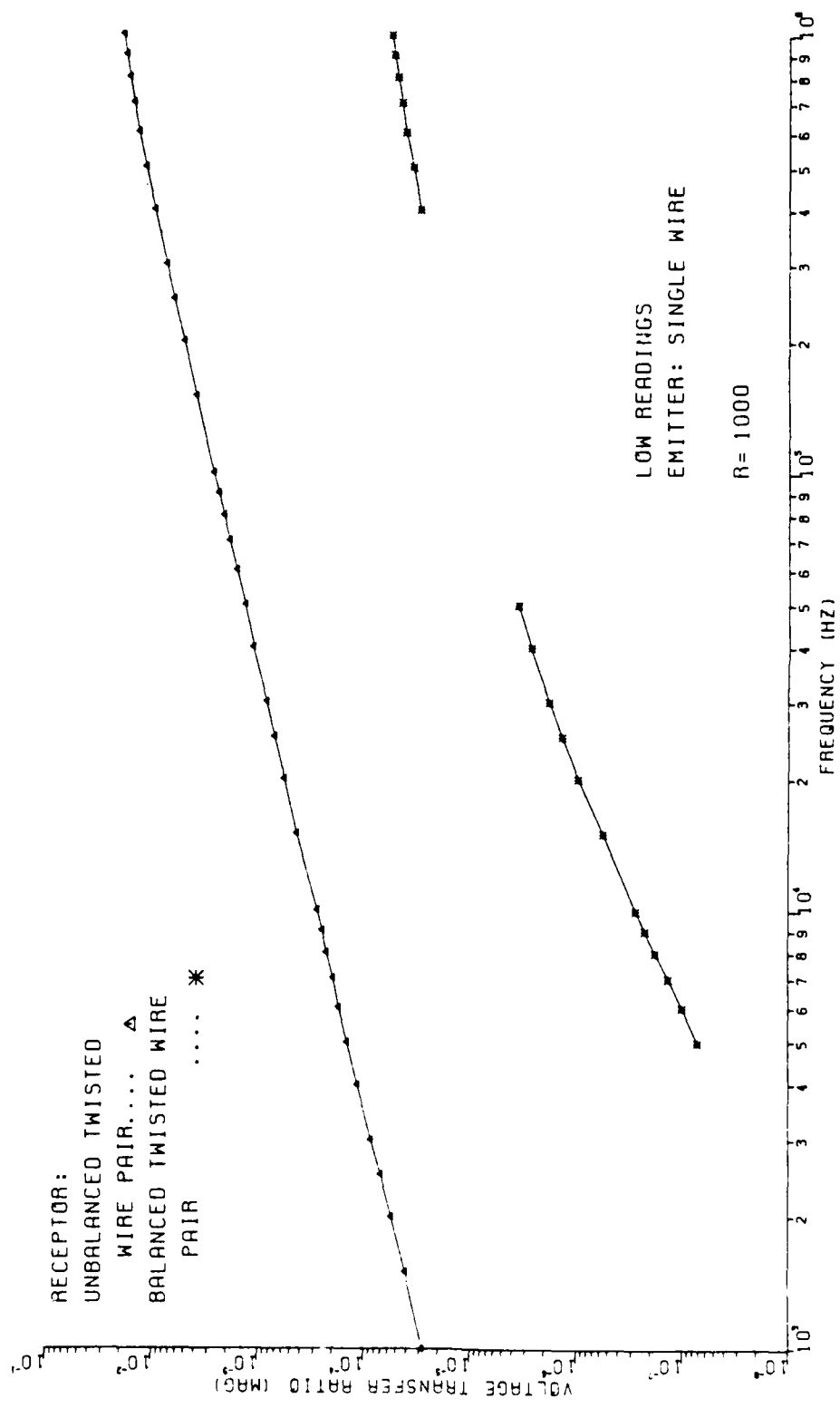
PLOT 5-2(a)

ratio was measured for all four impedance values with the TWP in this minimum position. These measurements constitute the low sensitivity readings. The $1\ \Omega$ impedances and the EMC-25 (tuned to 15 kHz) were again attached. The right end of the TWP was then rotated (no more than 180°) until a maximum response in V_{out} was found. The high sensitivity readings were taken for all impedance values with the TWP in the position of the maximum $1\ \Omega$ reading.

The results of the sensitivity experiment are given in Plots 5-2(a) - 5-2(d). There was no equipment available to measure the voltage transfer ratio for the $R = 1\ k\Omega$ load impedances (Plot 5-2(d)) between the frequencies of 60 kHz and 300 kHz, so the plot is discontinued in that frequency range. As was mentioned previously, it was thought that balancing the terminal configurations of the TWP receptor circuit would reduce the capacitive-coupling contribution to the crosstalk. With the reduction of this capacitive-coupling, it was expected that the sensitivity shown only for the low-impedance loads in the unbalanced TWP configuration would appear for all values of load impedance for the balanced TWP. The $R = 1\ \Omega$ and $R = 3\ \Omega$ results, Plots 5-2(a) and 5-2(b), respectively, show about the same amount of sensitivity as when the receptor circuit was an unbalanced TWP. The $R = 1\ \Omega$ plot shows a maximum difference in coupling of about 35 dB and the

the experimental measurements show some deviation from this behavior below 10 kHz, especially when $R = 1 \text{ k}\Omega$ (Plot 5-1(d)). The transformer used to balance the left end of the receptor circuit was a Vari-L LF-428 transformer. The specifications of these transformers are only valid over the 10 kHz to 100 MHz frequency range. Since the discrepancy between experimental and prediction results occurs for frequencies less than 10 kHz, it is believed that the permeability of the core of the transformer is deteriorating, causing the experimental measurements to roll-off at a faster rate below 10 kHz. Since the equivalent circuit used to model the transformer (See Appendix B) in both the low-frequency and transmission line models assumes the core permeability is infinite, neither model will predict any effects caused when the core permeability departs from this ideal assumption. However, when this roll-off does not appear in the experimental results, the prediction models give reasonable results for the cross-talk.

The SWP receptor circuit was replaced with a TWP receptor circuit and the sensitivity experiment was performed in the same way as outlined for the experiments in Chapters III and IV. The $R = 12$ loads were connected and the EMC-25 was attached to measure V_{out} and tuned to 15 kHz. By rotating the right end of the receptor TWP (no more than 180°) a minimum reading was found in V_{out} . The voltage transfer



PLOT 5-4(d)

crosstalk induced in the receptor circuit.

Thus, balancing the terminal configurations of the receptor TWP produced a large reduction in the crosstalk level when the load impedance was $1\text{ k}\Omega$ (and a significant, but somewhat less, reduction when $R = 50\Omega$). However, the high and low TWP readings for $R = 1\text{ k}\Omega$ still showed virtually no sensitivity to line twist. For this case of the balanced receptor TWP, a calculation of SWP^{CAP} does not provide a good prediction for the low TWP sensitivity readings for any value of load impedance. In fact, for the low-impedance loads, SWP^{CAP} falls very much below the TWP low readings whereas for the high-impedance loads SWP^{CAP} is greater than the TWP low readings. This might make one suspect that, for the balanced receptor TWP, TWP^{CAP} is sensitive to line twist. There is evidence to suggest that this is the case. Recall that because the second TWP wire was grounded in the unbalanced TWP configuration, TWP^{CAP} appeared to be insensitive to changes in line twist. If, for the balanced TWP configuration, TWP^{CAP} is sensitive to line-twist, the crosstalk level would be as difficult to predict as TWP^{IND} was in the previous configurations. Indeed, for the balanced TWP receptor circuit, both contributions to the crosstalk, inductive-coupling and capacitive-coupling, appear to be sensitive to variations in line twist, since the capacitive coupling current sources (see Figure 5-7) appear as differences with the result being

determined by the presence of an odd or even number of half twists. Since it is not possible to either determine or control the amount of twist in a practical installation, prediction of the crosstalk levels does not seem reasonable.

The purpose of this chapter was to determine the effectiveness of the balanced TWP receptor circuit. It was conclusively shown that the balanced TWP produced significant reduction in the crosstalk levels for both low and high-impedance loads. This was expected, qualitatively, from the concepts of inductive and capacitive coupling. Unlike the previous two chapters, however, the results of the TWP sensitivity experiments could not be predicted using the concepts of inductive- and capacitive-coupling, although these concepts adequately predicted the SWP results.

CHAPTER VI

SUMMARY AND CONCLUSIONS

Whenever transmission lines are used in close proximity to one another, electromagnetic fields will couple from one wire to another. The primary intent of this report was to investigate the crosstalk to a balanced (with respect to the terminal configurations) twisted wire pair (TWP). Also, the crosstalk from an unbalanced TWP to an unbalanced TWP was examined. The effectiveness of the TWP was explained in terms of inductive-coupling and capacitive-coupling. For example, for the case of the unbalanced TWP to unbalanced TWP configuration, the TWP's reduced the inductive-coupling, which was dependent on the amount of twist in the line, whereas the capacitive-coupling appeared to be insensitive to line twist and was not reduced by the twist. Thus, for low-impedance loads, where inductive-coupling dominated the crosstalk (when the wires were straight wire pairs (SWP's)), twisting the wires substantially reduced the crosstalk level. Also, for the low-impedance loads, the crosstalk to the receptor TWP was very sensitive to slight variations in line twist. This sensitivity was also explained using the concept that inductive-coupling is dependent on the number of half-twists, even or odd, in the receptor TWP but, for this configuration, capacitive-coupling is insensitive to line twist.

The results of using a balanced TWP receptor circuit were, qualitatively, easily explained using the concepts of inductive- and capacitive-coupling. As was expected, balancing the TWP terminal configurations provided a significant reduction in crosstalk over the unbalanced configuration for the high-impedance loads, when capacitive-coupling was dominant. This was thought to occur because balancing the terminations reduced the capacitive-coupling floor. However, with the reduction of the capacitive-coupling, the same sensitivity to variations in line twist formerly only exhibited by low-impedance loads for the unbalanced TWP was expected for all loads. This sensitivity was not observed for the high-impedance loads. Also, it was no longer possible to provide a good prediction of the low TWP sensitivity results with the capacitive-coupling floor. Further investigation seems to indicate that for the balanced TWP configuration, both inductive-coupling and capacitive-coupling are dependent on the amount of twist in the line.

For the TWP configurations examined in Chapters III, IV and V, the crosstalk was computed with the low-frequency inductive- and capacitive-coupling model and with a transmission line model. For sufficiently low frequencies, both models provided adequate predictions of the crosstalk. For higher frequencies, only the transmission line model was able to predict the crosstalk, although the results at

high frequencies were not as good as at low frequencies. The low-frequency model changes linearly with frequency, so the results of this model can be easily determined with a small calculator. The transmission line model, however, must be calculated by solving simultaneous equations for each value of frequency desired, and is therefore more readily determined through the use of a computer program. Thus, for sufficiently small frequencies, the low-frequency model is significantly more efficient, computationally, than the transmission line model. Also, the low-frequency model provides a qualitative analysis of the crosstalk through the concepts of inductive- and capacitive-coupling, and the dominance of one type of coupling over the other.

Better models to predict the crosstalk to a TWP, balanced or unbalanced, are still needed. The sensitivity that was observed for some load impedances appears to rule out the possibility of exact prediction models. One alternative could be a model that would provide upper and lower bounds on the crosstalk. An attempt was made to determine an upper bound for the single wire with ground return generator circuit to unbalanced TWP receptor circuit for the low-impedance loads. By using the low-impedance of $R = 1\Omega$ and $R = 3\Omega$, the high bound could essentially be determined by the inductive-coupling to one half-twist of the TWP. Representing the TWP as a circular helix, the

magnetic flux penetrating one loop of the TWP can be found by determining the total magnetic flux, $\int B \cdot ds$, over one half-twist. Substitution of the proper parameters into this integral and setting the limits for integration over one half-twist yields an integral of the form

$$\int_0^{\pi/2} \ln(1 + a \sin\theta + b \cos\theta) d\theta$$

which is not possible to integrate in closed form. Therefore, a computer program was written to calculate this integral using a Gaussian quadrature routine. The results of this analysis did not give good predictions of the high readings of the low-impedance loads. This analysis seemed to indicate, however, that the nonuniformity of the twist of the TWP could greatly affect the high readings, so that the upper bound of a prediction model would not simply depend on one half-twist of the TWP, but would depend on the nonuniformity of the twists. Obviously, a model that must know the nonuniformity in the twist of a line is not useful. From a purely theoretical view, a TWP could be constructed to have uniform twist, so that the above analysis could be tested, but since such TWPs do not exist in practical situations, such an experiment did not seem worthwhile.

In an effort to achieve optimum system design, it is important to know when crosstalk will cause a problem and how to reduce crosstalk to prevent those problems. In the past, it was widely accepted that using twisted wire pairs reduced crosstalk, and that using balanced TWP's further reduced crosstalk. Both statements are true, but the degree to which the crosstalk is reduced has been shown to be strongly dependent on such parameters as the values of load impedance. At a time when the efficiency of a system is in part determined by weight and size, an understanding of the manner in which electromagnetic coupling occurs, even if it is only through a simple low-frequency model like examined in this report, could help prevent the addition of unnecessary bulk to a system. It can also serve to provide an optimum system design from the standpoint of reduction of crosstalk to acceptable levels. The results of this report should provide this type of understanding.

APPENDIX A

The transmission line model used to calculate the voltage transfer ratio of the SWP configurations investigated in Chapters III - VI is explained in this Appendix. Before the specific transmission line model which was used is examined, a general $(n + 1)$ conductor line (Figure A-1) will be reviewed [8]. This line consists of n conductors and a ground plane return. Under the assumption of TEM mode of propagation on the line, the voltages and currents of the line can be uniquely defined and are represented by $n \times 1$ vectors

$$\underline{V}(x) = \begin{bmatrix} V_1(x) \\ V_2(x) \\ \vdots \\ V_n(x) \end{bmatrix} \quad (\text{A-1a})$$

$$\underline{I}(x) = \begin{bmatrix} I_1(x) \\ I_2(x) \\ \vdots \\ I_n(x) \end{bmatrix} \quad (\text{A-1b})$$

The transmission line equations are given by

$$\underline{V}'(x) = - \left[\underline{Z}_0 + j\omega \left(\underline{L}_0 + \underline{L}_{ex} \right) \right] \underline{I}(x) \quad (\text{A-2a})$$

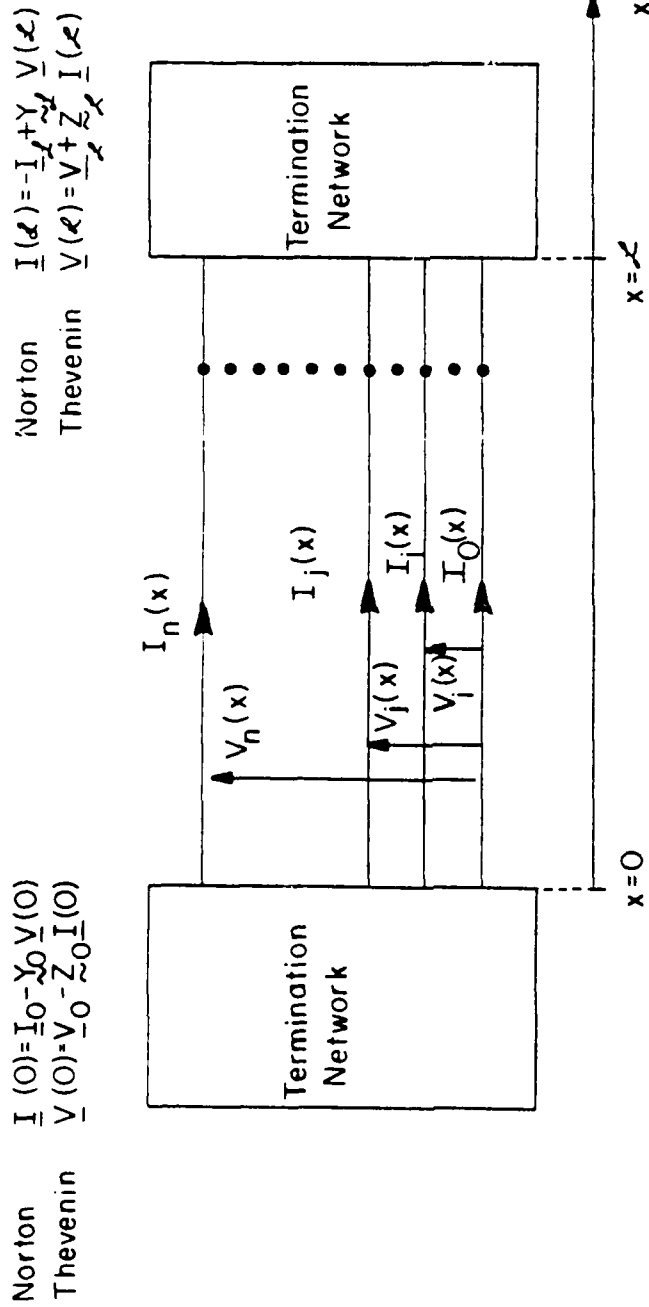


FIGURE A-1. A GENERAL (n + 1) CONDUCTOR LINE.

and

$$\underline{\dot{I}}(x) = -j\omega \underline{C} \underline{V}(x) \quad (A-2b)$$

$\underline{\dot{V}}(x)$ and $\underline{\dot{I}}(x)$ signify the differentiation of each element of the vectors with respect to x . For example,

$$\underline{\dot{V}}(x) = \begin{bmatrix} \frac{d V_1(x)}{dx} \\ \frac{d V_2(x)}{dx} \\ \vdots \\ \frac{d V_n(x)}{dx} \end{bmatrix} \quad (A-3)$$

The matrices \underline{R} , \underline{L}_c , \underline{L}_{ex} and \underline{C} are of dimension $n \times n$ and contain the per-unit-length parameters of the line. \underline{L}_{ex} contains the per-unit-length parameters of self inductance and mutual inductance. \underline{C} contains the per-unit-length self and mutual capacitances. The presence of \underline{R} and \underline{L}_c is due to imperfect conductors. \underline{R} represents ohmic resistances of the conductors and \underline{L}_c represents the internal inductances of the conductors. This report, however, assumes perfect conductors so that \underline{R} and \underline{L}_c are removed. Therefore, to simplify notation, \underline{L}_{ex} will simply be referred to as \underline{L} . The transmission line equations then become

$$\dot{\underline{V}}(x) = -j\omega \underline{L} \underline{I}(x) \quad (\text{A-4a})$$

$$\dot{\underline{I}}(x) = -j\omega \underline{C} \underline{V}(x) \quad (\text{A-4b})$$

In deriving a transmission line model to evaluate the configuration shown in Figure A-1, it is necessary to relate the voltages and currents at one end of the line, $\underline{V}(0)$ and $\underline{I}(0)$, to the voltages and currents at the other end of the line, $\underline{V}(L)$ and $\underline{I}(L)$. This can be accomplished through the use of chain parameter matrix by

$$\begin{bmatrix} \underline{V}(L) \\ \underline{I}(L) \end{bmatrix} = \underbrace{\begin{bmatrix} \underline{\rho}_{11}(L) & \underline{\rho}_{12}(L) \\ \underline{\rho}_{21}(L) & \underline{\rho}_{22}(L) \end{bmatrix}}_{\underline{\rho}} \begin{bmatrix} \underline{V}(0) \\ \underline{I}(0) \end{bmatrix} \quad (\text{A-5})$$

where $\underline{\rho}$ is the $2n \times 2n$ chain parameter matrix of the line. The line is now completely characterized by $\underline{\rho}$. For no dielectric insulation and perfect conductors, the $n \times n$ $\underline{\rho}_{ij}$ are given by [1]

$$\underline{\rho}_{11} = \cos(\beta L) \underline{1}_n \quad (\text{A-6a})$$

$$\underline{\rho}_{12} = -j \sin(\beta L) \underline{1}_n \quad (\text{A-6b})$$

$$\underline{\rho}_{21} = -j \sin(\beta L) \underline{C} \quad (\text{A-6c})$$

$$\underline{\rho}_{22} = \cos(\beta L) \underline{1}_n \quad (\text{A-6d})$$

where β is the phase constant defined by

$$\beta = \omega/v \quad (A-7)$$

and v is the velocity of propagation in the surrounding medium defined by

$$v = \frac{1}{\sqrt{\mu\epsilon}} \quad (A-8)$$

We will assume free space as the medium so that

$v = 3 \times 10^8$ m/s. The radian frequency of excitation is ω .

The terminal networks of Figure A-1 can be represented by either generalized Thevenin Equivalents

$$\underline{V}(0) = \underline{V}_0 - \underline{Z}_0 \underline{I}(0) \quad (A-9a)$$

$$\underline{V}(L) = \underline{V}_L + \underline{Z}_L \underline{I}(L) \quad (A-9b)$$

or Generalized Norton Equivalents

$$\underline{I}(0) = \underline{I}_0 - \underline{Y}_0 \underline{I}(0) \quad (A-10a)$$

$$\underline{I}(L) = -\underline{I}_L + \underline{Y}_L \underline{I}(L) \quad (A-10b)$$

The vectors \underline{V}_0 and \underline{V}_L represent open circuit voltages between each wire and ground for the appropriate terminal network. Similarly, \underline{I}_0 and \underline{I}_L represent the short circuit currents of the appropriate circuit. \underline{Z}_0 and \underline{Z}_L are the $n \times n$ impedance matrices which characterize these terminations. Similarly \underline{Y}_0 and \underline{Y}_L are the $n \times n$ admittance matrices which also characterize the terminations. For the configurations investigated in this report, it was easiest to represent the left end of the line by a Thevenin Equivalent (Equation A-9a) and the right end of the line by a Norton Equivalent (Equation A-10b).

The currents $\underline{I}(0)$ can be determined, through substitution of the terminal conditions into Equation A-5, from

$$\begin{aligned} & [\underline{Y}_L \underline{Z}_{11}(L) \underline{Z}_0 - \underline{Z}_L \underline{\phi}_{12}(L) - \underline{\phi}_{21}(L) \underline{Z}_0 + \underline{\phi}_{22}(L)] \underline{I}(0) \\ & = [\underline{Y}_L \underline{Z}_{11}(L) - \underline{\phi}_{21}(L)] \underline{V}_0 + \underline{I}_L \end{aligned} \quad (A-11)$$

The voltage transfer ratio of the configurations of this report can be found once $\underline{I}(0)$ is known.

The following three sections pertain to the specific configurations of this report. Each section will define

$$\underline{\tilde{y}}_L = \begin{bmatrix} \frac{1}{\underline{B}_L G} & 0 & 0 \\ 0 & \frac{1}{\underline{B}_L R} & -\frac{1}{\underline{B}_L R} \\ 0 & -\frac{1}{\underline{B}_L R} & \frac{1}{\underline{B}_L R} \end{bmatrix} \quad (A-31)$$

The entries of \underline{I}_L are all equal to zero.

and

$$I_G (L) = \left(\frac{1}{Z_{LG}}\right) V_G (L) \quad (A-28a)$$

$$I_{R1} (L) = \left(\frac{1}{Z_{LR}}\right) V_{R1} (L) - \left(\frac{1}{Z_{LR}}\right) V_{R2} (L) \quad (A-28b)$$

$$I_{R2} (L) = -\left(\frac{1}{Z_{LR}}\right) V_{R1} (L) + \left(\frac{1}{Z_{LR}}\right) V_{R2} (L) \quad (A-28c)$$

Equation A-9a and A-27 yield

$$\underline{Z}_{00} = \begin{bmatrix} 0 & 0 & 0 \\ 0 & Z_{OR} & -Z_{OR} \\ 0 & -Z_{OR} & Z_{OR} \end{bmatrix} \quad (A-29)$$

and

$$\underline{V}_0 = \begin{bmatrix} 1 \\ 0 \\ 0 \end{bmatrix} \quad (A-30)$$

Equations A-19b and A-28 yield

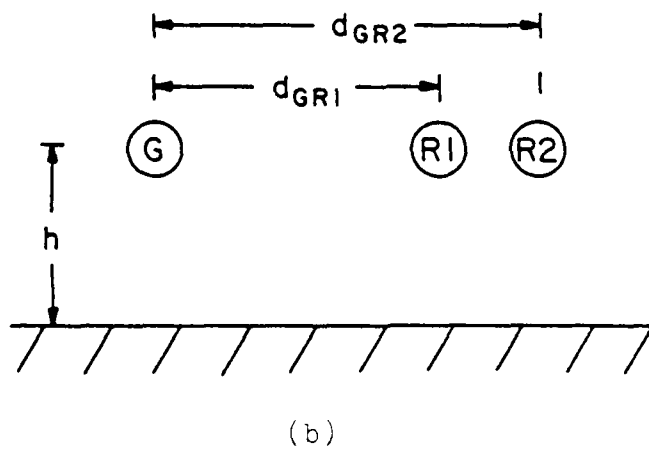
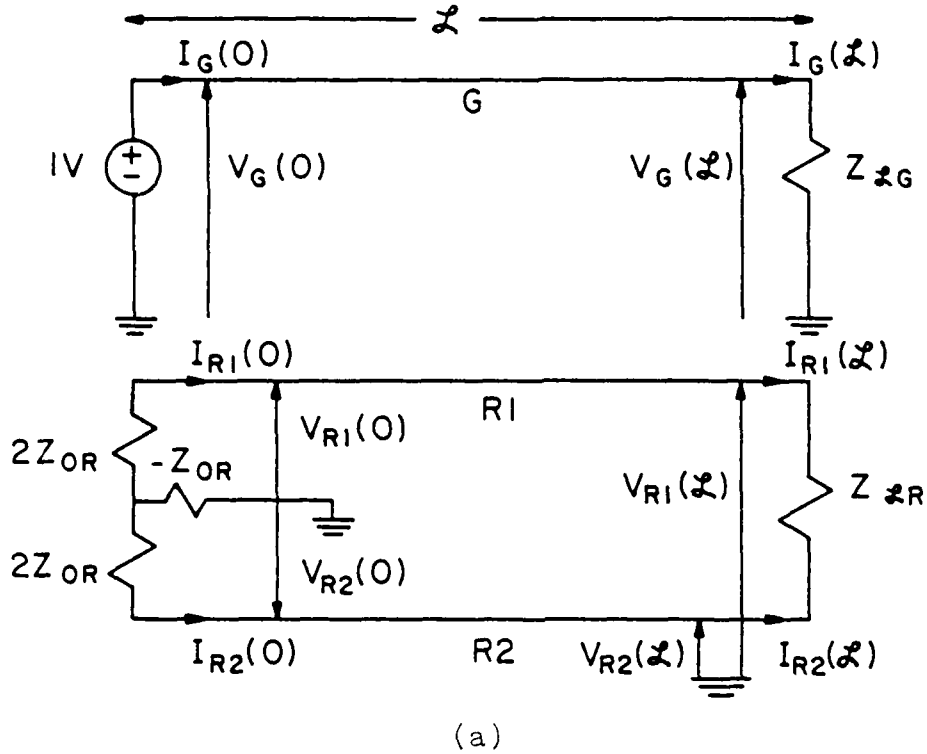


FIGURE A-4. THE SINGLE WIRE GENERATOR CIRCUIT TO BALANCED SWP RECEPTOR CIRCUIT.
 (a) LONGITUDINAL VIEW. (b) CROSS-SECTIONAL VIEW.

A.2 The Single Wire Generator Circuit to Balanced,
SWP Receptor Circuit Configuration

The configuration (Figure A-4) described in Chapter V is examined here. The generator circuit is a single wire with ground return. The receptor circuit is a balanced SWP. This is a four conductor line, therefore \underline{L} , \underline{C} , \underline{R}_0 and \underline{Y}_0 are matrices of dimension 3 x 3 and \underline{V}_0 and \underline{I}_0 are vectors of dimension 3 x 1.

Notice that the cross-sectional view of the SWP configuration of this section is the same as the cross-sectional view of the SWP configuration of Section A.1. This means that the per-unit-length inductance matrix, \underline{L} , of this section is the same as that given in Section A.1.

The terminal conditions are found by examining Figure A-4. Notice that the 1:2 transformer used to balance the left end of the receptor circuit SWP has been modeled as described in Appendix B.

$$V_{RL}(0) = 1 \quad (A-27a)$$

$$V_{RL}(0) = -S_{BR} I_{RL}(0) + S_{BR} I_{RC}(0) \quad (A-27b)$$

$$V_{RL}(0) = S_{FR} I_{FL}(0) - S_{FR} I_{RC}(0) \quad (A-27c)$$

Equations A-10b and A-23 yield

$$\underline{y}_L = \begin{bmatrix} \frac{1}{\bar{b}L_G} & -\frac{1}{\bar{b}L_G} & 0 & 0 \\ -\frac{1}{\bar{b}L_G} & \frac{1}{\bar{b}L_G} & 0 & 0 \\ 0 & 0 & \frac{1}{\bar{z}L_R} & -\frac{1}{\bar{z}L_R} \\ 0 & 0 & -\frac{1}{\bar{z}L_R} & \frac{1}{\bar{z}L_R} \end{bmatrix} \quad (\text{A-26})$$

The elements of \underline{I}_L are equal to zero.

Notice that the generator wires of this section are numbered differently than they were in Chapter IV. This is done to facilitate the use of the computer program which analyzes the transmission line model. The numbering of the wires in Chapter IV is still correct for the low-frequency SWF model described there.

and

$$I_{G1}(\mathcal{L}) = \left(\frac{1}{Z_{LG}}\right) V_{G1}(\mathcal{L}) - \left(\frac{1}{Z_{LG}}\right) V_{G2}(\mathcal{L}) \quad (\text{A-23a})$$

$$I_{G2}(\mathcal{L}) = \left(\frac{1}{Z_{LG}}\right) V_{G1}(\mathcal{L}) + \left(\frac{1}{Z_{LG}}\right) V_{G2}(\mathcal{L}) \quad (\text{A-23b})$$

$$I_{R1}(\mathcal{L}) = \left(\frac{1}{Z_{LR}}\right) V_{R1}(\mathcal{L}) - \left(\frac{1}{Z_{LR}}\right) V_{R2}(\mathcal{L}) \quad (\text{A-23c})$$

$$I_{R2}(\mathcal{L}) = -\left(\frac{1}{Z_{LR}}\right) V_{R1}(\mathcal{L}) + \left(\frac{1}{Z_{LR}}\right) V_{R2}(\mathcal{L}) \quad (\text{A-23d})$$

Equations A-9a and A-22 yield

$$\underline{I}_G = \begin{bmatrix} 0 & 0 & 0 & 0 \\ 0 & 0 & 0 & 0 \\ 0 & 0 & Z_{OR} & 0 \\ 0 & 0 & 0 & 0 \end{bmatrix} \quad (\text{A-24})$$

and

$$\underline{V}_G = \begin{bmatrix} 0 \\ 1 \\ 0 \\ 0 \end{bmatrix} \quad (\text{A-25})$$

$$L_{G1G2} = \frac{\mu_0}{4\pi} \ln \left(1 + \frac{4h^2}{d_{G1G2}^2} \right) \quad (\text{A-21e})$$

$$L_{G1R1} = \frac{\mu_0}{4\pi} \ln \left(1 + \frac{4h^2}{d_{G1R1}^2} \right) \quad (\text{A-21f})$$

$$L_{G1R2} = \frac{\mu_0}{4\pi} \ln \left(1 + \frac{4h^2}{d_{G1R2}^2} \right) \quad (\text{A-21g})$$

$$L_{G2R1} = \frac{\mu_0}{4\pi} \ln \left(1 + \frac{4h^2}{(d_{G1G2} - d_{G1R1})^2} \right) \quad (\text{A-21h})$$

$$L_{G2R2} = \frac{\mu_0}{4\pi} \ln \left(1 + \frac{4h^2}{(d_{G1G2} - d_{G1R2})^2} \right) \quad (\text{A-21i})$$

$$L_{R1R2} = \frac{\mu_0}{4\pi} \ln \left(1 + \frac{4h^2}{(d_{G1R1} - d_{G1R2})^2} \right) \quad (\text{A-21j})$$

The other elements of \underline{L} are found by realizing that \underline{L} is symmetric and again all wires are identical with radii r_w .

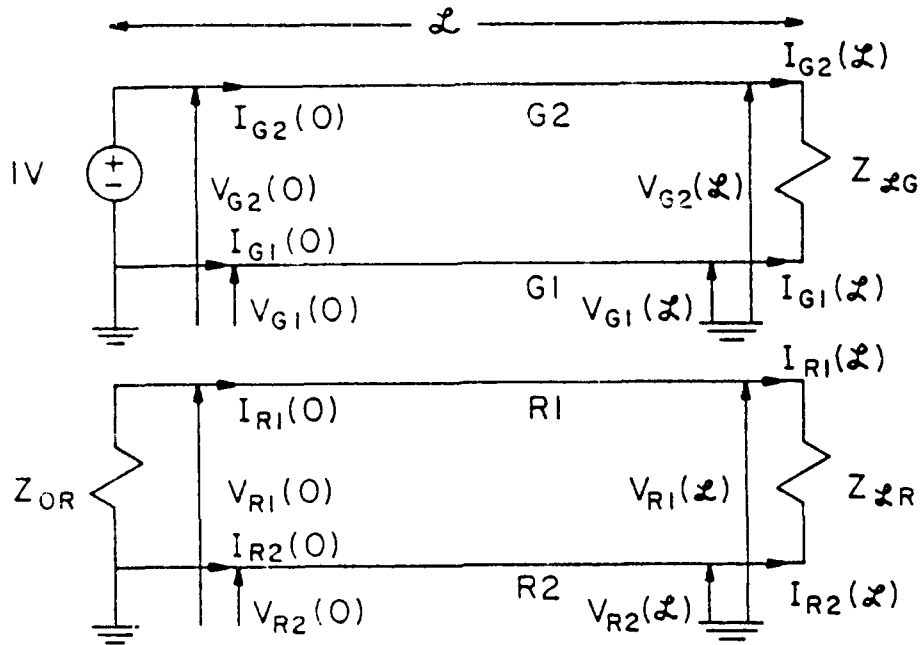
The terminal conditions are found by analyzing Figure A-3.

$$V_{G1}(0) = 1 \quad (\text{A-22a})$$

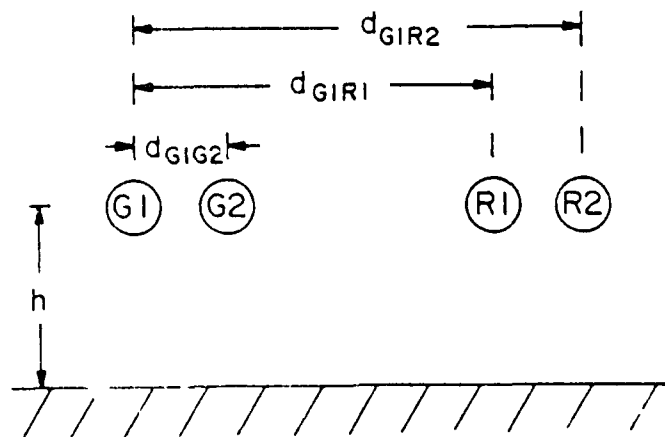
$$V_{G2}(0) = 0 \quad (\text{A-22b})$$

$$V_{R1}(0) = -S_{GR} I_{R1}(0) \quad (\text{A-22c})$$

$$V_{R2}(0) = 0 \quad (\text{A-22d})$$



(2)



(3)

1. Diagram of the equivalent circuit of the generator circuit of a transmission line of length L .
 2. Diagram of the physical layout of the conductors in the cross-sectional view.

A.2 The Unbalanced SWP Generator Circuit to Unbalanced SWP Receptor Circuit Configuration

The unbalanced SWP generator circuit to unbalanced SWP receptor circuit (Figure A-3) described in Chapter IV is examined here. This is a five conductor line, therefore \underline{L} , \underline{C} , \underline{Z}_0 and \underline{Y}_L are 4 x 4 matrices. \underline{V}_0 and \underline{I}_L are vectors of dimension 4 x 1.

The per-unit-length inductance matrix is

$$\underline{L} = \begin{bmatrix} L_{G1G1} & L_{G1G2} & L_{G1R1} & L_{G1R2} \\ L_{G2G1} & L_{G2G2} & L_{G2R1} & L_{G2R2} \\ L_{R1G1} & L_{R1G2} & L_{R1R1} & L_{R1R2} \\ L_{R2G1} & L_{R2G2} & L_{R2R1} & L_{R2R2} \end{bmatrix} \quad (A-20)$$

The elements of L are given by [9]

$$L_{G1R1} = \frac{\mu_0}{2\pi} \ln \frac{2h}{r_w} \quad (A-21a)$$

$$L_{G2R1} = \frac{\mu_0}{2\pi} \ln \frac{2h}{r_w} \quad (A-21b)$$

$$L_{R1R1} = \frac{\mu_0}{2\pi} \ln \frac{2h}{r_w} \quad (A-21c)$$

$$L_{R2R2} = \frac{\mu_0}{2\pi} \ln \frac{2h}{r_w} \quad (A-21d)$$

Equations A-9a and A-16 yield

$$\underline{z}_0 = \begin{bmatrix} 0 & 0 & 0 \\ 0 & z_{CR} & 0 \\ 0 & 0 & 0 \end{bmatrix} \quad (A-18)$$

and

$$\underline{v}_0 = \begin{bmatrix} 1 \\ 0 \\ 0 \end{bmatrix} \quad \underline{I}_L = \begin{bmatrix} 0 \\ 0 \\ 0 \end{bmatrix} \quad (A-19)$$

Equations A-10b and A-17 yield

$$\underline{y}_L = \begin{bmatrix} \frac{1}{z_{LG}} & 0 & 0 \\ 0 & \frac{1}{z_{LR}} & -\frac{1}{z_{LR}} \\ 0 & -\frac{1}{z_{LR}} & \frac{1}{z_{LR}} \end{bmatrix} \quad (A-20)$$

$$L_{GR1} = \frac{\mu_0}{2\pi} \ln \left(1 + \frac{4 h^2}{d_{GR1}^2} \right) \quad (A-15d)$$

$$L_{GR2} = \frac{\mu_0}{2\pi} \ln \left(1 + \frac{4 h^2}{d_{GR2}^2} \right) \quad (A-15e)$$

$$L_{R1R2} = \frac{\mu_0}{2\pi} \ln \left(1 + \frac{4 h^2}{(d_{GR2} - d_{GR1})^2} \right) \quad (A-15f)$$

L is symmetric and all three wires are identical with radii r_w .

The terminal conditions are found through evaluation of Figure A-2.

$$V_G (0) = 1 \quad (A-16a)$$

$$V_{R1} (0) = -Z_{OR} I_{R1} (0) \quad (A-16b)$$

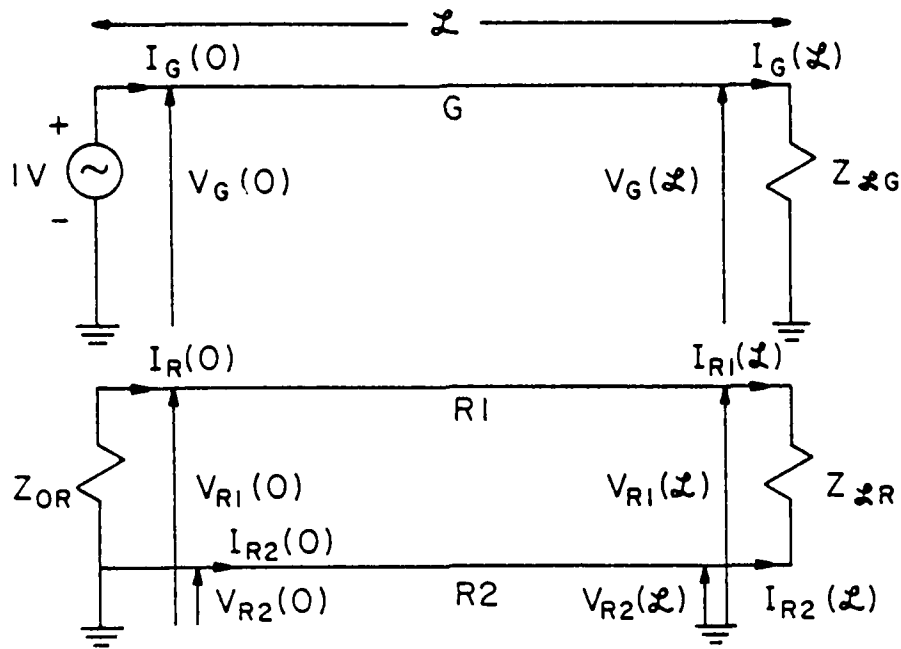
$$V_{R2} (0) = 0 \quad (A-16c)$$

and

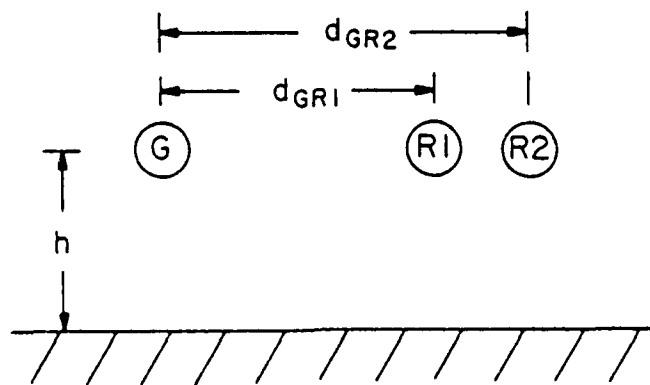
$$I_G (L) = \left(\frac{1}{Z_{LG}} \right) V_G (L) \quad (A-17a)$$

$$I_{R1} (L) = \left(\frac{1}{Z_{LR}} \right) V_{R1} (L) - \left(\frac{1}{Z_{LR}} \right) V_{R2} (L) \quad (A-17b)$$

$$I_{R2} (L) = - \left(\frac{1}{Z_{LR}} \right) V_{R1} (L) + \left(\frac{1}{Z_{LR}} \right) V_{R2} (L) \quad (A-17c)$$



(a)



(b)

FIGURE A-2. THE SINGLE WIRE GENERATOR TO STRAIGHT WIRE PAIR (SWP) RECEPTOR CONFIGURATION.
 (a) LONGITUDINAL VIEW. (b) CROSS-SECTIONAL VIEW.

A.1 The Single Generator Wire to Straight Wire Pair
(SWP) Receptor Configuration

The SWP configuration described in Chapter III is examined here (Figure A-2). The generator circuit consists of a single wire with ground return. The receptor circuit is an unbalanced SWP. This is a four conductor line (the three conductors and ground plane return), therefore \underline{L} , \underline{C} , \underline{Z}_0 and \underline{Y}_L are of dimension 3 x 3.

The per-unit-length inductance matrix is

$$\underline{L} = \begin{bmatrix} L_{GG} & L_{GR1} & L_{GR2} \\ L_{RG} & L_{R1R1} & L_{R1R2} \\ L_{R2G} & L_{R2R1} & L_{R2R2} \end{bmatrix} \quad (A-14)$$

The elements of \underline{L} for the cross-sectional configuration investigated and shown in Figure A-2(b) are given by [8]

$$L_{GG} = \frac{\mu_0}{2\pi} \ln\left(\frac{2h}{r_w}\right) \quad (A-15a)$$

$$L_{R1R1} = \frac{\mu_0}{2\pi} \ln\left(\frac{2h}{r_w}\right) \quad (A-15b)$$

$$L_{R2R2} = \frac{\mu_0}{2\pi} \ln\left(\frac{2h}{r_w}\right) \quad (A-15c)$$

the per-unit-length matrix \underline{L} and will determine the terminal conditions \underline{Z}_0 , \underline{Y}_L , \underline{V}_0 and \underline{I}_L necessary to use the transmission line model. Recall that \underline{C} can be found from

$$\underline{C} = \frac{1}{v^2} \underline{L}^{-1} \quad (\text{A-13})$$

and therefore does not need to be given explicitly.

APPENDIX B

This appendix explains the equivalent circuit used to model the center-tapped transformer (Figure B-1) in Chapter V. The transformer consists of three coils wound on a ferromagnetic, high permeability core (Figure B-2). A comparison of Figures B-1 and B-2 shows that the dot convention was used to define the proper polarities (directions) of the voltages (currents) of the windings. The windings are numbered 0, 1 and 2 and consist of N_0 , N_1 or N_2 turns, respectively.

To determine voltage relationships between the primary and secondary windings, consider Faraday's law:

$$\oint_C \mathbf{E} \cdot d\mathbf{l} = - \frac{d}{dt} \Psi \quad (\text{B-1})$$

For an ideal transformer, the same flux links all three coils. Therefore,

$$v_0 = -N_0 \frac{d\Psi}{dt} \quad (\text{B-2a})$$

$$v_1 = -N_1 \frac{d\Psi}{dt} \quad (\text{B-2b})$$

$$v_2 = -N_2 \frac{d\Psi}{dt} \quad (\text{B-2c})$$

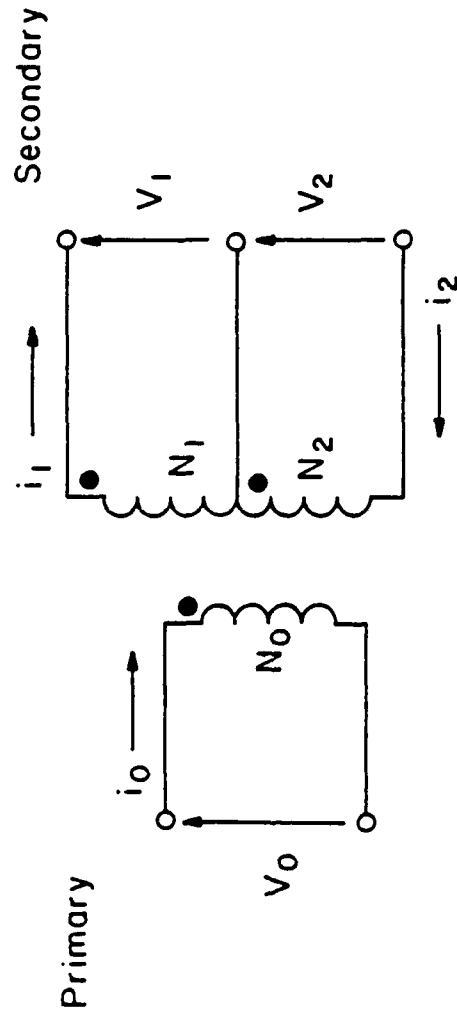


FIGURE B-1. THE CENTER-TAPPED TRANSFORMER.

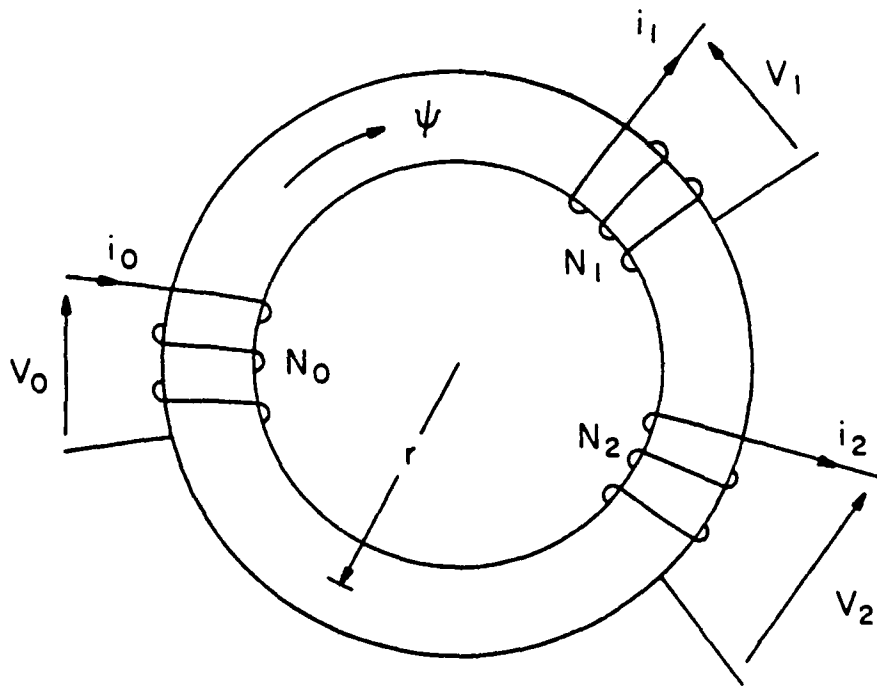


FIGURE B-2. THE TRANSFORMER WINDINGS.

Equations B-2a and B-2b yield

$$v_1 = \frac{N_1}{N_0} v_0 \quad (\text{B-3a})$$

and Equations B-2a and B-2c yield

$$v_2 = \frac{N_2}{N_0} v_0 \quad (\text{B-3b})$$

The current relationships between the primary and secondary windings are determined through use of Ampere's law

$$\oint_C \mathbf{H} \cdot d\mathbf{l} = i \quad (\text{B-4})$$

Notice that the displacement current has been neglected in Ampere's law; that is, quasi-static conditions are assumed. Integration of Ampere's law around the mean axis of the toroid yields

$$H (2 \pi r) = N_0 i_0 - N_1 i_1 - N_2 i_2 \quad (\text{B-5})$$

However, H is related to the flux, Ψ , by

$$B = \mu H \quad (\text{B-6})$$

$$\Psi = BA \quad (\text{B-7})$$

Therefore

$$H = \frac{\Psi}{\mu A} \quad (B-8)$$

Now, consider that the magnetomotive force is defined by

$$F = H \cdot dl \quad (B-9)$$

and the reluctance of the core is defined by

$$\mathcal{R} = \frac{F}{\Psi} = \frac{2 \pi r}{\mu A} \quad (B-10)$$

Equations B-4 through B-10 yield

$$\mathcal{R} \Psi = N_0 i_0 - N_1 i_1 - N_2 i_2 \quad (B-11)$$

For an ideal transformer, the permeability of the core, μ , is infinite, so the reluctance of the core, \mathcal{R} , is zero. Equation B-11 becomes, for an ideal transformer,

$$N_0 i_0 = N_1 i_1 + N_2 i_2 \quad (B-12a)$$

or

$$i_0 = \frac{N_1}{N_0} i_1 + \frac{N_2}{N_0} i_2 \quad (B-12b)$$

The equivalent circuit model (see Figure B-3) is derived from Equations B-3 and Equation B-12b.

The transformer used to balance the terminal configuration of the SWP in Chapter V was center-tapped and its primary winding was terminated in an impedance R. The equivalent circuit derived above can be used to model this configuration (Figure B-4), by finding the impedance matrix of the two ports of the secondary windings.

The two-port parameters of Figure B-4 can be found from

$$V_1 = \bar{B}_{11} I_1 + \bar{B}_{12} I_2 \quad (\text{B-13a})$$

$$V_2 = \bar{B}_{21} I_1 + \bar{B}_{22} I_2 \quad (\text{B-13b})$$

which can be written in matrix notation

$$\begin{bmatrix} V_1 \\ V_2 \end{bmatrix} = \begin{bmatrix} \bar{B}_{11} & \bar{B}_{12} \\ \bar{B}_{21} & \bar{B}_{22} \end{bmatrix} \begin{bmatrix} I_1 \\ I_2 \end{bmatrix} \quad (\text{B-14a})$$

or simply

$$\underline{V} = \underline{\bar{B}} \underline{I} \quad (\text{B-14b})$$

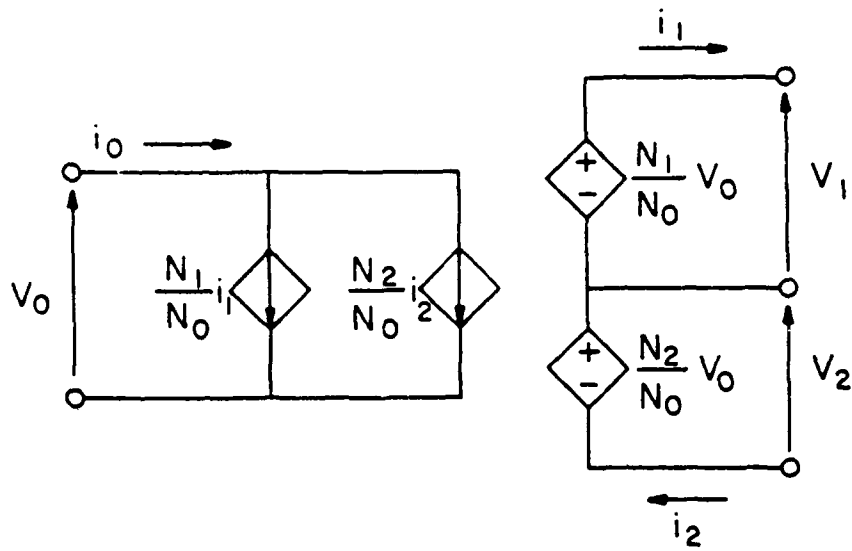


FIGURE B-3. THE EQUIVALENT CIRCUIT.

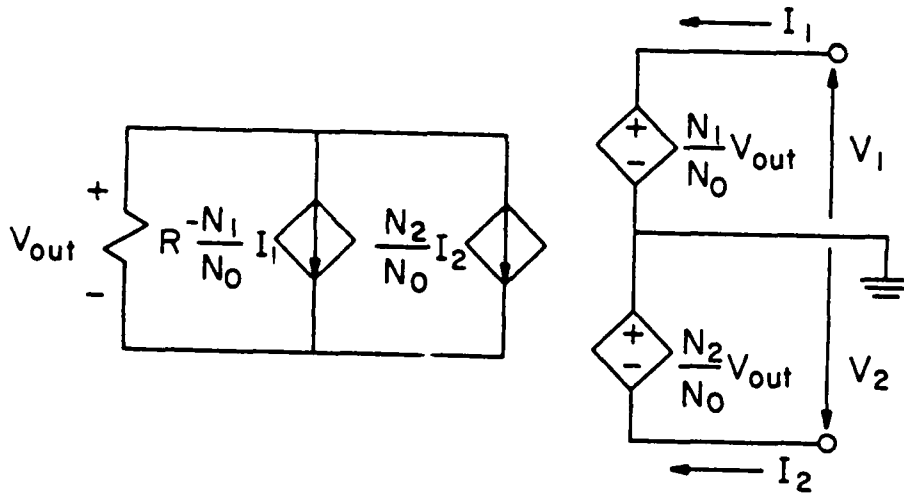


FIGURE B-4. THE EQUIVALENT CIRCUIT WITH ITS PRIMARY WINDING TERMINATED IN IMPEDANCE R.

The elements of Z are found in the following manner.

$$\begin{aligned} Z_{11} &= \left. \frac{V_1}{I_1} \right|_{I_2 = 0} \\ &= \begin{pmatrix} N_1 & \\ N_0 & V_0 \end{pmatrix} \begin{pmatrix} N_0 & \\ N_1 & R \end{pmatrix} \\ Z_{11} &= \left(N_1/N_0 \right)^2 R \end{aligned} \tag{B-15a}$$

$$\begin{aligned} Z_{12} &= \left. \frac{V_1}{I_2} \right|_{I_1 = 0} \\ &= \begin{pmatrix} N_1 & \\ N_0 & V_0 \end{pmatrix} \begin{pmatrix} -N_0 & \\ N_2 & R \end{pmatrix} \\ Z_{12} &= \left(-\frac{N_1 N_2}{N_0^2} \right) R \end{aligned} \tag{B-15b}$$

$$\begin{aligned} Z_{21} &= \left. \frac{V_2}{I_1} \right|_{I_2 = 0} \\ &= \begin{pmatrix} -N_2 & \\ N_0 & V_0 \end{pmatrix} \begin{pmatrix} N_0 & \\ N_1 & R \end{pmatrix} \\ Z_{21} &= \left(-\frac{N_1 N_2}{N_0^2} \right) R \end{aligned} \tag{B-15c}$$

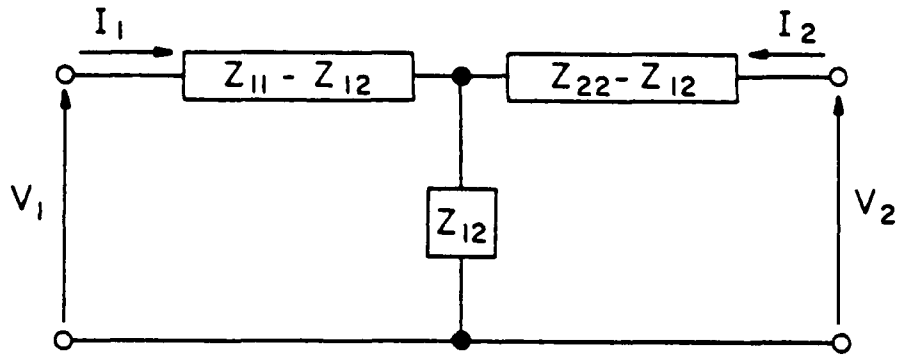


FIGURE B-5. A T NETWORK.

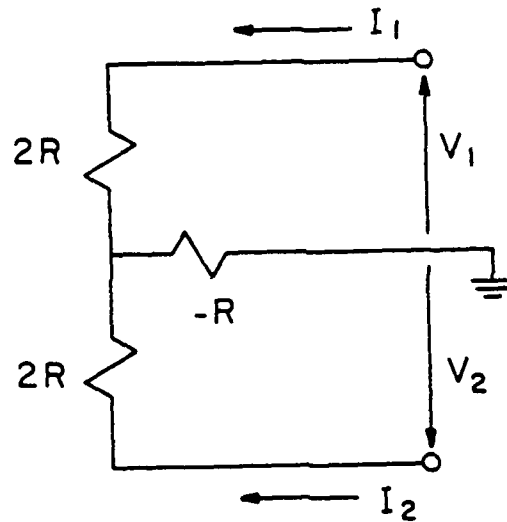


FIGURE B-8. EQUIVALENT CIRCUIT USED IN CHAPTER V.

$$\begin{aligned} Z_{22} &= \left. \frac{V_2}{I_2} \right|_{I_1 = 0} \\ &= \begin{pmatrix} -\frac{N_2}{N_0} & V_0 \\ & \frac{N_0}{N_2} & \frac{V_0}{R} \end{pmatrix} \\ Z_{22} &= \left(\frac{N_2}{N_0} \right)^2 R \end{aligned} \tag{B-15d}$$

Notice that $Z_{12} = Z_{21}$. \underline{Z} is symmetric.

A T network is often used to represent the equivalent circuit found by impedance parameters (see Figure B-5). If the center-tapped transformer used in Chapter V is assumed to be ideally balanced, then $N_1 = N_2$. The specific transformer used had a turns ratio of 1:2. Therefore $N_0 = 1$ and $N_1 = N_2 = 1$. Then the T network of Figure B-5 becomes the equivalent circuit used in Chapter V (Figure B-6).

Finally, note that the impedance matrix, \underline{Z} , formed with the elements defined in Equations B-15, has a determinant equal to zero. When the determinant of a matrix is equal to zero, the matrix is said to be singular and its inverse does not exist. The inverse of the impedance matrix is the admittance matrix. Therefore, there is no admittance matrix that can represent the two-port network of Figure B-4.

REFERENCES

- [1] C. R. Paul and J. W. McKnight, "Prediction of Cross-talk Involving Twisted Pairs of Wires - Part 1: A Transmission - Line Model for Twisted-Wire Pairs", IEEE Transactions on Electromagnetic Compatibility, Vol. EMC-21, No. 2, pp. 92-105, May 1979.
- [2] C. R. Paul and D. Koopman, "Sensitivity of Cross-talk in Balanced Twisted Pair Circuits to Line Twist", 1983 International Symposium and Technical Exhibition on Electromagnetic Compatibility, Zurich, Switzerland, March 1983.
- [3] C. R. Paul and M. B. Jolly, Crosstalk in Twisted-Wire Circuits, Technical Report, RADC-TR-82-286, Vol. IV C, Rome Air Development Center, Griffis AFB, Ni., November 1982.
- [4] A. Y. Alksne, "Magnetic Fields Near Twisted Wires", IEEE Transactions on Space Electronics and Technology, Vol. SET-10, No. 3, p. 324, September 1968.
- [5] G. Barker, E. Gray, and R. M. Showers, "Preliminary Measurements Related to Procedures for Measuring Systems Susceptibility", presented at Unclassified Proc. Eighth Tri-Service Conf. EMC, 1962.

- [6] J. Moser and R. F. Spencer, Jr., "Predicting the Magnetic Fields from a Twisted-Pair Cable", IEEE Transactions on Electromagnetic Compatibility, Vol. EMC-10, pp. 324-329, September 1968.
- [7] S. Shenfield, "Magnetic Fields of Twisted-Wire Pairs", IEEE Transactions on Electromagnetic Compatibility, Vol. EMC-11, pp. 164-169, November 1969.
- [8] C. R. Paul, Applications of Multiconductor Transmission Line Theory to the Prediction of Cable Coupling, Vol. 1, Multiconductor Transmission Line Theory, Technical Report, RADC-TR-76-101, Rome Air Development Center, Griffis AFB, NY, April 1976.
(A025028)
- [9] F. M. Tesche, "Coupling Between Twisted Wire Bundles: Analysis and Description of Computer Code TWERP", LeTech, Inc., Report for Martin Marietta Aerospace, under subcontract BPA-1290, May 1981.
- [10] C. R. Paul and J. W. McKnight, "Prediction of Crosstalk Involving Twisted Pairs of Wires - Part II: A Simplified Low-Frequency Prediction Model", IEEE Trans on Electromagnetic Compatibility, Vol. EMC-21 No. 2, pp. 105-114, May 1979.

- [11] C. R. Paul, "Effect of Pigtails to Braided - Shield Cables", IEEE Transactions on Electromagnetic Compatibility, Vol. EMC-22, No. 3, pp. 161-172, August 1980.

- [12] C. R. Paul and M. B. Jolly, "Sensitivity of Crosstalk in Twisted-Pair Circuits to Line Twist", IEEE Trans. on Electromagnetic Compatibility, Vol. EMC-24, No. 3, pp. 359-364, August 1982.

- [13] C. R. Paul, "Solution of the Transmission-Line Equations for Three-Conductor Lines in Homogeneous Media", IEEE Trans on Electromagnetic Compatibility, Vol. EMC-20, No. 1, pp. 216-222, February 1978.

- [14] R. E. Matick, Transmission Lines for Digital and Communication Networks, New York: McGraw-Hill, 1969.



MISSION
of
Rome Air Development Center

RADC plans and executes research, development, test and selected acquisition programs in support of Command, Control Communications and Intelligence (C³I) activities. Technical and engineering support within areas of technical competence is provided to ESD Program Offices (POs) and other ESD elements. The principal technical mission areas are communications, electromagnetic guidance and control, surveillance of ground and aerospace objects, intelligence data collection and handling, information system technology, ionospheric propagation, solid state sciences, microwave physics and electronic reliability, maintainability and compatibility.

END

FILMED

6-85

DTIC